Institut für Medizinische Mikrobiologie, Immunologie und Hygiene der
Technischen Universität München

Analysis of immune-modulatory effects of NKG2D ligands on T cells

Anja Kerstin Kriegeskorte

Vollständiger Abdruck der von der Fakultät Wissenschaftszentrum Weihenstephan für Ernährung, Landnutzung und Umwelt der Technischen Universität zur Erlangung des akademischen Grades eines

Doktors der Naturwissenschaften

genehmigten Dissertation.

Vorsitzender:	Univ.-Prof. Dr. S. Scherer
Prüfer der Dissertation:	
	1. Univ.-Prof. Dr. M. Hrabé de Angelis
	2. Univ.-Prof. Dr. D. Busch

Die Dissertation wurde am 19.04.2007 bei der Technischen Universität München eingereicht und durch die Fakultät Wissenschaftszentrum Weihenstephan für Ernährung, Landnutzung und Umwelt am 16.07.2007 angenommen.

Die Ergebnisse dieser Arbeit sind zum Teil veröffentlicht:

Kriegeskorte, A. K., Gebhardt, F. E., Porcellini, S., Schiemann, M., Stemberger, C., Franz, T. J., Huster, K. M., Carayannopoulos, L. N., Yokoyama, W. M., Colonna, M., Siccardi, A. G., Bauer, S., and Busch, D. H. (2005). NKG2D-independent suppression of T cell proliferation by H60 and MICA. *PNAS* 102, 11805-11810.

I TABLE OF CONTENTS

II INDEX OF FIGURES AND TABLES

III ABBREVIATIONS

Ab	Antibody
AP-1	Activation protein-1
APC	Allophycocyanin
APCs	Antigen-presenting cells
ATP	Adenosine 5'-triphosphate
BCR	B cell receptor
β_2m	β_2m-microglobuline
Bq	Becquerel
BrdU	Bromodeoxyuridine
BSA	Bovine serum albumin
BTLA	B and T lymphocyte attenuator
CD	Cluster of differentiation
Cdk	Cyclin-dependent kinase
CFSE	5-(and-6) Carboxy-fluoresceindiacetat succinimidyl ester
CHO	Chinese hamster ovary
ConA	Concanavalin A
CTL	Cytotoxic T lymphocyte
CTLA-4	Cytotoxic T lymphocyte associated antigen-4
CTP	Cytidine 5'triphosphate
DAP10/12	DNAX-activating protein of 10/12 kDa
DC	Dendritic cell
ddH_2O	Double-distilled water
DMEM	Dulbecco's modified eagle medium
DNA	Deoxyribonucleic acid
E.coli	*Escherichia coli*
EDTA	Ethylendiamintetraacetate
EMA	Ethidiummonazid-bromide
ERK	Extracellular receptor-activated kinase
FACS	Fluorescence activated cell sorting
FCS	Fetal calf serum
FITC	Fluorescein-isothiocyanat
FoxP3	Forkhead box P3
FPLC	Fast performance liquid chromatography
GITR	Glucocorticoid-induced TNF receptor family-related protein
GPI	Glycosylphosphatidylinositol
h	Hour
HEK 293	Human embryonic kidney 293 cells
HCMV	*Human cytomegalovirus*
HRP	Horseradish peroxidase
HSP	Heat shock protein
ICOS	Inducible costimulatory molecule
IFN	Interferon
IL	Interleukin
IPTG	Isopropylthiogalactoside
ITAM	Immunoreceptor tyrosine activatory motif
ITIM	Immunoreceptor tyrosine inhibitory motif
JNK	c-Jun N-terminal kinase
KARAP	Killer cell activatory receptor-associated protein

KIR	Killer immunoglobulin-like receptor
kDa	Kilo Dalton
ko	Gene knockout
L.m.	*Listeria monocytogenes*
LPS	Lipopolysaccharide
mAb	Monoclonal antibody
MACS	Magnetically activated cell sorting
MAPK	Mitogen-activated protein kinase
MCMV	*Murine cytomegalovirus*
MHCI/II	Major histocompatibility complex class I/II
MICA/B	MHC class I-related molecule A/B
mRNA	Messenger RNA
MULT1	Murine UL16-binding protein like transcript
MyD88	Myeloid differentiation marker 88
NFAT	Nuclear factor of activated T cells
NFκB	Nuclear factor κB
NK/NKG2D	Natural killer/natural killer group 2-D
NKT	Natural killer-like T cell
dNTP	Deoxynucleosid-triphosphat
hPBMC	Human peripheral blood mononuclear cell
PBS	Phosphate buffered saline
PCR	Polymerase chain reaction
PD	Programmed death
PE	Phycoerythrin
PFA	Paraformaldehyde
PHA	Phytohemagglutinin
PI	Propidium iodide
PI3K	Phosphatidylinositol-3-kinase
PLC	Phospholipase C
PMA	Phorbol 12-myristate 13-acetate
Rae1	Retinoic acid early inducible gene 1
Rb	Retinoblastoma protein
RNA	Ribonucleic acid
rpm	Rounds per minute
RT	Room temperature
RT-PCR	Reverse transcription PCR
SA	Streptavidin
SDS	Sodium dodecyl sulfate
7-AAD	7-aminoactinomycin
TCR	T cell receptor
TEMED	N, N, N‘, N‘-Tetramethylethylendiamine
TGF-β	Transforming growth factor-β
Th	T helper
TLR	Toll-like receptor
TNF	Tumor necrosis factor
Tr1	antigen-induced regulatory T cell 1
Treg	$CD4^+CD25^+$ regulatory T cell
TREM	Triggering receptor expressed by myeloid cells
Tris	Tris-(Hydroxylmethyl-)Aminomethan
ULBP	UL16-binding protein
ZAP-70	ζ-associated protein of 70kDa

1 INTRODUCTION

1.1 Components of the cellular immune system

The mammalian immune system can be divided into two main parts: the innate and the adaptive immune system. Both arms interact tightly to initiate and maintain protective immune responses. The innate immune system is specialized for the immediate rejection of pathogens with limited and germline imprinted specificity. It consists of leukocyte populations that include macrophages, granulocytes, dendritic cells (DCs) and natural killer (NK) cells (Hsieh et al., 1993). Some innate cells, like NK cells, are involved in discrimination between self and non-self, others are essential for presentation of foreign antigen to cells of the adaptive immune system (Medzhitov and Janeway, 1998).

The adaptive or acquired immune system is characterized by its enormous variability to recognize and eliminate pathogens due to their highly diverse antigen-specific receptors. The two main effector cells of the adaptive immune system are the B and the T cells. Upon antigen-recognition by the B cell receptor (BCR), B cells, the carriers of the humoral immune response, differentiate and proliferate in the B cell regions of secondary lymphatic organs to become antibody producing plasma cells. The secreted antibodies can bind to antigen, and subsequently activate the complement system to lyse target cells, neutralize bacterial toxins or opsonize pathogens.

T cells, on the other hand, express a heterodimeric T cell receptor (TCR) usually consisting of an α and β chain, which enables them to specifically recognize peptides presented by professional antigen-presenting cells (APCs). While expressing two different types of coreceptors, CD4 or CD8, $\alpha\beta$ T cells can be phenotypically discriminated. These coreceptors play an important role in antigen recognition, as they are crucial for the recognition of MHC class I and MHC class II molecules. Peptide-MHC complexes on the surface of APCs present peptide-epitopes from pathogen-derived antigens to the TCR of T cells; $CD8^+$ T cells recognize peptides bound to MHC I and $CD4^+$ T cells peptides bound to MHC II. After antigen encounter, $CD4^+$ T cells, also known as T helper cells (Th), divide based on their effector function into Th1 cells, which can activate macrophages or DCs, and Th2 cells, which can stimulate B cells to differentiate and produce antibodies. Naïve $CD8^+$ T cells differentiate into cytotoxic T lymphocytes (CTLs) after recognition of antigen and can lyse target cells by the release of effector molecules from cytotoxic granula, like granzyme B and perforin, or via Fas/FasL interaction (Janeway and Travers, 2001).

In addition to αβ T cells, there exists another population of about 5% of all T cells that expresses a TCR comprising a γ and δ chain. The γδ T cells have been described to share characteristics typical for both the innate and the adaptive immunity, as they can respond with their restricted TCR rapidly after antigen encounter but also express rearranged surface receptors and are able to develop into memory cells. Their occurrence is mainly limited to epithelia, like epidermis and the mucosa of the gastro-intestinal tract. Interestingly, γδ T cells have been proposed to play a role in regulation of immune responses (Girardi, 2006; Hayday and Tigelaar, 2003), and in humans γδ T cells have been implicated to function like APCs, being able to present ligands to other γδ T cells (Brandes et al., 2005).

Another small, but important subpopulation of T cells (less than 1 %) are NKT cells, which coexpress the αβ TCR and NK cell-associated molecules as NK1.1 (CD161) (Bendelac et al., 1997). NKT cells are not restricted by classical MHC molecules and can be subdivided into CD1d-restricted and CD1d-independent NKT cells, while of the latter until now very little is known. CD1d-restricted NKT cells recognize lipid antigens presented by CD1d, a less polymorphic variant ("non-classical") of MHC I, and seem to influence immune responses such as suppression of autoimmune diseases in mice and humans, and prevention of tumor metastasis in liver and lung (Kronenberg, 2005; Kronenberg and Gapin, 2002).

Within the $CD4^+$ T cell compartment one can further distinguish a specialized cell population (about 10-15% of peripheral $CD4^+$ T cells), named regulatory T cells (Treg), which seem to play a dominant role in inhibiting the activation of T cells by self-peptides. The majority of $CD4^+$ Treg cells expresses CD25 (IL-2Rα chain), CD62L, CD103, CD152, CTLA-4 and GITR and need for their development the recently identified transcription factor Foxp3 (Cantor, 2004; Fehervari and Sakaguchi, 2004; Fontenot et al., 2003; Khattri et al., 2003). Extensive studies have separated Treg cells further into two major groups, the naturally occurring Tregs and the antigen-induced regulatory T cells. The naturally occurring Treg cells, on the one hand, develop in the thymus, express self-reactive TCRs and function to prevent activation of self-reactive T cells in the periphery (Hsieh et al., 2004). Costimulation by CD28 seems to be required in addition to TCR ligation for their development out of immature precursors and for their maintenance (Salomon et al., 2000; Takahashi et al., 1998; Thornton and Shevach, 1998). On the other hand, antigen-induced regulatory T cells are generated in the periphery upon antigen-stimulation and can develop from classical T cell subsets. It has been proposed that their main function is to maintain homeostatic control over various adaptive immune responses; they also might play a role in the maintenance of self-tolerance. For survival, they need continuous activation through antigen in a cell-contact

dependent manner. Based on their cytokine secretion profile, one further discriminates Tr1 cells, which produce high levels of IL-10 and TGF-β and require IL-10 for their differentiation and function, and Th3 cells that produce IL-10, TGF-β and IL-4, and depend on TGF-β for their suppressive function (Oldenhove et al., 2003; Vieira et al., 2004). The immune suppressive mechanisms of regulatory T cells have been described to include inhibition of upregulation of costimulatory molecules (Liu et al., 1999), secretion of TGF-β and IL-10, Fas/FasL interaction (Zhang et al., 2000), and other poorly defined cell contact-dependent mechanisms (Vieira et al., 2004).

1.2 Regulation of antigen-specific T cell responses

After their development in the thymus, T cells circulate in the blood and the periphery until they encounter appropriate antigen presented by professional APCs. For proliferation and differentiation from naïve T cells to effector cells, at least two signals, one over the TCR another via costimulatory molecules, are necessary. A vigorous expansion phase is followed by a contraction phase, where more than 90% of antigen-specific T cells die by apoptosis, leaving only a small pool of long living memory cells. These memory T cells can be immediately activated by re-encounter with antigen to rapidly proliferate, therefore providing protection against re-infection with pathogen. With the help of recently identified markers, one can discriminate in the murine model between short living effector T cells ($CD127^{low}$, $CD62L^{low}$), effector memory T cells (T_{EM}, $CD127^{high}$, $CD62L^{low}$), which are characterized by their ability to immediately exert effector functions but only a poor proliferative capacity, and central memory T cells (T_{CM}, $CD127^{high}$, $CD62L^{high}$), which have a high proliferative activity, but don't show immediate effector functions (Huster et al., 2004).
In order to initiate, amplify and terminate immune responses, a complex system of activation and inhibition, mediated by modulatory receptors and signaling molecules, is needed.

1.2.1 Immune-stimulatory events

For effective activation of T cells, at first a so called "signal 1" is required. Binding of peptide-MHC complexes usually provides this signal to the TCR together with the coreceptor CD8 or CD4. Recognition of MHC-associated peptides leads to a clustering of the TCR complex and coreceptors, followed by the activation of tyrosine kinases and phosphorylation of tyrosines associated with the cytoplasmic domains of CD3 and the ζ chain, which belong to

the TCR complex. The phosphorylation of tyrosines takes place on immunoreceptor tyrosine-based activation motifs (ITAMs), a common activation motif of nine conserved peptide sequences present in many immune-stimulatory receptors. Further intracellular signaling events include recruitment of ZAP-70 and Syk, phosphorylation of PLCγ-1 and e.g. activation of Ras signaling pathway or signaling through membrane inositol phospholipid metabolism, which lead to synthesis and activation of transcription factors like AP-1, NFAT and NF-κB.

It is possible to artificially stimulate T cells by providing anti-CD3 antibodies, which circumvent TCR activation via peptide-MHC complexes by directly cross-linking and thereby stimulating CD3 molecules. Similarly, other polyclonal activators like concanavalin A (Con-A) or phytohemagglutinin (PHA), so called lectins, activate T cells by binding specifically to certain sugar residues on glycoproteins of the TCR and CD3 proteins. Another pharmacologic reagent to stimulate T cells of any antigen specificity (mitogen) is provided by combining phorbol ester PMA with the calcium ionophore ionomycin, thereby mimicking signals generated by the TCR complex (Abbas and Lichtman, 2003).

As mentioned before, T cells need in addition to their signal 1 also a costimulatory signal 2, otherwise they will fail to develop effector functions and die by apoptosis, or they enter a stage of unresponsiveness called anergy. The best-characterized costimulatory molecule is CD28, which binds to B7-1 (CD80) and B7-2 (CD86) on activated APCs. Its cytoplasmic tail doesn't contain a typical ITAM sequence but a different cytosolic domain with a tyrosine motif, YXXM, which is capable of recruiting the p85 subunit of phosphatidylinositol-3-kinase (PI3K) and Grb2 (growth factor receptor-bound protein 2), thereby activating the Ras-Sos pathway, which mainly functions to enhance T cell responses and survival by e.g. production of IL-2 as well as T cell differentiation. Other important costimulators of T cells are interactions of CD40L (CD154) with CD40 on APCs, ICOS with B7RP-1, OX40 (CD134) with OX40L, 4-1BB (CD137) with 4-1BBL or CD27L (CD70) with CD27, just to name a few (Lipscomb and Masten, 2002).

For the innate immune system, at least three main groups of immune-stimulatory receptors with different functions have been described so far. NKG2D (CD314), which also plays a role in costimulation of $CD8^+$ T cells in a similar manner like CD28, recognizes non-classical MHC molecules and will be discussed in detail under 1.3. Ly49H (and Ly49D), another stimulatory receptor, is expressed on a subset of NK cells, associates with the adaptor protein DAP12 and recognizes directly a virus-encoded protein expressed by cells infected with murine cytomegalovirus (MCMV). Furthermore, the group of triggering receptors expressed

by myeloid cells (TREMs), which are exclusively expressed on myeloid cells, have been shown to magnify cytokine responses to bacterial products (Diefenbach and Raulet, 2003).

1.2.2 Immune-suppressive events

Immune-inhibitory receptors play an essential role in the control of immune responses and their loss often leads to auto-reactivity and uncontrolled inflammation (Long, 1999). A common feature is their capacity to weaken activatory signals. Most cells contain activatory and inhibitory receptors, so that after ligand binding the relative strength of both types of receptors determines the outcome. In analogy to the ITAM motif in stimulatory receptors, many inhibitory receptors share in their cytoplasmic domain an immunoreceptor tyrosine inhibitory motif (ITIM) that recruits upon ligand-induced receptor clustering the tyrosine phosphatases SHP-1 or SHP-2 (Src homology 2 domain containing phosphatase), or the inositol phosphatase SHIP (SH2 domain containing inositol 5-phosphatase), which dephosphorylate and thereby inactivate signaling intermediates generated by activatory receptors. An overview over the main immune inhibitory receptors, their ligands and their distribution is given in Table 1 (Chen, 2004; Ravetch and Lanier, 2000); selected examples are discussed in the following section.

Receptor	Predominant cell distribution	Ligands
FcγRIIB	B, myeloid, mast	IgG complexes
BTLA (CD272)	B, T, some APCs	HVEM
CTLA-4 (CD152)	T	CD80, CD86
Unknown	T	B7-H3
Unknown	T	B7-H4
PD-1	T, B, myeloid	PD-L1 (B7-H1), PD-L2 (B7-DC)
CD5	T, subset of B	Unknown
PILRα	Myeloid	Unknown
CD72	B	Unknown
MAFA	Myeloid, mast, NK	Unknown
NKG2A/CD94	NK, T	HLA-E / $Qa1^b$
CD31	Myleoid, platelet, endothelial cells, subset of NK and T	CD31
KIR2DL/3DL	NK, T	MHC class I
Ly49A-I (not D or H)	NK, T	MHC class I
ILT2-5; LIR8	Myeloid, NK, B, subset of T	MHC class I and unknown
LAIR-1	Leukocytes	Unknown
gp49B1	Myeloid, mast, NK	Unknown
PIR-B	Myeloid, B	Unknown
CMRF35H	Leukocytes	Unknown

CD22	B	Sialic acid
CD66a/d	Granolocytes, T, B, subset NK, epithelial cells	CD66, CD62E and unknown
CD33	Myeloid	Sialic acid
SIGLEC5-7	Myeloid, B, NK, subset T	Sialic acid
SIRPα	Myeloid, nonhematopoietic cells	CD47

Table 1: Immune-inhibitory receptors and their distribution pattern

Members of the B7 family are involved in costimulation and coinhibition of lymphocytes. As illustrated before, CD28 is constitutively expressed on T cells and mediates activatory signals via B7-1 and B7-2. In comparison, the expression of the structurally homologous CTLA-4 (cytotoxic T lymphocyte associated antigen) is inducible by T cell activation. CTLA-4 binds with a higher affinity to the very same ligands as CD28 but serves as negative regulator of immune responses in lymphoid organs, e.g. by blocking cell cycle progression (Greenwald et al., 2002). Similar to CTLA-4, BTLA (B and T lymphocyte attenuator) is upregulated during T cell activation. BTLA binds to a member of the tumor necrosis factor family, HVEM (herpersvirus entry mediator), and has been postulated to negatively influence generation of $CD8^+$ T cell memory and homeostasis (Krieg et al., 2007). Another negative regulator of T cells from the B7 family is PD-1 (programmed death) with its ligands PD-L1 and PD-L2, which can inhibit cytokine production and T cell proliferation in peripheral tissues (Greenwald et al., 2005).

In addition to the inhibitory B7 family members, also inhibitory Fc (fragment crystalline) receptors have been described. Fc receptors bind to the Fc parts of immunoglobulins (Igs), normally leading to activation of leukocytes or triggering of phagocytosis of opsonized particles. In contrast, IgG antibody complexes ligating the FcγRIIB (CD32) receptor expressed on B cells, macrophages and mast cells, deliver negative signals, which terminate e.g. antibody production of B cells (Ravetch and Lanier, 2000).

For the negative regulation of NK cells and memory T cells, further receptor types are involved like the family of killer immunoglobuline-like receptors (KIR, CD158), CD94/NKG2A and Ly49 (only in mice), which all bind to classical or non-classical MHC molecules. Only when target cells as a result of e.g. virus infection or tumorigenesis downregulate their MHC molecules, NK cells can be activated, e.g. by NKG2D, to lyse target cells (Ravetch and Lanier, 2000).

1.2.3 Immune-regulation via cell cycle arrest

T cell proliferation is essential during most types of T cell-mediated immune responses, as it allows a low frequency of antigen-specific T cells to reach numbers sufficient to eradicate an infection or to exert other effector functions. It has been proposed, that CD28 among other costimulatory molecules is needed to provide the signal to enter the cell cycle, but the main intracellular targets and the molecular nature of checkpoints controlling T cell division remain to be identified (Croft, 2003; Harding et al., 1992). The cell cycle is divided into two major phases, the S phase (S for synthesis), which requires 10-12 hours and where the DNA duplication takes place, and the M phase (M for mitosis), which lasts about one hour and leads to chromosome segregation. But as most cells need more time to grow and double their proteins and organelles, extra gap phases are inserted between S and M phase; a G1 phase (G for gap) between M and S phase, and a G2 phase between S phase and mitosis, leading to an approximately 24 hour cycle. Furthermore, the length of the G1 phase can vary greatly, as cells can also enter a specialized G0 phase, if conditions are not prone to divide, which can last even for years. If a cell receives signals to grow, it passes the restriction point, whereby the cell proceeds autonomously from G1 phase to S phase and initiates DNA replication.

Of course, there have to exist several points in the cell cycle, called checkpoints, at which the cell can be arrested by negative intracellular signals. Cyclins and cyclin-dependent kinases (cdks) are essential for cell cycle control in eukaryotes. Cyclins (regulatory subunits) bind to cdks (catalytic subunits) to form active cyclin-cdk complexes. The cdk subunits are by themselves inactive and require binding to a cyclin for activation. The cyclins, on the other hand, undergo periodic synthesis and degradation, thereby regulating cdk activity. In addition to the cyclins, cdk activity is regulated by activating or inhibitory phosphorylation, and by small proteins (p15, p18, p21 and p27) called inhibitors of cdk activity, that can bind to cdks, cyclins or their complexes. Active cyclin-cdk complexes drive cells through the cell cycle by phosphorylating protein substrates needed to achieve transition to the next phase.

D- and E-type cyclins are expressed during G0 and G1 and are called start cyclins. Cdks 2,4,5 and 6 form complexes with D-type cyclins, which lead to phosphorylation of the retinoblastoma protein Rb, removing the G1 block caused by underphosphorylated Rb. This results in the release of transcription factor E2F, required for transcription of S phase genes. Further, interaction of Cyclin E and cdk2 initiates and progresses DNA replication. Cell cycle regulators as p15, p16, p18, p21, and p27 can block the activity of these cyclin-cdk complexes and thereby prevent phosphorylation of their targets, leading to arrest of G1 phase or S phase transition, respectively.

Cyclins A and B are mitotic cyclins. Cyclin A is synthesized during S phase and degrades during anaphase. In complex with cdk2, it plays a role in progression of DNA replication, which can be negatively regulated by p21 and p27. In late G2 phase, cdk1 (also known as cdc2 for cell-division-cycle) binds to cyclin B1, which finally drives the cell to enter mitosis. DNA damage or other forms of cell stress can lead to downstream activation of p53, which inhibits cell cycle progression to G1 phase or later at G2/M transition in order to activate DNA repair mechanisms (Alberts et al., 2002). A summary of the cell cycle steps and their regulation is shown in Figure 1 (taken from www.pharmingen.com).

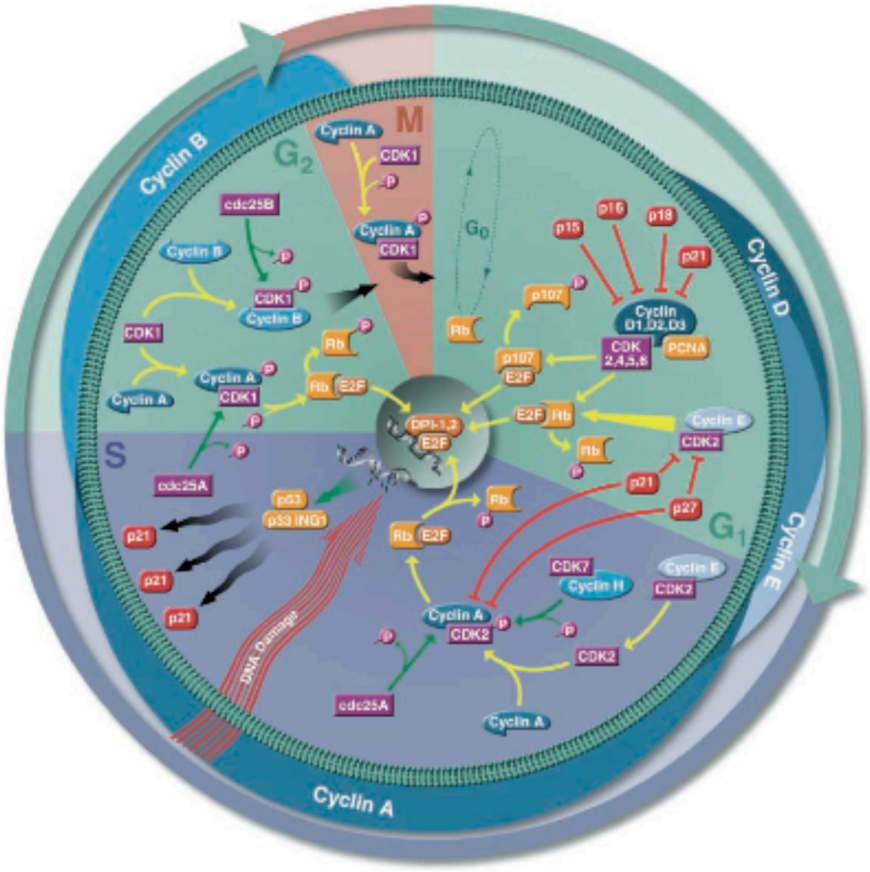

Figure 1: The cell cycle and its major regulation steps

With the help of immune-suppressive agents, it is possible to manipulate cell cycle progression. Cyclosporine, which is often used in patients to prevent transplant rejection, inhibits transcription of IL-2, a mitogen needed for cell cycle initiation, so that cells cannot leave the G1 phase and subsequently enter the cell cycle. In contrast, rapamycin inhibits through FK506 binding protein the kinase mammalian target of rapamycin (mTOR), thereby preventing G1 to S phase progression (Powell et al., 1999). A different block is caused by the drug nocodazole, a microtubule-interfering agent, which leads to a delay at G2/M phase transition (Rieder and Cole, 2000).

1.3 NKG2D and its ligands

1.3.1 The NKG2D receptor

NKG2D is part of a sub-family of C type lectin-like receptors and consists as a homodimeric type II (i.e. the C-terminus is extracellular) transmembrane glycoprotein (Wolan et al., 2001). For signaling, NKG2D depends on the association with adaptor proteins. In humans NKG2D forms exclusively non-covalent complexes with DAP10 (Rosen et al., 2004; Wu et al., 1999), whereas mouse NKG2D can associate with DAP10 and DAP12 (or KARAP) (Diefenbach et al., 2002). Mouse NKG2D is expressed as two distinct splice variants, a short form (NKG2D-S) and a long form (NKG2D-L), which differ by 13 amino acids at the NH_2-tail (Diefenbach et al., 2002). While the short NKG2D can associate with both adaptor molecules, the longer cytoplasmic domain of NKG2D-L seems to disturb pairing with DAP12, although a recent report has questioned this (Rabinovich et al., 2006). Interestingly, one NKG2D homodimer can assemble with two other dimers, so that in mice for example also one DAP10 and one DAP12 homodimer can form a hexameric complex (Garrity et al., 2005).

On most innate immune cells in mice and humans, as NK cells, subsets of NKT cells (only mouse), and most γδ T cells, NKG2D is constitutively expressed (Gumperz et al., 2002; Jamieson et al., 2002). Furthermore, it has been recently demonstrated that also a subset of murine interferon-producing killer DCs (IKDCs) express NKG2D (Chan et al., 2006; Taieb et al., 2006). Of the cells of the adaptive immune system, human $CD8^+$ T cells constitutively express NKG2D, whereas only activated and memory $CD8^+$ T cells in mice express NKG2D (Jamieson et al., 2002). On $CD4^+$ T cells, NKG2D is normally not expressed, but it has been found in humans on subsets of $CD4^+$ cells in rheumatoid arthritis patients, in late-stage tumor settings (Groh et al., 2003; Groh et al., 2006), and on $CD4^+$ T cells specific for HCMV (Saez-Borderias et al., 2006).

As before mentioned, NKG2D signaling depends on the adaptor proteins DAP10 and DAP12. DAP12 contains an ITAM (Lanier et al., 1998) leading upon engagement to recruitment of ZAP-70 and Syk as discussed under 1.2.1. DAP10 instead contains a YINM motif similar to costimulatory receptors like CD28 and ICOS, and signaling via NKG2D occurs by recruitment of the p85 subunit of PI3-Kinase and binding of a Grb2-Vav1 intermediate (Upshaw et al., 2006). Unstimulated NK cells in mice express mainly the DAP10-associated form NKG2D-L, whereas activation with IL-2 or polyI:C leads to upregulation of NKG2D-S enabling also binding to DAP12 (Diefenbach et al., 2002). However, activated NK cells lacking DAP12 or Syk kinases retain significant NKG2D-dependent mediated killing and

cytokine production, thus making NKG2D to a primary activation receptor in NK cells (Andre et al., 2004; Billadeau et al., 2003; Zompi et al., 2003), which can dominate inhibitory effects of MHC I molecules (Bauer et al., 1999; Cosman et al., 2001). Since T cells generally don't express DAP12, DAP10 is the only adaptor molecule, and NKG2D signaling is believed to play more a costimulatory role in combination with TCR signaling than a primary activation function (Gilfillan et al., 2002; Groh et al., 2001; Maasho et al., 2005; Roberts et al., 2001), although this has been doubted by a recent report claiming not to see any costimulatory effect of NKG2D engagement on cytolytic activity and IFN-γ production by human and mouse $CD8^+$ T cells (Ehrlich et al., 2005). Nevertheless, NKG2D can also serve as TCR-independent primary activation receptor of cytotoxicity in $CD8^+$ T cells, which have been long term cultivated with high amounts of IL-15 or IL-2, causing a priming of the NKG2D signal transduction via induction of ERK phosphorylation (Meresse et al., 2004; Roberts et al., 2001).

1.3.2 NKG2D ligands

The receptor NKG2D recognizes a large number of distantly related non-classical MHC I molecules. First described as NKG2D ligands were the highly polymorphic human ligands MICA/B (MHC class I-chain-related protein A and B), with almost 60 alleles already identified for MICA and 25 for MICB (Bahram et al., 2005). Like MHC I molecules, they contain three immunoglobulin (Ig) –like domains (α1, α2 and α3), but do not associate with β2-microglobulin or peptide (Bahram et al., 1994). Expression in healthy tissue has only been observed on gastro-intestinal epithelium (Groh et al., 1996) and on bone marrow stem cells (Poggi et al., 2005). MICA/B allele frequency is varying in between ethnic groups, with MICA*008 being the most frequent allele in caucasian and oriental populations, followed by *002, *010 and *004. Interestingly, the abundantly used MICA*008 allele lacks due to a frameshift mutation the cytoplasmic tail, which led to speculations of encoding a secreted or dysfunctional allele. Up to now, MICA allele frequency has been linked by several reports to the occurrence of various diseases, such as Crohn's disease, Behçet's disease, psoriasis, ulcerative colitis and type I diabetes, but further investigations are needed to functionally discriminate the different alleles (Bahram et al., 2005; Stephens, 2001). Another family of human NKG2D ligands is represented by the ULBPs (UL-16 binding proteins), of which some can interact with the UL-16 protein of HCMV (Cosman et al., 2001); they have also been called RAET1s (retinoic acid early inducible gene 1 like transcript), due to their

homology with the murine Rae1 genes. ULBPs contain only α1 and α2 domains, while the ULBPs1-3 are GPI (glycosylphosphatidylinositol) –anchored (Cosman et al., 2001), and ULBP-4 (also named RAET1E or Letal) and RAET1G are transmembrane glycoproteins like the MICs (Bacon et al., 2004; Conejo-Garcia et al., 2003). ULBP1-3 mRNA is detected in various healthy tissues (Cosman et al., 2001), while ULBP-4 mRNA is expressed in the skin (Chalupny et al., 2003) and RAET1G in the colon like the MIC molecules (Bacon et al., 2004).

The murine NKG2D ligands can all be contemplated as ULBP homologs containing only α1 and α2 domains. The five Rae1 molecules (α-ε) are differentially possessed by BALB/c (α,β,γ) and C57BL/6 (δ,ε) mice and can be induced by retinoic acid in embryocarcinoma cells *in vitro*. Furthermore, Rae1 mRNA expression is detectable in the early embryo (Nomura et al., 1996) and on bone marrow stem cells (Ogasawara et al., 2005). Another ligand, H60, was originally identified as minor histocompatibility antigen in immunization of C57BL/6 mice with haplo-identical BALB/b cells (Malarkannan et al., 1998); indeed, until now H60 protein expression has not been detected in C57BL/6 mice. In BALB/c mice, H60 is expressed on some activated lymphoblasts and on immature $CD4^+8^+$ thymocytes (Diefenbach et al., 2000; Li et al., 2005). Of the recently identified MULT1 (murine UL16 binding protein like transcript 1) mRNA expression is measured in a wide array of adult tissue, but seems to be regulated post-transcriptionally (Carayannopoulos et al., 2002a; Diefenbach et al., 2003).

1.3.3 Role of NKG2D/ligand system in tumor and disease

Expression of NKG2D ligands is very low in normal tissue, but all ligands can be upregulated on stressed or transformed cells, the so called “induced self” mechanism, providing a marker for abnormal body cells (Diefenbach and Raulet, 1999). The first hint to the regulation of NKG2D ligands was provided by the finding that MICA/B promoters contain regions similar to heat shock proteins like HSP70 (Groh et al., 1996). In addition, T cell activation by antigen pulsed APCs or ConA upregulates NKG2D ligands, turning them into a target for NK cells (Diefenbach et al., 2000; Rabinovich et al., 2003).

Furthermore, different types of infection can induce NKG2D ligands. MICA expression is triggered by infection with enteric bacteria by binding of *E.coli* adhesin to CD55 on epithelial cells (Tieng et al., 2002), providing an explanation for the high MICA/B expression in human gut. Infection with Sendai or Influenza virus in humans upregulates MICB on macrophages (Siren et al., 2004), HCMV infection leads to expression of MICs in lung tissue, and further

MCMV-infected mouse macrophages upregulate Rae1 expression (Lodoen et al., 2003). In addition, MCMV can selectively interfere with NK cell activation for encoding several genes (m145, m152 and m155), which can specifically downregulate surface expression of NKG2D ligands (MULT1, Rae1 and H60) (Hasan et al., 2005; Krmpotic et al., 2002; Krmpotic et al., 2005; Lodoen et al., 2003; Lodoen et al., 2004). Moreover, Toll–like receptor (TLR) stimuli induce NKG2D ligands on murine macrophages and DCs (Hamerman et al., 2004; Krug et al., 2004).

Oddly enough, a large number of tumor cells and cell lines express NKG2D ligands constitutively. On many types of epithelial tumors MICA/B expression is found (Busche et al., 2006; Groh et al., 1999; Jinushi et al., 2003), but less in myeloid and lymphoblastic leukemia (Carbone et al., 2005; Romanski et al., 2005; Salih et al., 2003). In contrast, ULBPs are mostly expressed on freshly isolated lymphoid leukemia cells (Salih et al., 2003) and *in vitro* cultured cell lines (Pende et al., 2002). In mice Rae1 and H60 are detected on skin, renal and lung carcinoma cell lines (Girardi et al., 2001; Smyth et al., 2004), as well as on various hematopoietic tumor cell lines (Cerwenka et al., 2000; Diefenbach et al., 2000).

How the expression of NKG2D ligands during transformation is regulated, is currently not well understood. Oncogenes of adenovirus and chronic myeloid leukemia have been shown to be involved in ligand upregulation (Boissel et al., 2006; Routes et al., 2005). A recent report identified the DNA damage response mechanism as upregulator of distinct NGK2D ligands, contributing to alert the immune system to the occurrence of potentially dangerous cells (Gasser et al., 2005).

As tumors develop from self-cells, they are generally poorly immunogenic and often not recognized efficiently by the adaptive immune system. NKG2D ligands can serve on tumor cells to sense the recognition of transformed cells, and indeed, mouse tumor cells expressing endogenous NKG2D ligands or transfected with cDNA encoding NKG2D ligands are efficiently rejected by NK cells and $CD8^+$ T cells (Cerwenka et al., 2001; Diefenbach et al., 2001). Moreover, high levels of MICA are correlated with a good prognosis in colorectal cancer (Watson et al., 2006), and chemically induced skin cancer, which specifically upregulates NKG2D ligands on transformed cells, was found to be enhanced in the absence of γδ T cells (Girardi et al., 2001).

However, despite high expression of NKG2D ligands *in vivo*, numerous tumors are not rejected by the host. Several mechanisms may account for the selection of NKG2D ligand bearing tumors. Soluble factors as TGF-β secreted by tumors themselves, can trigger downregulation of NKG2D on NK cells and $CD8^+$ T cells in the tumor microenvironment

(Castriconi et al., 2003; Lee et al., 2004). Furthermore, sustained exposure to NKG2D ligands can cause loss of signaling adaptor proteins DAP10 and DAP12, and CD3ζ, impairing also other stimulatory functions (Coudert et al., 2005). Additionally, it has been shown that in some cancer patients, metalloproteinases can cleave MICA/B from the surface of tumor cells, reducing NKG2D recognition (Groh et al., 2002; Salih et al., 2002). Moreover, soluble MIC proteins can bind to NKG2D leading to internalization and degradation of the NKG2D receptor (Jinushi et al., 2005; Wu et al., 2004). In addition, the occurrence of a unique $NGK2D^{+}CD4^{+}$ T cell population in late-stage tumor patients was recently presented, being able to suppress proliferation of $CD8^{+}$ T cells and kill them via Fas/FasL interaction (Groh et al., 2006). Another possible explanation for the high NKG2D ligand expression on tumor cells could be that not all NKG2D ligands mediate the same redundant (co-) stimulatory effects, but that distinct ligands can also cause inhibitory effects, thereby impairing the immune response and giving NKG2D ligand positive tumors a selective advantage.

1.4 Aim of this PhD work

The NKG2D receptor binds to a large array of structurally diverse ligands. Although these ligands seem to be differentially expressed, until recently only redundant stimulatory functions have been described for them. Based on these observations, especially the high expression of NKG2D ligands on tumor cells remains puzzling. Interestingly, we could recently demonstrate that distinct ligands, namely H60 and MICA-8, can beneath their stimulatory role also mediate suppressive functions. This observation might be crucial to better understand the role of NKG2D ligand expression under physiological, as well as pathological conditions.

On the basis of this finding, the major aim of this thesis work was to further analyze the obviously non-redundant capacities of NKG2D ligands on T cell activation and expansion, and to investigate the nature of the suppressive effect. With the help of several gene deficient mice it was intended to characterize the cell populations and molecules, which are essential for the H60- or MICA-8 mediated inhibition of T cells. Moreover, murine splenocytes should be compared with hPBMCs for analogous effects, because the NKG2D system is rather conserved between the two species. As our data pointed early to an effect independent of NKG2D, the third main part of the work was dedicated to several approaches to identify the receptor that binds exclusively to H60 and MICA-8. Therefore, a cDNA library of Phoenix cells, which highly express the unknown receptor under certain growth conditions, should be

generated and screened for the corresponding gene. Further strategies to find the receptor were anticipated with an Affymetrix microarray analysis of differential gene transcription of receptor positive and negative cells, by the generation of monoclonal antibodies against the receptor, and upon a receptor-ligand pull-down approach followed by mass spectrometric measurements.

Beyond this, the fate of the inhibited T cells should be characterized in more detail. Therefore, it is of special interest, if the suppressed cells die or if they are just temporarily arrested. These results could further help to link the suppressive effects of H60 or MICA-8 to distinct signaling pathways regulating cell cycle progression.

2 MATERIALS AND METHODS

2.1 Materials

2.1.1 Equipment

Equipment	Supplier
β-Counter	Matrix 9600 Direct Beta Counter, Packard Bioscience, Dreieich
Cell-harvester	Micro96 Harvester, Skatron Instruments, Lier, Norway
Flow cytometer	FACSCalibur, Becton Dickinson, Heidelberg
	Cyan, Dako Cytomation, Freiburg
	MoFlo Cell Sorter, Dako Cytomation, Freiburg
Centrifuges	Biofuge fresco, Heraeus, Hanau
	Sorvall® RC 26 Plus, Hanau
	Multifuge 3 SR, Heraeus, Hanau
FPLC	Amersham Biosciences, Europe GmbH, Freiburg
Heating block	Thermomixer compact, Eppendorf
Incubator	Cytoperm 2, Heraeus, Hanau
Laminar flow hood	HERA safe, Heraeus, Hanau
Microscope	Axiovert S100, Carl Zeiss, Jena
Neubauer counting device	Schubert, München
Phospho-Imager	STORM 840, Amersham Biosciences, Europe GmbH, Freiburg
Photometer	BioPhotometer, Eppendorf
Shaker	Multitron® Version 2, INFORS AG, Bottmingen, Switzerland
Thermocycler	T3 Thermocycler, Biometra, Göttingen
Waterbath	LAUDA ecoline 019, Lauda-Königshofen

2.1.2 Chemicals and reagents

Reagents	Supplier
Acrylamide/Bis 30%	Biorad, München
[α-^{32}P]dATP	Amersham Biosciences, Europe GmbH, Freiburg
BL21 Codon (DE3) plus	Stratagene, Amsterdam, Netherlands
β-Mercapto-ethanol	Invitrogen, Paisley, U.K.
Bovine Serum Albumin	SIGMA-Aldrich, Steinheim

BrdU	SIGMA-Aldrich, Steinheim
CELLection Biotin Binder Kit (artificial APCs)	Dynal, Oslo, Norway
CFSE	SIGMA-Aldrich, Steinheim
Cyclosporine	Novartis Pharma GmbH, Nürnberg
DMEM	Gibco Life Technologies, Gaithersburg MD, USA
Dimethylformamid (DMF)	SIGMA-Aldrich, Steinheim
DMSO	SIGMA-Aldrich, Steinheim
1kb/100bp DNA ladder	Fermentas, St. Leon-Rot
EMA	GIBCO, Invitrogen, Paisley, U.K.
Ethanol	Pharmacy, Klinikum rechts der Isar, München
Ethidiumbromide	Life Technologies, Paisley, U.K.
ExGen 500	Fermentas, St. Leon-Rot
FCS	Invitrogen, Paisley, U.K.
Ficoll	Biochrom AG, Berlin
Geneticin (G418)	GIBCO, Invitrogen, Paisley, U.K.
Gentamycin	GIBCO, Invitrogen, Paisley, U.K.
Goat Serum	GIBCO, Invitrogen, Paisley, U.K.
HEPES	GIBCO, Invitrogen, Paisley, U.K.
Ionomycin	SIGMA-Aldrich, Steinheim
IPTG	SIGMA-Aldrich, Steinheim
Isopropanol	Roth, Karlsruhe
Kanamycin	SIGMA-Aldrich, Steinheim
Lambda ZAP®-CMV XR Library Construction Kit	Stratagene, Amsterdam, Netherlands
Leupeptin	SIGMA-Aldrich, Steihnheim
L-Glutamin	GIBCO, Invitrogen, Paisley, U.K.
Methanol	Roth, Karlsruhe
Milk powder	Roth, Karlsruhe
Nitrocellulose Membrane	Invitrogen, Carlsbad, USA.
Nocodazole	SIGMA-Aldrich, Steihnheim
Oligotex mRNA-Kit	QIAGEN GmbH, Hilden
PageRuler Protein Ladder	Fermentas, St. Leon-Rot
PBS	Biochrom AG, Berlin

Penicillin	GIBCO, Invitrogen, Paisley, U.K.
Pepstatin	SIGMA-Aldrich, Steinheim
pET 3a/27b	Novagen, Madison USA
PFA	SIGMA-Aldrich, Steinheim
PI	Molecular Probes, Invitrogen, Paisley, U.K.
PMA	SIGMA-Aldrich, Steinheim
Protease inhibitors	Roche Diagonostics GmbH, Mannheim
QIAprep Miniprep Kit	QIAGEN GmbH, Hilden
QIAquick Extraction Kit	QIAGEN GmbH, Hilden
Rapamycin	Calbiochem, San Diego, USA
RNeasy Mini Kit	QIAGEN GmbH, Hilden
RPMI 1640	Gibco Life Technologies, Gaithersburg MD, USA
7-AAD	Molecular Probes, Invitrogen, Paisley, U.K.
Streptavidin –PE/-APC	Molecular Probes, Invitrogen, Paisley, U.K.
Streptomycin	SIGMA-Aldrich, Steinheim
SuperScript II	Invitrogen, Paisley, U.K.
Taq-Polymerase	Invitrogen, Paisley, U.K.
Temed	Bio-Rad, München
Tetracyclin	SIGMA-Aldrich, Steinheim
TRI REAGENT	SIGMA-Aldrich, Steinheim
Tween20	SIGMA-Aldrich, Steinheim
Triton X-100	Bio-Rad, München
Trypan Blue Solution	SIGMA-Aldrich, Steinheim
Western Lightning	Perkin Elmer, Boston, USA

2.1.3 Buffers and media

All buffers prepared for FACS or sterile preparations were filtered using a Stericup 0.22µM vacuum filtering system (Millipore, Bedfore, USA). Proper pH adjustment was performed with NaOH or HCl.

Buffer	Composition	
Ammoniumchloride-Tris (ACT)	0.17M	NH_4Cl
	0.3M	Tris-HCl, pH 7.5

Annexin V-binding buffer, pH 7.4	10mM	HEPES
	140mM	NaCl
	2.5mM	$CaCl_2$
Blocking buffer (200ml)	10g	Milk powder or BSA
	6ml	Goat serum
	194ml	PBT
Blotting buffer (1l)	100ml	10x Tris-Glycine
	200ml	Methanol
	700ml	dH_2O
$DMEM^+$	1x	DMEM
	10% (v/v)	FCS
	5% (v/v)	SC^+
FACS staining buffer, pH 7.45	1x	PBS
	0.5% (w/v)	BSA
	0.02% (w/v)	NaN_3
Lysis buffer, pH 7.4	150mM	NaCl
	50mM	HEPES
	1mM	EDTA
	10%	Glycerol
	1%	Triton-X-100
	10mM	$Na_4P_2O_7$
	1Tabl.	Protease inhibitors/100ml
6x Orange G	50µg	Orange G
	1µl	1M Tris-HCl, pH 8.0
	35µl	ddH_2O
	15µl	Glycerol
PBT (1l)	995ml	PBS
	5ml	Tween20
$RP10^+$	1x	RPMI 1640
	10% (v/v)	FCS
	5% (v/v)	SC^+
2x Sample Buffer (SB)	10ml	dH_2O
	10µl	0.5M Tris, pH 6.8
	20µl	10% SDS

	10µl	Glycerol
	1.543g	DTT
	0.1g	Bromophenol blue
SC^+ (supplement complete, in 1l RPMI)	1ml	β-Mercapto-ethanol
	20ml	Gentamycin
	23.83g	HEPES
	4g	L-Glutamin
	200ml	Penicillin/Streptomycin
SOC medium	100ml	SOB
	2ml	20% Glucose
4x Running buffer (2l)	24g	Tris
	115.2g	Glycine
	8g	SDS
5x TBE buffer (2l), pH 8.0	108g	Tris Ultra
	55g	Boric acid
	40ml	EDTA (0.5M)
10x Tris-Glycine (1l)	29g	Glycine
	58g	Tris

2.1.4 Gels

Running gel 10% (SDS-PAGE)	7ml	dH_2O
	4.38ml	1.5M Tris, pH 8.8
	5.8ml	30% Acryl 1% bis
	170µl	10% SDS
	8.8µl	Temed
	170µl	10% APS
Stocking gel (SDS-PAGE)	6.2ml	dH_2O
	2.5ml	0.5M Tris, pH 6.8
	1.2ml	30% Acryl 1% bis
	100µl	SDS
	5µl	Temed
	100µl	10% APS
Agarose gel 1.1%	0.45g	Agarose

40ml	1x TBE
1µl	Ethidium bromide

2.1.5 MHC multimers and peptides

The production of multimers of MHC class I and MHC-like molecules is routinely performed in the laboratory of Prof. Busch according to well-established protocols (Busch et al., 1998). The following multimers of non-classical MHC molecules of human and mouse NKG2D ligands were used: MICA-8, Rae1-γ, H60 and MULT1.

To stimulate TCR transgenic L9.6/RAG$^{-/-}$ mice antigen-specifically, the peptide p60$_{217\text{-}225}$ (KYGVSVQDI-COOH) (Affina Immuntechnik, Berlin) and the peptide-loaded MHC I molecule H2-K^{d}/p60$_{217\text{-}225}$ conjugated to artificial APCs were used.

2.1.6 Primers

Following primers were synthesized from TIB Molbiol (Berlin) and used for PCR out of cDNA samples:

Mouse:	NKG2D-S:	5’ TCCCTTCTCTGCTCAGAG 3’
		5’ TTACACCGCCCTTTTCATGCAGATG 3’
	NKG2D-L:	5’ CAGGAAGCAGAGGCAGATTATCTC 3’
		Second primer as for NKG2D-S (Diefenbach et al., 2002)
	β-Actin:	5’ TGCGTGACATCAAAGAGAAG 3’
		5’ GATGCCACAGGATTCCATA 3’ (Steuerwald et al., 1999)
Human:	NKG2D:	5’ CTGGGAGATGAGTGAATTTCATA 3’
		5’ GACTTCACCAGTTTAAGTAAATC 3’
	DAP10:	5’ CATCTGGGTCACATCCTCTT 3’
		5’ CAGAAGTCAAAGGTCCAAGC 3’ (Verneris et al., 2004)
	DAP12:	5’ CCGCAAAGACCTGTACGCCA 3’
		5’ TGGACTTGGGAGAGGACTGG 3’ (Karimi et al., 2005)
	β-Actin:	5’ GGCCACGGCTGCTTC 3’
		5’ GTTGGCGTACAGGTCTTTGC 3’ (Steuerwald et al., 1999)

2.1.7 Antibodies and second step reagents

Unless otherwise declared, all antibodies are directed against mouse antigens and have been titrated for optimal dilutions.

2.1.7.1 FACS and *in vitro* stimulation

Antibody/reagent	Clone	Supplier
Annexin V-FITC		BD Pharmingen, San Diego, USA
BrdU-FITC		BD Pharmingen, San Diego, USA
CD3ε	145-2C11	BD Pharmingen, San Diego, USA
Anti-human CD3	OKT-3	Hematology, TUM, München
CD4-FITC	RM4-5	BD Pharmingen, San Diego, USA
CD4-PerCP	RM4-5	BD Pharmingen, San Diego, USA
CD4-APC	RM4-5	BD Pharmingen, San Diego, USA
Anti-human CD4-FITC	RPA-T4	BD Pharmingen, San Diego, USA
CD8α-PE	5H10	Caltag Laboratories, Hamburg
CD8α-APC	5H10	Caltag Laboratories, Hamburg
Anti-human CD8-APC	HIT8a	BD Pharmingen, San Diego, USA
CD16/32 (Fc-block)	2.4 G2	BD Pharmingen, San Diego, USA
CD28	JJ316	BD Pharmingen, San Diego, USA
Anti-human CD79a-FITC	ZL7.4	AbD Serotec, Oxford, U.K.
Anti-human EMP3		Abnova Corp., Taipei City, Taiwan
Anti-human Fas	SM1-23	BenderMedSystems, Wien, Austria
Anti-human HSP70	OBT1688	AbD Serotec, Oxford, U.K.
IL-10	JES5-2A5	BD Pharmingen, San Diego, USA
NKG2D-PE	CX5	eBioscience, San Diego, USA
Anti-human NKG2D-APC	1D11	BD Pharmingen, San Diego, USA
NKG2D	C7	W. Yokoyama, St. Louis
NKG2D	A10	W. Yokoyama, St. Louis
PanNK-FITC	DX5	BD Pharmingen, San Diego, USA
Rat IgG1 isotype	R3-34	BD Pharmingen, San Diego, USA
Anti-hamster IgG-PE		BD Pharmingen, San Diego, USA
Anti-rabbit IgG-FITC		BD Pharmingen, San Diego, USA
SA-PE		Molecular Probes, Paisley, U.K.

SA-APC		Molecular Probes, Paisley, U.K.
TGF-β	1D1	BD Pharmingen, San Diego, USA

2.1.7.2 Westernblot

Antibody/reagent	Clone	Supplier
β-Actin	AC-15	SIGMA-Aldrich, Steinheim
Akt	5B5	Cell Signaling, Danvers, USA
Phospho-Akt	193H12	Cell Signaling, Danvers, USA
Cyclin A	H-432	Santa Cruz Biotech., Santa Cruz, USA
Cyclin B1	GNS1	Santa Cruz Biotech., Santa Cruz, USA
JNK1	C-17	Santa Cruz Biotech., Santa Cruz, USA
p21	F-5	Santa Cruz Biotech., Santa Cruz, USA
p27	C-19	Santa Cruz Biotech., Santa Cruz, USA
p44/42 MAP Kinase	3A7	Cell Signaling, Danvers, USA
Phospho-p44/42 MAP Kinase	E10	Cell Signaling, Danvers, USA
p53	CM1	Vision BioSystems, Newcastle, U.K.
p85α-PI3K	12929	Santa Cruz Biotech., Santa Cruz, USA
PLCγ-1	1249	Santa Cruz Biotech., Santa Cruz, USA
ZAP-70	LR	Santa Cruz Biotech., Santa Cruz, USA
Anti-mouse IgG + IgM-HRP		Dianova, Hamburg
Anti-rabbit IgG + IgM-HRP		Dianova, Hamburg

2.1.8 Reagents for the cDNA library

Additionally to the Lambda ZAP®-CMV Library Construction Kit following media and reagents were needed to prepare the cDNA library.

Alkaline agarose 2x loading buffer	200µl	Glycerol
	750µl	dH_2O
	46µl	saturated Bromophenolblue
	5µl	5M NaOH
10x Alkaline buffer	3ml	5M NaOH
	2ml	0.5M EDTA
	45ml	dH_2O

Nondenaturing acrylamide gel (5%)	16.6ml	30% Acrylamide
	62.7ml	dH_2O
	20ml	5x TBE buffer
	0.5ml	10% Ammonium persulfate
	50µl	TEMED
LB broth with supplements	1l	LB broth
	10ml	1M $MgSO_4$
	3ml	2M Maltose solution
NZY broth (1l), pH 7.5	5g	NaCl
	2g	$MgSO_4 \cdot 7H_2O$
	5g	Yeast extract
	10g	NZ amine
NZY agar (1l)	1l	NZY broth
	15g	Agar
NZY top agar	1l	NZY broth
	0.7% (w/v)	Agarose
SM buffer (1l)	5.8g	NaCl
	2g	$MgSO_4 \cdot 7H_2O$
	50ml	1M Tris-HCl, pH 7.5
	5ml	2% Gelatine
1x TAE buffer	40mM	Tris-acetate
	1mM	EDTA

2.1.9 Mice and hPBMCs

BALB/c and C57BL/6 mice were obtained from Harlan Winkelmann (Borchen). $DAP10^{-/-}$, $DAP12^{-/-}$ and $DAP10/12^{-/-}$ mice were housed at the animal facility at Washington University by Marco Colonna; $NKG2D^{-/-}$ mice were bred at the animal facility at Berkeley University by David Raulet. Spleens from $CD1d^{-/-}$ and $TCR\gamma\delta^{-/-}$ mice were obtained from H.W. Mittrücker (Max Planck Institute for Infection Biology, Berlin); L9.6/$RAG^{-/-}$ were provided by Eric Pamer (Memorial Sloan-Kettering, New York); MRL/lpr mice were made available by Bruno Luckow (LMU, München). $MHCII^{-/-}$ ($I\text{-}A\alpha^{-/-}$), $TLR4^{-/-}$, $MyD88^{-/-}$, and $IL10^{-/-}$ mice were derived from in-house breeding at the TUM under specific pathogen-free conditions.
Human PBMCs were prepared of blood samples of voluntary donors from the TUM.

2.1.10 Cell lines

Tumor cell lines HEK293, Phoenix, and CHO were maintained in $DMEM^+$; NKL cells were provided by Stefan Bauer (Marburg). For preparation of floating cells, formerly adherently growing Phoenix cells (150mm polystyrene tissue culture dish, Falcon BD, Franklin Lakes, USA) were cultured for three to four days in petri dishes (150mm polystyrene petri dish, Peske, Aindling-Arnhofen), which prevent a sticking of the cells to the surface, thereby generating floating cells. By thymidine excess synchronized 3T3 cells were kindly provided by Christine von Klitzing (TU München).
Polyclonal LLO_{91-99}-specific T cell line was expanded by *in vitro* peptide stimulation as described (Busch and Pamer, 1998).

2.2 Methods

2.2.1 Production of multimer reagents

A C-terminal biotinylation site was added to the extracellular domains of Rae1-γ, H60 (cDNA kindly provided by N. Shastri), MULT1 (cDNA kindly provided by W. Yokoyama) and MICA-8 by using standard PCR techniques on full-length cDNA. Recombinant biotinylated proteins were generated by using pET27b or pET3a expression vectors, expressed in *E. coli* BL21 Codon (DE3) plus, followed by an inclusion bodies purification and subsequent *in vitro* refolding procedures as described (Busch et al., 1998; Wolan et al., 2001). For multimerization, PE- or APC-conjugated streptavidin was added to the monomeric NKG2D ligands at an optimally titrated ratio (approximately 1:1) shortly before each experiment.

2.2.2 Spleen preparation

For staining or short term *in vitro* culture of naive splenocytes, approximately six to ten weeks old animals were sacrificed by cervical dislocation. Spleens were removed and single cell suspensions generated with the help of a syringe plunger by homogenization over a cell strainer into $RP10^+$ medium. After centrifugation (7', 1500rpm), the erythrocytes were lysed by ACT buffer (7', RT) and centrifuged again. In $RP10^+$-resuspended cells were then filtered over a nylon filter and counted.

2.2.3 Preparation of hPBMCs

For the preparation of human peripheral blood mononuclear cells (hPBMCs), blood of healthy individuals was mixed with an equal amount of PBS and separated from erythrocytes over a Ficoll-gradient (20', 1200g, RT, no brake). After washing, cells were resuspended in $RP10^{+}$, filtered, and counted.

2.2.4 FACS staining and flow cytometry

2.2.4.1 Antibody and multimer staining

For antibody and tetramer staining, about $2x10^{6}$ cells were used per sample and the staining was performed in 96 well plates. To block Fcγ receptors and for live/dead discrimination, cells were at first incubated for 20' under light in 100µl of Fc block (1:400) and EMA (1:2000) solution. Cells were then washed once with FACS buffer in a total volume of 200µl (2', 1500rpm) and incubated in 50µl of antibody mix (usually 1:100) in the dark on ice for 25', if only fluorescence-conjugated antibodies were used, or for 45', if also multimer-reagents were used. The samples were then washed three times with FACS buffer and fixed in 1% PFA or stained for another 20' followed by washing and fixation, if a secondary staining was needed. Until analysis on a flow cytometer (FACSCalibur or Cyan), cells were stored in the dark at 4°C. Analysis of raw data was performed using FlowJo software (Tree Star, Ashland, USA).

2.2.4.2 FACS sorting

In order to highly purify distinct cell populations, fresh splenocytes (as under 2.2.2) or cultured cells were stained on ice as $1x10^{7}$/100µl in FACS or $RP10^{+}$ (25' or 45' with multimers), washed three times and resuspended in $2x10^{8}$ cells per ml. Just before sorting with a MoFlo cytometer, cells were treated 1:1 with propidium iodide to allow live/dead discrimination. Fluorescence-positive and –negative cells were sorted directly into cold FCS.

2.2.4.3 Annexin and PI staining

To determine occurrence of apoptosis, cells were washed with PBS after surface staining without EMA as under 2.2.4.1, and stained with AnnexinV-FITC and the vital dye 7-AAD (15', RT) in Annexin binding buffer, followed by immediate flow cytometric analysis.

For analysis of cell cycle progression, living cells were surface stained without EMA as under 2.2.4.1, washed with FACS, resuspended in PBS, and fixed with 70% cold ethanol by dropwise addition while vortexing. After 1h on ice, cells were washed twice with PBS (2000rpm, 5'), treated for 5' with RNase A (1mg/ml) and stained with PI (50µg/ml) at 37°C for 15', followed by immediate flow cytometric analysis on the Cyan cytometer.

2.2.4.4 BrdU Analysis

To analyze cell proliferation and cell cycle status, BrdU can be incorporated into DNA instead of thymidine and identified by an anti-BrdU antibody. To achieve this, cell cultures were pulsed for 30-60' with 10µM BrdU in the incubator at 37°C. Cells were then washed once with 1% BSA/PBS, counted, and equal cell numbers per sample (usually $5x10^5$) were resuspended in 200µl PBS. For fixation, cells were added to 5ml 70% cold ethanol dropwise while vortexing and incubated 30' on ice. After centrifugation (500g, 10', 10°C), pellets were vortexed and 1ml 2N HCl/0.5% TritionX-100 was added dropwise while maintaining a vortex to denature the DNA. Cells were incubated for another 30' at room temperature, centrifuged and resuspended in neutralizing 0.1M $Na_2B_4O_7 \cdot 10H_2O$ (pH 8.5). Cells were washed once with 1ml 0.5% Tween-20/1% BSA/PBS and stained in 20µl 1:8 diluted anti-BrdU-FITC for 30' in the dark at RT. Cells were washed again, resuspended in 500µl PBS containing 0.5µg/ml PI and analyzed on the Cyan cytometer.

To chemically arrest cells in different cell cycle phases, cultures were treated with 1µg/ml cyclosporine (G1-arrest), 0.1µg/ml rapamycin (G1/S-arrest) or 0.5µg/ml nocodazole (G2/M-arrest).

2.2.5 CFSE proliferation assay and *in vitro* stimulation of splenocytes

For CFSE proliferation assays, murine splenocytes or hPBMCs prepared as under 2.2.2/2.2.3 were washed twice with PBS and labeled with CFSE (2.5µM) at $5x10^7$ cells per ml (10', 37°C). Staining was stopped by addition of cold $RP10^+$ and incubation for 5' on ice. Cells were washed twice with $RP10^+$ and counted again.

To stimulate splenocytes *in vitro*, $1x10^6$ CFSE-labeled or unlabeled cells were cultured in 500µl $RP10^+$ in 48 well plates with, or as a control without, 0.2µg/ml anti-CD3 mAb in the presence or absence of daily-added 20µg/ml NKG2D ligand multimer (equal to 10µg/ml NKG2D ligand monomer). Murine enriched $CD8^+$ and $CD4^+$ T cells were stimulated with plate-bound anti-CD3 (wells pre-incubated with 5µg anti-CD3/ml PBS), while hPBMCs were

either anti-CD3 (30ng/ml) stimulated or alternatively with PMA (20ng/ml)/Ionomycin (100ng/ml). Transgenic L9.6/RAG$^{-/-}$ CD8^{+} T cells were stimulated with their cognate epitope ($p60_{217-225}$, 1µM) or artificial APCs loaded with 1µg MHC (H2-K^{d}/$p60_{217-225}$)/10^{7} beads. NKG2D blocking experiments were performed by adding mAb A10 or C7 (10µg/ml) to the culture. Mediators of T cell suppression were tested with blocking or neutralizing mAbs for IL-10 (10µg/ml), TGF-β (50µg/ml) and Fas (2µg/ml). After three days of culture (usually 65-68h), cells were stained and analyzed as described under 2.2.4.

2.2.6 ^{3}H-Thymidine assay

Human PBMCs as described in 2.2.3 were stimulated in triplicates in 96 well plates at 1x10^{5} cells/100µl RP10^{+} with PMA (20ng/ml)/Ionomycin (100ng/ml) in the presence or absence of daily-added 20µg/ml NKG2D ligand multimer at 37°C. 1µl ^{3}H-thymidin (37MBq/ml) in 10 µl RP10^{+} was added after 48h and the assay was incubated for another 16h. Afterwards, cell-DNA was immobilized to a glass fiber filter with a cell-harvester and incorporated radioactivity was measured with a β-counter. Antagonist Fas (2µg/ml) mAb was added daily.

2.2.7 RNA isolation and RT-PCR

Two different RNA isolation methods have been used for this thesis.

For the isolation of high amounts of RNA, cell pellets were treated with TRI REAGENT™ (Trizol, Sigma) at 5-10x10^{6} cells/ml (5', RT). Thereafter, 0.2ml chloroform per ml TRI REAGENT was added, the samples were shaken vigorously for 15 seconds and allowed to stand for 2-15' at RT. The mixture was centrifuged (4000rpm, 30', 4°C), and the colorless upper aqueous phase containing RNA transferred to a fresh tube. RNA was precipitated by addition of 0.5ml isopropanol per ml TRI REAGENT and incubation (5', RT), followed by centrifugation (4000rpm, 1h, 4°C). The resulting RNA pellet was washed with 75% ethanol (≥1ml/ml TRI REAGENT; 4000rpm, 10'), briefly air-dried and resuspended in an appropriate volume of RNase free ddH_2O. The isolated RNA could further be enriched for mRNA with the help of an Oligotex mRNA Kit (Qiagen).

Another protocol of RNA isolation was used to obtain RNA for sequential PCR analysis. Total RNA was extracted with RNeasy Mini Kit (Qiagen). Equal amounts of RNA (1ng-5µg) were subjected to first-strand cDNA synthesis with SuperScript II Reverse Transcriptase (Invitrogen) as follows:

Oligo $(dT)_{12-18}$ primer (500µg/ml)	1µl
RNA	3µg (max. 10µl)
10mM dNTP Mix	1µl
RNase free ddH_2O	added to 12µl

The mixture was heated to 65°C for 5', chilled on ice, spun down and mixed with:

5x first-strand buffer	4µl
0.1M DTT	2µl
RNase OUT (Invitrogen)	1µl

The contents were incubated for 2' at 42°C. 1µl (200U) of SuperScript II was added and synthesis perfomed for 50' at 42°C, followed by heat inactivation (70°C, 15'). To remove residual RNA, cDNA products were treated with RNase H (Invitrogen; 37°C, 30').

2.2.8 PCR

To qualitatively measure mRNA transcript levels, cDNA products obtained from RT-PCR were subjected to PCR as follows:

10x PCR buffer	5µl
10mM dNTP Mix	0.5µl
Primer forward (diluted 1:10)	3.5µl
Primer reverse (diluted 1:10)	3.5µl
cDNA (from first-strand synthesis)	2-5µl
Taq-Polymerase	1µl
ddH_2O	ad 50µl

Taq-Polymerase was added after heating ("Hot Start") and two different PCR programs were used depending on the product size.

Program 1 (large products):	1	94°C	5'
30 cycles from 3-5	2	80°C	2'
	3	94°C	2'
	4	56°C	.0
	5	72°C	2' 30''
	6	72°C	5'
	7	4°C	.0
Program 2 (small products):	1	95°C	3'
30 cycles from 3-5	2	80°C	2'

3	95°C	15''
4	60°C	30''
5	72°C	30''
6	72°C	5'
7	4°C	.0

PCR products were analyzed on agarose gels.

2.2.9 Generation of cDNA-library

In order to identify the unknown H60/MICA-8 receptor, an expression library out of floating Phoenix cells, which were found to express the receptor, was generated with the help of the Lambda ZAP®-CMV XR Library Construction Kit (Stratagene). Total RNA was extracted from floating Phoenix cells with Trizol and mRNA was enriched via its poly(A) tail as described under 2.2.7. The basic steps are described in the following.

To synthesize first-strand cDNA

10x first-strand buffer	5µl
first-strand methyl nucleotide mix	3µl
linker-primer (1.4µg/µl)	2µl
poly(A)$^+$ RNA	5µg (max. 37.5µl)
DEPC-treated water	added to 50µl
RNase Ribonuclease Inhibitor (40U/µl)	1µl

were mixed in an RNase-free microcentrifuge tube and incubated for 10' at RT. A control reaction was performed with 5µg of test RNA. 1.5µl StrataScript RT (50U/µl) was added, the sample mixed, and 5µl of the reaction transferred to a separate tube containing 0.5µl of [α-^{32}P]dATP (800Ci/mmol) for the first-strand synthesis control reaction. After 1h incubation at 42C°, the samples were placed on ice and the radioactive control reaction was stored at -20°C.

For second-strand synthesis

10x second-strand buffer	20µl
second-strand dNTP mix	6µl
ddH_2O	114µl
[α-^{32}P]dATP (800Ci/mmol)	2µl
RNase H (1.5U/µl)	2µl
DNA polymerase I (9U/µl)	11µl

were mixed on ice with the first-strand reactions and incubated for 2.5h at 16°C. To blunt cDNA termini 23µl blunting dNTP mix and 2µl cloned *Pfu* DNA polymerase (2.5U/µl) were added to the second-strand reaction, vortexed and incubated (30', 72°C). The samples were then treated with 200µl phenol-chloroform (1:1), spun 2' at maximum speed, and the upper aqueous layer transferred to a new tube, followed by an identical chloroform extraction step. DNA was precipitated overnight at -20°C by addition of 20µl 3M sodium acteate and 400µl 100% (v/v) ethanol.

The next day samples were centrifuged (60', 4°C, 13.000rpm), the resulting pellet was washed by addition of 500µl 70% ethanol (2', RT, 13.000rpm), and dried by vacuum centrifugation, followed by resuspension in 9µl *Eco*RI adapters (30', 4°C). 1µl of this second-strand synthesis reaction was transferred to a separate tube and analyzed together with the first-strand control reaction on a 1% alkaline agarose gel by using the slide technique, where a small, thin gel is poured on a glass slide (3x7 cm), which can be analyzed after running with a phospho-imager. The remaining sample was ligated with *Eco*RI adapters by adding

10x ligase buffer	1µl
10mM rATP	1µl
T4 DNA ligase (4U/µl)	1µl

and incubating overnight at 8°C.

The next morning, the ligase was heat inactivated (30', 70°C) and the adapter ends were phosphorylated by mixing the following components:

10x ligase buffer	1µl
10mM rATP	2µl
sterile water	5µl
T4 polynucleotide kinase (5U/µl)	2µl

The reaction was incubated (30', 37°C), the kinase heat inactivated (30', 70°C), and digested (1.5h, 37°C) by adding 28µl *Xho*I buffer supplement and 3µl *Xho*I (40U/µl). Afterwards, DNA was precipitated overnight at -20°C by addition of 5µl 10x STE buffer and 125µl 100% ethanol. An overview of the cDNA synthesis steps is given in Figure 2 (Stratagene).

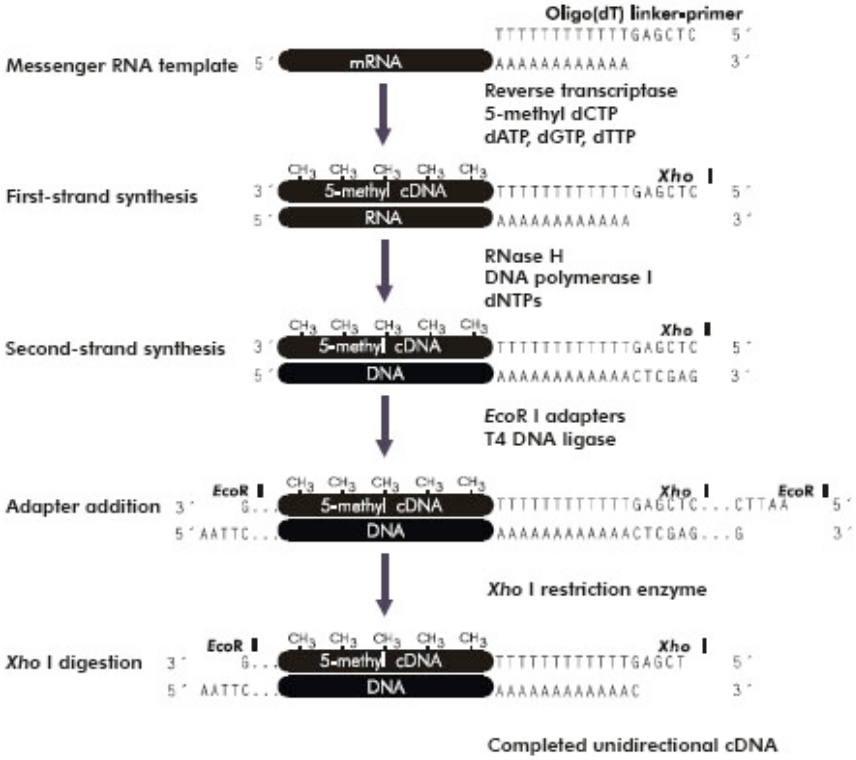

Figure 2: cDNA synthesis steps

The next day, the reaction was centrifuged (60', 4°C, 13.000rpm), and the dried pellet was resuspended in 14µl 1xSTE buffer plus 3.5µl column loading dye. A drip column was assembled by filling Sepharose CL-2B gel filtration medium together with 1x STE buffer air bubble-free in a 1ml plastic pipet connected on the top to a 10ml syringe serving as buffer reservoir. Into the tip of the pipet, a cotton plug was inserted to achieve a slower dripping of the column resulting in a better separation of the cDNA fractions. Thereafter, the column was equilibrated with 10ml 1x STE buffer before the cDNA sample was loaded into 50µl of remaining STE buffer above the surface of the resin. As the cDNA sample eluted through the column, the progress of the blue loading dye was monitored and three drops (~100µl) per fraction were collected, when the leading edge of the dye reached the -0.4ml gradation on the pipet. Fractions were continuously collected until the trailing edge of the dye reached the 0.3ml gradation. About 12 fractions were collected. 8µl of each fraction was removed and gelelectrophoresed on a 5% nondenaturing acrylamide gel followed by exposition to a phospho-imager to check the effectiveness of the size fractionation and to determine, which fractions would be used for ligation. The selected fractions were extracted with equal volumes phenol-chloroform and chloroform, and precipitated overnight with 100% ethanol at -20°C.

The next day, samples were centrifuged (60', 4°C, 13.000rpm), the resulting pellets were washed by addition of 200µl 80% ethanol (2', RT, 13.000rpm), and shortly dried by vacuum centrifugation. Using a handheld Geiger counter, it was verified that the cDNA had been recovered and the number of counts per seconds (cps) were recorded. cDNA pellets were resuspended, pooled in 5-10µl ddH_2O, and quantified by an ethidium bromide plate assay (0.8% agarose in 100ml TAE buffer, 5µl EtBr), where several standard DNA concentrations were spotted (10-200ng/µl) together with the sample, so that the concentration of the sample could be estimated by comparison with the standards. To ligate the obtained unidirectional cDNA to the Lambda ZAP-CMV XR vector, following components were mixed:

resuspended cDNA (~100ng)	Xµl (max. 2.5µl)
10x ligase buffer	0.5µl
10mM rATP	0.5µl
Lambda ZAP-CMV XR vector (1µg/µl)	1.0 µl
ddH_2O	ad 4.5µl
T4 DNA ligase (4U/µl)	0.5µl

A control ligation was set up by using 1.6µl test insert (0.4µg). The reaction was incubated overnight at 12°C or for up to two days at 4°C, and then packaged with the help of Gigapack III Gold Packaging Extract. 1-4µl of the ligation were added to a just thawing packaging extract, gently mixed and incubated (2h, RT). 500µl SM buffer were added, followed by 20µl chloroform. To determine the titer of the packaged ligation product, 1µl and 1µl of a 1:10 dilution of the reaction were mixed with 200µl XL1-Blue MRF´cells (grown in LB broth with supplements to an OD_{600} of 0.5; resuspended in 10mM $MgSO_4$), incubated (37°C, 15') and plated together with 3ml NZY top agar (~48°C) onto pre-warmed NZY agar plates. After 10' the plates were inverted and incubated at 37°C for 6-8h. Plaques were counted and the size of the primary library determined in plaque-forming units per ml (pfu/ml, should be 1-2x10^6 pfu/ml).

To amplify the primary library in order to produce a large, stable quantity of a high-titer stock, aliquots of the packaging reaction containing ~5x10^4 pfu bacteriophage were mixed with 600µl XL1-Blue MRF´cells (grown in LB broth with supplements to an OD_{600} of 0.5; resuspended in 10mM $MgSO_4$) in Falcon 2059 polypropylene tubes, incubated (15', 37°C), combined with 6.5ml NZY top agar (~48°C), and spread onto fresh 150mm NZY agar plates. Plates were inverted after 10' and incubated 6-8h at 37°C, until the plaques were touching and of about 1-2mm size. The plates were then overlaid with 8-10 ml SM buffer and incubated overnight at 4°C to allow the phage to diffuse into the SM buffer. Bacteriophage suspension

was pipetted from each plate and pooled in polypropylene container. Plates were rinsed with additional 2ml SM buffer, and chloroform was added to a 5% final concentration (15', RT). The cell debris was removed by centrifugation (500g, 10') and the supernatant transferred to fresh 50ml tubes. Chloroform was added to the clear supernatant at a 0.3% final concentration. Afterwards, the titer of the amplified library (~10^9-10^{11} pfu/ml) was checked using XL1-Blue MRF´cells and serial dilutions. Aliquots of the amplified library were stored in 7% DMSO at -80°C.

To allow screening of the phagemid library in eukaryotic cells by transfections, the library was mass excised. In a 50ml tube 10^7 pfu of amplified lambda phage (10- to 100-fold above the primary library size) were mixed with 10^8 XL1-Blue MRF´cells and 10^9 pfu of ExAssist helper phage, incubated (37°C, 15'), and enriched with 20ml LB broth with supplements, followed by incubation (2.5h, 37°C). Thereafter, the reaction was heated (20', 65-70°C) to lyse lambda phage particles and cells and centrifuged (1000g, 10'). Aliquots of the supernatant were combined with 200µl XLOLR cells and incubated (15', 37°C); then 40µl 5x NZY broth was added, incubated (45', 37°C), and the mixture was plated onto LB-kanamycin agar plates (50µg/ml) to obtain 200-500 colonies per plate (37°C, overnight). These colonies were pooled in LB medium, glycerol stocks were subsequently assembled, and plasmids were prepared with the QIAprep Miniprep Kit, leading to 600 cDNA pools each containing about 200-500 individual cDNA clones. A map of the obtained pCMV-Script® EX Vectors is depicted in Figure 3 (Stratagene).

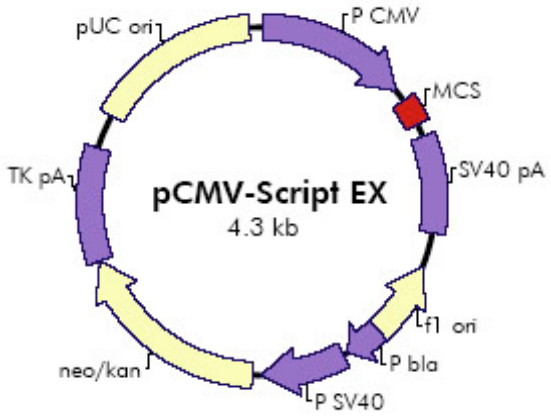

Figure 3: pCMV-Script EX Vector Map

To determine the representation of the library concerning insert size, plasmids were extracted from 18 single colonies and *Eco*RI/*Xho*I (Fermentas) control digested by using

mini prep DNA	2µl
5x buffer Tango (Fermentas)	2µl
*EcoR*I (10U/µl)	0.5µl
*Xho*I (10U/µl)	0.5µl
ddH_2O	added to 10µl

and incubating 1.5h at 37°C. Whole plasmids and digested plasmids were analyzed on agarose gels (1.1%).

2.2.10 Transfection of cell lines

To screen the generated cDNA library, H60/MICA-8 receptor negative cell lines, HEK293 and CHO, were transfected with the 600 cDNA pools by using ExGen 500 *in vitro* Transfection Reagent (Fermentas), a cationic polymer (polyethylenimine) reagent. For single transfections 1-2µl cDNA pool (~0.3µg) were diluted in 20µl 150mM NaCl and vortexed. 1µl ExGen 500 was added and immediately vortexed for 10 seconds. The mixture was incubated for at least 10' at RT; thereafter, 20µl were added onto $2x10^4$ the evening before transfection seeded cells (200µl in 96well plates). Plates were rocked from side to side, centrifuged (280g, 5'), and incubated for two days at 37°C. Transfected cells were either directly analyzed by staining with H60 or MICA-8 multimers for transient gene expression, or incubated in G418 selection medium (500µg/ml) for three weeks for stable transfections, followed by flow cytrometric analysis with H60 or MICA-8 multimers as described under 2.2.4.1.

For simultaneous analysis of all 600 cDNA pools, 38 groups of 16 pools à 1µl cDNA each were diluted in 320µl 150mM NaCl, 16.45µl ExGen 500 were added, vortexed, and incubated as described above; the mixture was pipetted onto $6.5x10^5$ the day before transfection seeded cells (3ml in 60mm plates). Afterwards, the 38 plates were incubated for two days at 37°C and either immediately pooled and stained with H60 multimers followed by repeated FACS sorting as described under 2.2.4.2 to enrich transfectants, or first treated for three weeks with G418 (500µg/ml) and then stained and sorted.

Transfection efficiency was controlled by transfecting with histidine- or human CD4-plasmids (in pET3a), and monitoring after two days expression of human CD4 by staining with hCD4 antibody. Efficiencies of 65-95% were yielded.

2.2.11 Westernblot

To analyze protein levels, cultured or sorted cells were lysed by adding lysis buffer, incubated for 15' on ice, and centrifuged (15', 13000rpm, 4°C); thereafter, supernatants were transferred to fresh tubes and stored at -80°C. Protein concentration was determined by using the BCA assay (Pierce). Equal protein amounts were treated with 2x Sample Buffer, boiled (5', 96°C), resolved on 10% SDS-PAGE, and transferred to nitrocellulose membranes by electrophoretic blotting (1.5h, 100V, 400mA, 4°C). The blots were washed once with PBS (5'), and unspecific binding was prevented by incubating the rocking membranes in blocking buffer (1h, 4°C). Primary antibodies were diluted (1:400-1:30.000) in blocking buffer and incubated overnight at 4°C rockingly. The next day, blots were washed with PBT (3x 5') and incubated with secondary HRP-conjugated antibodies diluted in blocking buffer (1:5000-1:7000, 1h, RT). Afterwards, blots were washed (3x 10' PBT, 2x 5' PBS), and proteins were detected with 5ml Western Lightning (PerkinElmer), followed by autoradiography. When using phospho-antibodies, blocking buffer with BSA was applied instead of milk powder. For analysis of different proteins (e.g. β-actin), blots were stripped after washing (1x 10' PBS, 2x 10' ddH_2O) with 0.2M NaOH (20-30'), washed again (2x 10' ddH_2O), and subsequently reprobed as described before.

2.2.12 Microarray analysis of gene expression

To analyze differential gene expression patterns of floating Phoenix cells versus adherent Phoenix cells, RNA of FACS sorted (2.2.4.2) either MICA-8 tetramer positive floating Phoenix cells or MICA-8 tetramer negative adherent Phoenix cells, was extracted with Trizol (2.2.7), and datasets were generated using standard Affymetrix Expression Analysis GeneChips HG U133 Plus2.0 (>50.000 probe sets) and HG U133 A 2.0 (>20.000 probe sets), which have been described previously (Lang et al., 2002; Schmitz et al., 2004). Cel files were normalized using RMAExpress (Irizarry et al., 2003) or dChip (Li and Wong, 2001).

2.2.13 Generation of monoclonal antibodies against Phoenix cells

In order to generate monoclonal antibodies against Phoenix cells, our collaborators in Croatia immunized a group of five mice with $5x10^6$ H60/MICA-8 receptor expressing floating Phoenix cells, as confirmed by FACS staining (2.2.4.1), in complete Freund's adjuvant (CFA) subcutaneously. A boost immunization was given after three weeks with the same number of

cells in incomplete Freund's adjuvant (IFA) subcutaneously and intraperitoneally. A final boost containing 10^6 cells in PBS was given intraperitoneally three days before fusion. Fusion was performed by classic protocol using PEG (polyethylene glycol) as fusion promoter. Shortly, spleen and myeloma (SP2/O-Ag 14) cells were mixed at a 1:1 ratio and fused by adding PEG. Fusion was plated on 20 plates in HAT (hypoxanthine-aminopterin-thymidine) containing medium, which was replaced every day. Fusion efficiency was tested after ten days in cell ELISA. Supernatants were collected, and the entire fusion was frozen at -80°C. Supernatants were screened for binding and/or blocking capacities against the H60/MICA-8-binding receptor by FACS analysis of MICA-8 tetramer staining on floating Phoenix cells in the presence of the hybridoma supernatants.

3 RESULTS

3.1 Generation of recombinant NKG2D ligands

As the expression of NKG2D ligands is upregulated upon various forms of cell stress, including transfection (Diefenbach and Raulet, 1999), we needed a clean, controlled system without any type of stress to be able to study precisely interactions of defined NKG2D ligands with their receptor(s). Therefore, we decided not to use cell lines transfected with NKG2D ligands; instead, we generated recombinant soluble molecules for all three types of murine NKG2D ligands, as well as for one common human MICA allele (MICA-8). Analogous to the recently described generation of soluble murine NKG2D (Wolan et al., 2001), we expressed the extracellular domains of Rae1-γ, H60, MULT1, and MICA-8 combined with a biotinylation site as inclusion bodies in bacterial hosts (Figure 4A and B); these were purified and subsequently *in vitro* refolded together with further purification steps, followed by a targeted C-terminal biotinylation.

Correct refolding and functionality of the proteins were confirmed by staining NKG2D receptor-expressing T cell lines with fluorochrome-labeled (SA-PE) NKG2D ligand multimers. As shown in Figure 4C, a murine antigen-specific $CD8^+$ T cell line (10 days after the last stimulation), which expresses NKG2D as verified by staining with NKG2D-antibody, bound all murine NKG2D ligand multimers with similar staining intensity. In contrast, no binding of human MICA-8 to this murine expressed NKG2D could be observed. The opposite pattern was detected, when a human $CD8^+$ T cell line was stained with the multimerized NKG2D ligands: only the human ligand bound to human NKG2D-expressing cells (Figure 4D). Although it has been found that murine NKG2D can bind to some human NKG2D ligands with different binding modalities (Steinle et al., 2001), our data suggest that the MICA-8 allele does not bind strongly enough to murine NKG2D to result in detectable tetramer staining.

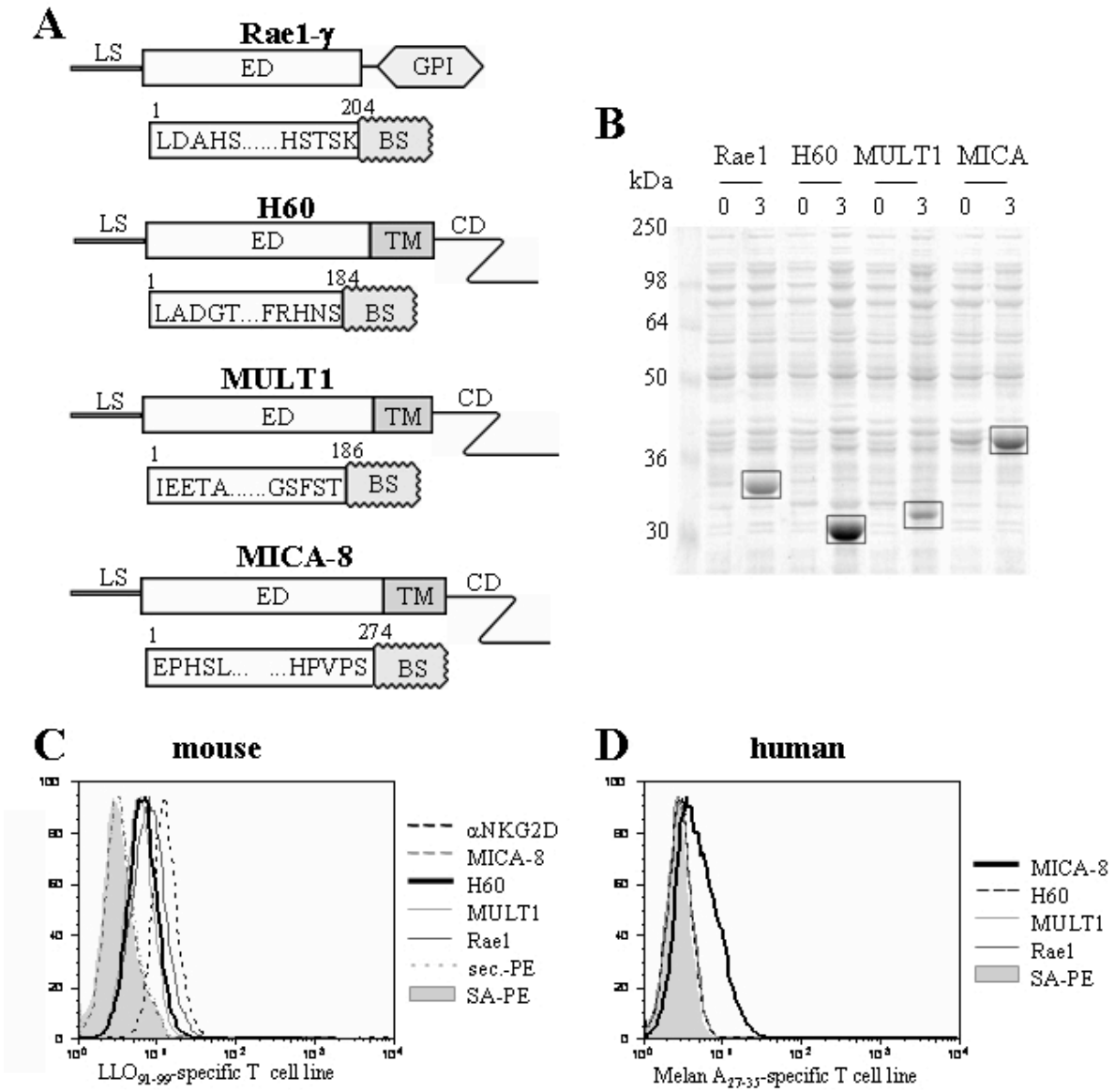

Figure 4: Generation of soluble NKG2D ligands

(A) *Schematic structure of NKG2D ligands from N to C terminus showing leader sequence (LS), extracellular domain (ED), transmembrane region (TM), and cytosolic domain (CD) or GPI-anchor. cDNAs were mutagenized at the positions indicated and a biotinylation sequence (BS) was added.* ***(B)*** *Expression of recombinant proteins in BL21(DE3) hosts. Samples before (0 h) and after (3 h) IPTG induction were run on a 10% SDS-PAGE. Murine* ***(C)*** *and human* ***(D)*** *antigen-specific $CD8^+$ T cell lines were stained with multimers of NKG2D ligands. Gray-filled histograms show control staining using streptavidin PE (SA-PE), and dotted gray lines show control staining with the PE-conjugated isotype-specific mAb used for visualization of anti-NKG2D (mAb C7) staining on murine cells.*

In addition, we tried to obtain some data on potential differences in relative binding affinities of murine NKG2D ligands for their receptor NKG2D. This was done by competition assays, where the concentration of one ligand was kept constant, whereas a second NKG2D ligand was added in increasing concentrations. The resulting data demonstrate clear differences between the ligands, showing much greater binding strengths of MULT1 and H60 to NKG2D than Rae1-γ (Figure 5), in accordance to data measured by other groups with BiaCore-based methods (Carayannopoulos et al., 2002a; Carayannopoulos et al., 2002b; O'Callaghan et al., 2001). In summary, these results indicate that all ligands were correctly refolded and can specifically bind to their species-matched NKG2D receptor molecules.

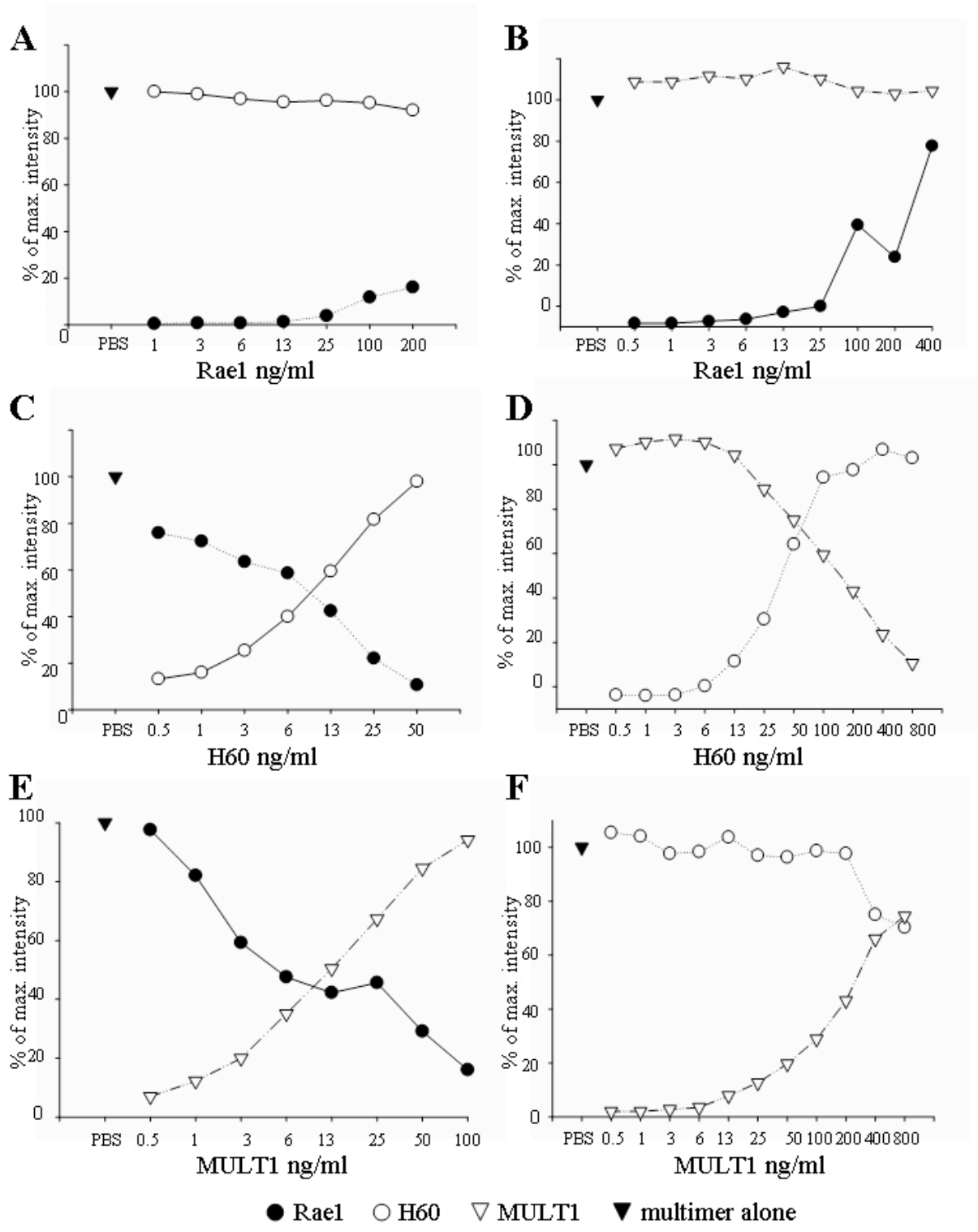

Figure 5: Relative binding affinities of NKG2D ligands for their receptor differ

(A and B) *Rae1-multimer ● was titratetd in the presence of H60 ○ (50 ng/ml, **A**) or MULT1 ▽ (50ng/ml, **B**) on a $CD8^+$ T cell line (LLO_{91-99} specific); changes in staining intensities were measured. (**C and D**) Same as in A, but H60-multimer was titrated in the presence of Rae1 (100 ng/ml, **C**) or MULT1 (50ng/ml, **D**). **(E and F)** Same as in A, but MULT1-multimer was titrated in the presence of Rae1 (100 ng/ml, **E**) or H60 (50ng/ml, **F**). ▼Multimer alone shows Rae1, H60 or MULT1 staining intensity in the absence of any other ligand.*

3.2 Distinct NKG2D ligands interfere with T cell proliferation

NKG2D has been described to mediate costimulatory signals upon ligand binding to $CD8^+$ T cells (Groh et al., 2001). In agreement with this interpretation, our group has measured a weak costimulatory influence of murine NKG2D ligand application on the sensitivity of target cell lysis by cytotoxic T cell lines (experiments performed by F. Gebhardt), observing identical results for all three ligands (Kriegeskorte et al., 2005). Surprisingly, when measuring T cell proliferation, we observed fundamental differences concerning NKG2D ligands, which had not been reported before.

3.2.1 H60 addition leads to inhibited proliferation of CD8 and CD4 T cells

We analyzed the effects of NGK2D ligands on lymphocyte proliferation by CFSE-dilution to daughter cells. CFSE-labeled bulk cultures of anti-CD3-stimulated splenocytes (C57BL/6 or BALB/c) were incubated in the absence or presence of NKG2D ligand multimers and their CFSE-profiles for $CD8^+$ and $CD4^+$ T cells were compared (Figure 6A and B). No costimulatory effect on T cell proliferation could be seen in the presence of Rae1 or MULT1, as cells proliferated as vigorously as control-treated (SA) cultures. In contrast, the application of H60 almost completely blocked $CD8^+$ T cell division (Figure 6A); comparable results were obtained, when additional CD28 costimulation was provided (Figure 6E). Surprisingly, also the division rate of $CD4^+$ T cells was strongly affected by H60 addition (Figure 6B), although NKG2D expression has only been described for rare T helper cell subsets (Groh et al., 2003; Groh et al., 2006; Saez-Borderias et al., 2006), but is absent from conventional $CD4^+$ T cells, as affirmed by reverse transcription PCR of the known NKG2D splice variants (Figure 6F). Furthermore, CFSE assays with plate-bound anti-CD3 stimulated, highly purified $CD8^+$ and $CD4^+$ T cells (Figure 6C and D), revealed still the same selective inhibitory effect in cultures treated with H60, but no other murine NKG2D ligand. When using cell lines “endogenously” overexpressing NKG2D ligands, similar to the recombinant proteins only H60 expressing cells inhibited T cell proliferation (experiments performed by F. Gebhardt), indicating that our findings are not restricted to recombinant proteins but also confer to native proteins.

Altogether, these results demonstrate that NKG2D ligands are not redundant but some of them (here: H60) are also potent suppressors of T cell proliferation. The inhibitory effects of H60 are detectable in *in vitro* stimulated bulk cultures as well as when using cultures of highly purified T cells, even with no measurable NKG2D expression.

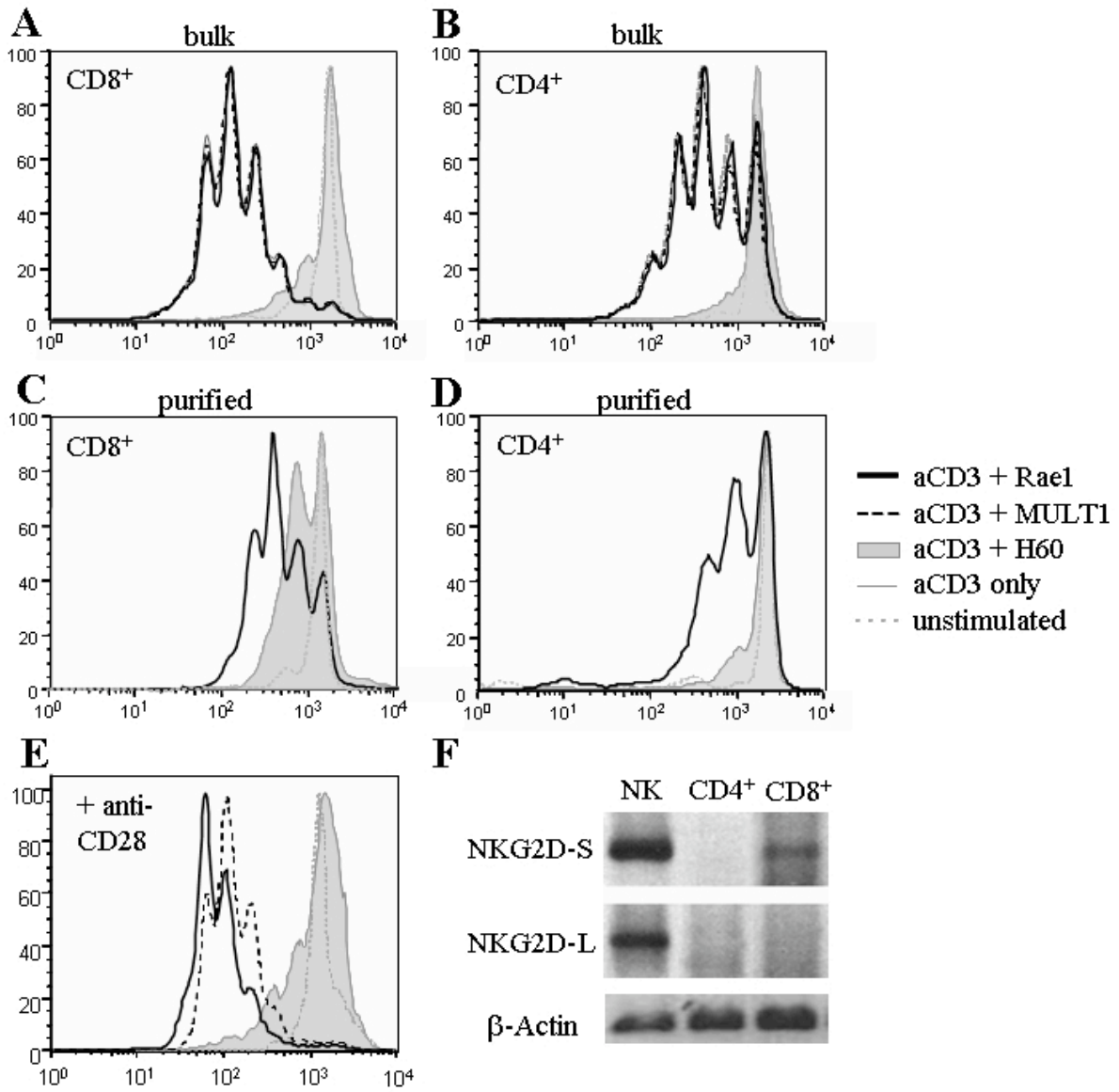

Figure 6: CD8$^+$ as well as CD4$^+$ T cells are specifically inhibited by H60

(A and B) *CFSE-labeled splenocytes (BALB/c) were analyzed 65h after stimulation with anti-CD3 in the presence or absence of different soluble NKG2D ligand multimers. For analysis, cells were gated on CD8$^+$* ***(A)*** *or CD4$^+$* ***(B)*** *T cells. Histograms represent cell divisions in the presence of Rae1 (bold line), MULT1 (dashes), H60 (filled gray), or no additional ligand as control; the dotted line indicates the CFSE profile in the absence of any stimulation.* ***(C and D)*** *Highly purified (>95%) CD8$^+$* ***(C)*** *and CD4$^+$* ***(D)*** *T cells were stimulated with plate-bound anti-CD3 under the same experimental conditions as in A and B.* ***(E)*** *Same settings as in A but in addition to anti-CD3 0.25µg/ml anti-CD28 mAb was provided.* ***(F)*** *Expression of NKG2D-S and -L splice variants was examined in highly purified NK cells and CD8$^+$ and CD4$^+$ T cells by RT-PCR. Loading control is shown by β-actin RT-PCR.*

3.2.2 Inhibition is independent of naturally occurring regulatory cells

Suppression of T cell proliferation is known as one of the characteristic effector functions of regulatory T cells (Treg). During the last years many different types of T cells with regulatory capacity have been described, as naturally arising $CD4^+CD25^+$ Tregs (Sakaguchi et al., 1985), antigen-induced regulatory T cells (Tr1; (Apostolou et al., 2002; Groux et al., 1997), and further subsets of NKT cells (Kronenberg and Gapin, 2002) and γδ T cells (Hayday and Tigelaar, 2003). We examined all these regulatory populations for responsiveness or selective binding to H60 and checked in cultures depleted of subpopulations or out of knockout mice deficient in these subpopulations for presence or absence of the inhibitory H60 effects. We found no involvement in H60-mediated suppressive effects for naturally arising $CD4^+CD25^+$ Tregs (with $MHCII^{-/-}$, Figure 7A), CD1d-restricted NKT cells (Figure 7B), or γδ T cells (Figure 7C), as T cell inhibition was as strong as in wildtype mice. To exclude possible LPS contaminations in the bacteria derived proteins, we determined endotoxin levels of the refolded NKG2D ligand proteins (below 0.1ng/ml) and measured proliferation of $MyD88^{-/-}$ (Figure 7D) and $TLR4^{-/-}$ (Figure 7E) splenocytes, which revealed no influence of TLR signaling on the observed phenotype. Also adding high LPS concentrations (500ng/ml) to the T cell cultures displayed no negative effect on the proliferation profile (Figure 7F). In order to examine the role of antigen-induced regulatory cells, we stimulated T cells from *Listeria*-specific TCR-transgenic mice on the $RAG^{-/-}$ background (L9.6tg/$RAG^{-/-}$, no T cells except from this one specificity) with their cognate epitope $p60_{217\text{-}225}$ (Figure 7G), and also further reduced the system by using FACS-sorted $CD8^+$ L9.6tg/$RAG^{-/-}$ T cells stimulated with artificial APCs (beads conjugated with H2-K^d/$p60_{217\text{-}225}$ complexes; Figure 7H). In these defined settings, where antigen-specific T cells are activated in an epitope-dependent fashion in the absence of any other cell population, T cells were still selectively inhibited by H60, suggesting that the regulatory effect can be indeed derived directly from antigen-specific T cell populations, without the “help” of any other additional cell population.

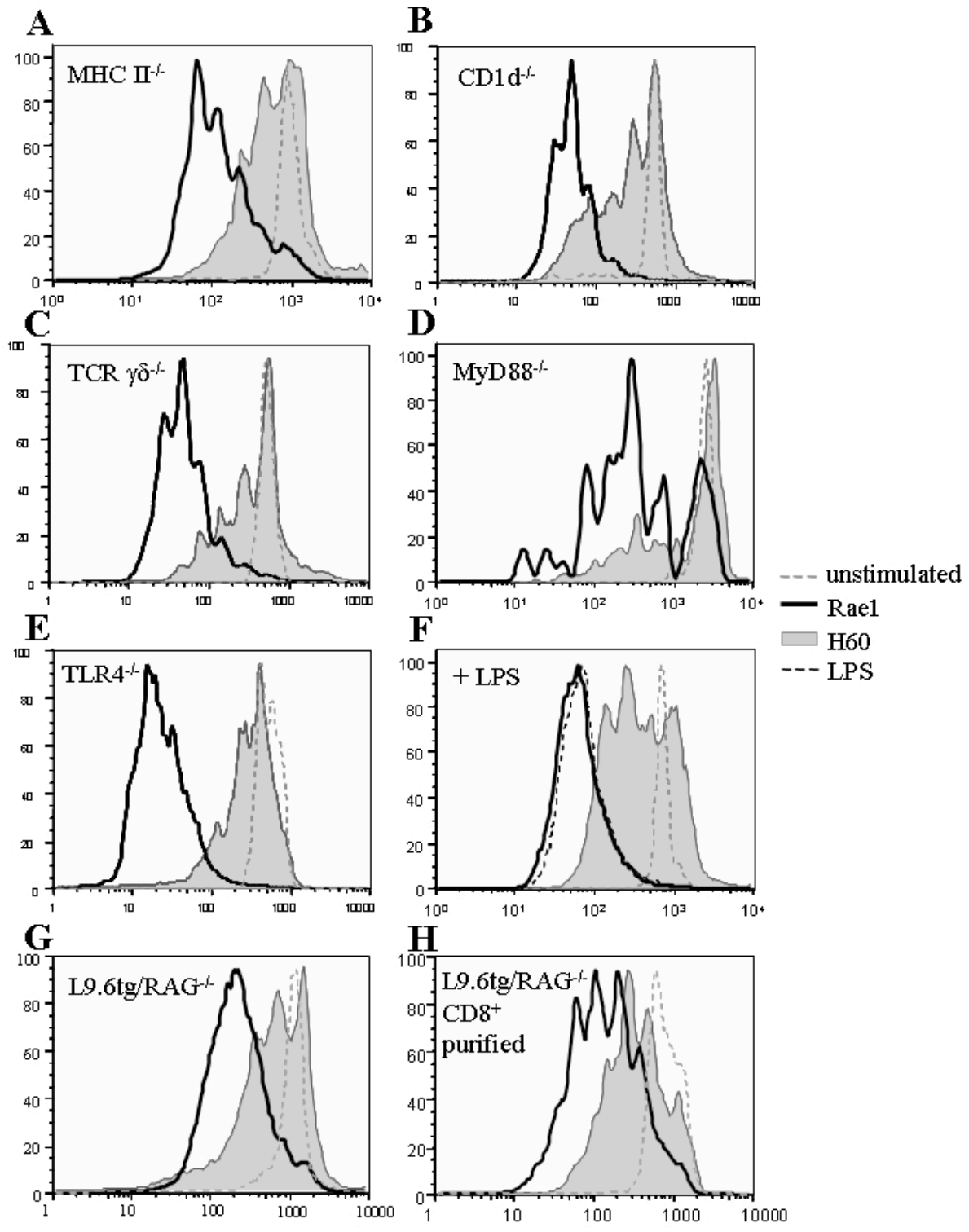

Figure 7: H60-mediated inhibition is independent of naturally arising Tregs

CFSE proliferation profiles of $CD8^+$ T cells upon anti-CD3 ***(A-F)****, peptide* ***(G)*** *or artificial APC stimulation* ***(H)*** *in the presence or absence of soluble NKG2D ligand multimers were determined as described in Figure 6. Histograms represent cell divisions in the presence of Rae1 (bold line) or H60 (filled gray); the dashed gray line indicates the CFSE profile in the*

absence of any stimulation. Splenocytes were derived from various gene-deficient ***(A-E)****, BALB/c* ***(F)*** *or transgenic mice* ***(G, H)****, as indicated at the top of each histogram.* ***(F)*** *Wildtype splenocytes were stimulated under addition of LPS (500ng/ml, long dashes).* ***(G and H)*** *L9.6tg/RAG$^{-/-}$ cells were stimulated in the presence of 1 µM p60$_{217-225}$ peptide* ***(G)*** *or purified for CD8^{+} T cells* ***(H)*** *and stimulated with artificial APCs (beads conjugated with H2-K^{d}/p60$_{217-225}$ complexes).*

3.2.3 Inhibition is dependent on IL-10, but independent of NKG2D

The observation that CD4^{+} T cells, although lacking NKG2D expression, can be substantially inhibited by the NKG2D ligand H60, led us to question the role of NKG2D in mediating these effects. DAP10 is the only known adaptor molecule for NKG2D signaling in T cells, and DAP10-deficient mice have been described to be devoid of NKG2D-mediated costimulation as well as NKG2D expression on CD8^{+} T cells (Diefenbach et al., 2002; Gilfillan et al., 2002). Most surprisingly, CD8^{+} and CD4^{+} T cells of DAP10$^{-/-}$ mice were as strongly inhibited as wildtype cells by addition of H60 multimers (Figure 8A). We further tried to block NKG2D with NKG2D-specific antibodies C7 (Figure 8B) or A10 (data not shown), but this treatment was not able to affect H60-specific suppression. Finally, the possibility to test NKG2D$^{-/-}$ mice (Figure 8C) in the laboratory of David Raulet (San Francisco, USA) revealed the same profound suppression level in mice with or without NKG2D. These observations demonstrate that H60-mediated inhibition of T cell proliferation occurs in a completely NKG2D-independent manner.

Antigen-induced Tr1 cells require IL-10 for their development, and their suppressive effects can be executed by secrection of inhibitory cytokines as IL-10 and TGF-β or also cell-contact-dependent mechanisms (Vieira et al., 2004). We applied neutralizing IL-10 or IL-10-receptor antibodies (Figure 8E and data not shown) to T cell cultures, but only minor effects on H60-suppression could be observed; similar results were obtained when using blocking TGF-β antibodies (data performed by F. Gebhardt). In addition, supernatants from H60-inhibited cultures did not transfer any detectable inhibitory effects onto primary T cells (data performed by F. Gebhardt). In contrast, splenocytes from IL-10$^{-/-}$ mice revealed almost complete unresponsiveness to the suppressive effects of H60 (Figure 8D). These data indicate that a mixture of executing effector functions, including cell-contact/IL-10/TGF-β-dependent mechanisms (like they are typical for Tr1 cells), contribute to the observed H60-mediated suppression of T cell proliferation.

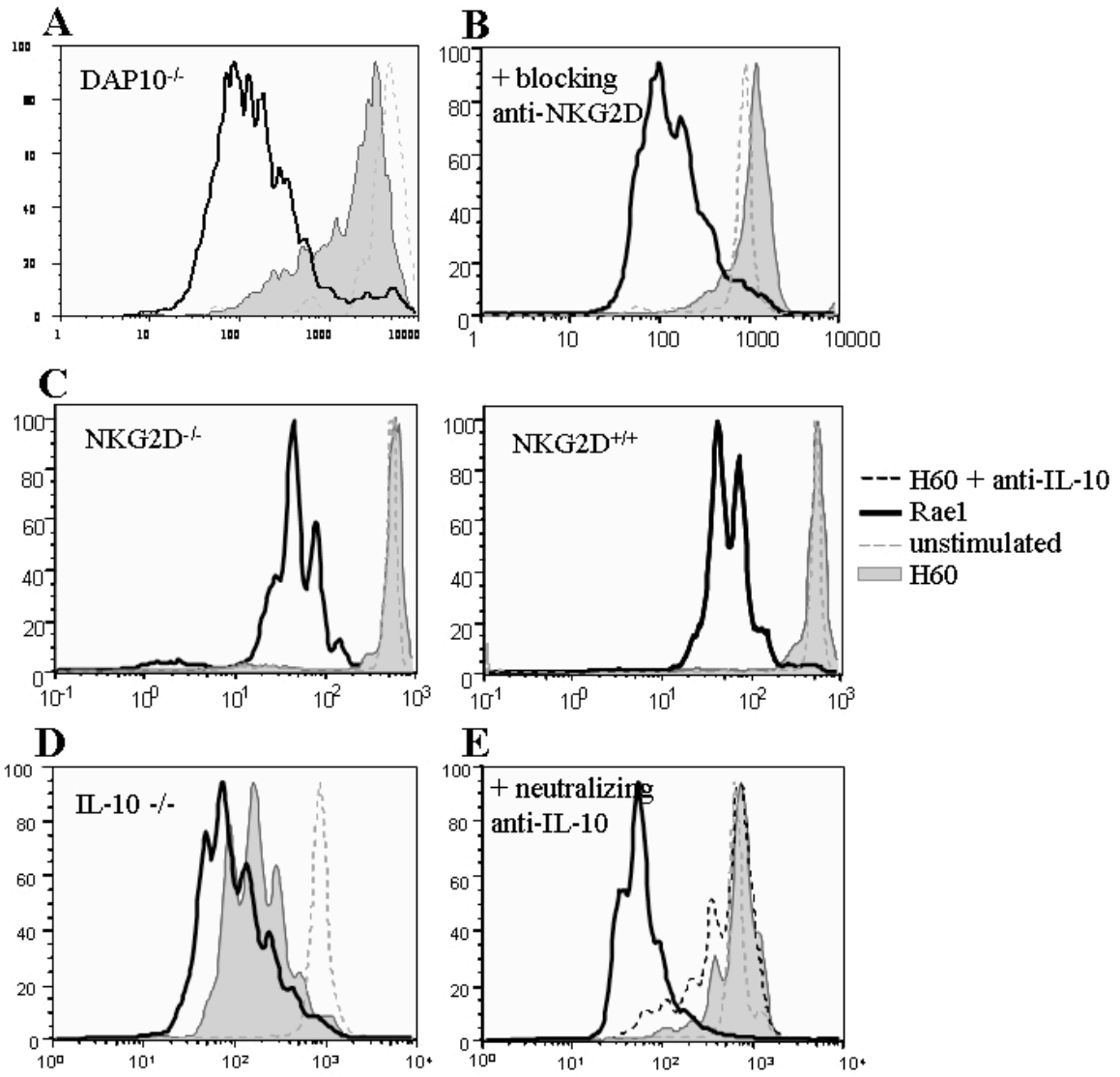

Figure 8: H60-mediated inhibition is independent of NKG2D, but dependent on IL-10

CFSE proliferation profiles of $CD8^+$ T cells upon anti-CD3 in the presence or absence of soluble NKG2D ligand multimers were determined as described in Figure 6. Histograms represent cell divisions in the presence of Rae1 (bold line) or H60 (filled gray); the dashed gray line indicates the CFSE profile in the absence of any stimulation. Splenocytes were derived from various gene-deficient ***(A, C left and D)*** *or wildtype mice* ***(B, C right and E)****, as indicated near the top of each histogram.* ***(B)*** *Summary of data obtained for splenocytes derived from wild-type BALB/c mice stimulated in the presence of high concentrations of blocking NKG2D mAb (clone C7).* ***(D, E)*** *Splenocytes derived from $IL10^{-/-}$* ***(D)*** *or wild-type* ***(E)*** *mice were stimulated in the presence or absence of H60; neutralizing anti-IL-10 antibody was added to wild-type cultures as indicated (dashed black line).*

During my diploma thesis, we performed a Biorad 8-Plex Assay with supernatants of CFSE cultures grown in the presence or absence of NKG2D ligands in order to determine cytokines possibly involved in the suppression. The measurements revealed elevated levels of IL-2 and IL-4 in H60-inhibited cultures, whereas at the same time the production of IFN-γ and IL-3 was strongly reduced (Kriegeskorte, 2003). Furthermore, addition of Rae1 as well as H60 resulted in higher secretion of MIP-1α and IL-12. All other tested cytokines as IL-1b, -5, -6, -17, GM-CSF, TNF-α, KC and Rantes, showed no significant differences. These preliminary data suggest that T cell inhibition by H60 is mediated by cells, which can be characterized by rapid secretion of IL-2 and IL-4, and that effector functions of T cells as IFN-γ production might be impaired in the presence of H60, further pointing to Tr1-like cells as executors of the H60-mediated inhibition.

3.2.4 Inhibition is cross reactive between man and mouse

As the murine and human NKG2D/ligand systems are rather homolog concerning the NKG2D receptor and *in vivo* functions, we further analyzed the effect of human NKG2D ligands on human T cells. We observed similar to the murine model a substantial reduction of proliferation of human PBMCs in the presence of human MICA-8 multimers (Figure 9A left). Surprisingly, application of the murine ligand H60 also inhibited human cells, whereas Rae1 and MULT1 had no effect on the proliferation of stimulated human T cells. A similar cross-reactivity was observed when MICA-8 was added to murine cells (Figure 9A right); MICA-8 was able to inhibit murine and human T cells like H60 (not always as strong).

As depicted in Figure 4, MICA-8 does not demonstrate any significant binding to murine NKG2D, but is able to inhibit murine splenocytes via a so far unknown receptor. We therefore tried to stain short-term activated T cells with MICA-8 multimers, which might have upregulated the unknown receptor. Indeed, substantial fractions (2-10%) of anti-CD3 stimulated $CD8^+$ and $CD4^+$ T cells could be stained with MICA-8 and H60 multimers (Figure 9B), and this staining could not be competed by blocking NKG2D antibodies (data not shown). A different staining pattern was observed with MULT1 multimers, which bound exclusively to NKG2D-expressing $CD8^+$ T cells. A combination of multimer staining with previously CFSE-labeled cells demonstrated that most of the MICA-8- and H60-binding cells have divided several times (Figure 9B lower panel). Highest absolute numbers of MICA-8-binding T cells were yielded early (day 3) after stimulation, whereas at later time points the staining decreased to background levels (> day 7, Figure 4C and data not shown), suggesting that the unknown receptor is strictly regulated during T cell activation, or that the MICA-8-

binding populations don't survive in the cell culture. Depletion experiments of MICA-8- and H60-binding cells before and during *in vitro* stimulation did not influence H60-mediated inhibition (Figure 9C), further indicating that the H60-responsive regulatory T cells are likely to be generated permanently out of conventional T cells during stimulation and expansion. In addition, as splenocytes derived from $IL10^{-/-}$ mice (Figure 8D) remained almost unresponsive to H60-mediated suppression, we measured MICA-8 multimer staining on *in vitro* stimulated $IL10^{-/-}$ cells (Figure 9D). MICA-8 multimer staining on $IL10^{-/-}$ lymphocytes never increased over background levels, again providing support that the MICA-8-positive populations are directly involved in our functional observations.

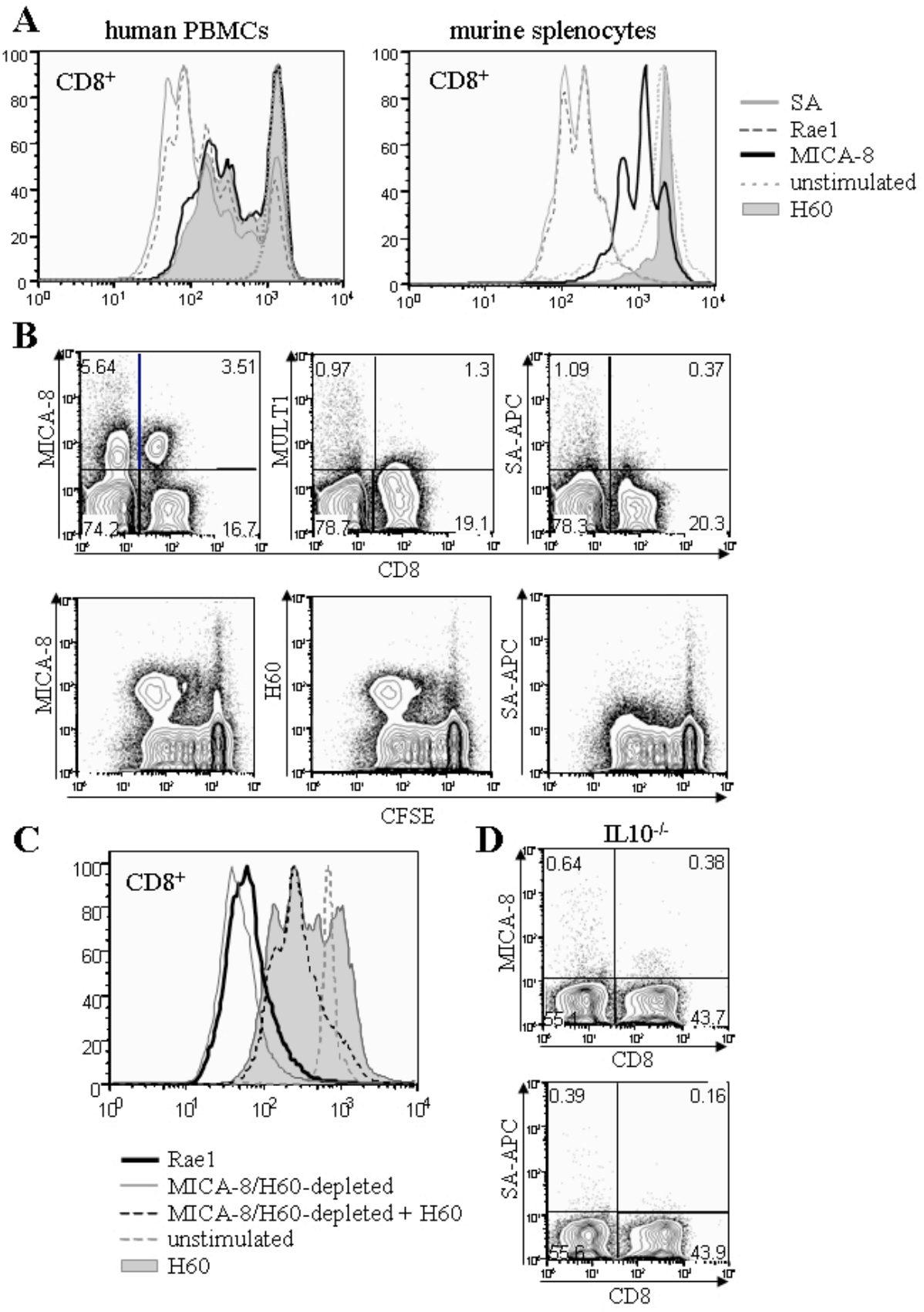

Figure 9: H60-mediated inhibition is cross-reactive between man and mouse

(A) *(Left) Freshly isolated CFSE-labeled human PBMC were stimulated with anti-CD3 in the presence or absence of soluble MICA (allele 8, bold line) or murine NKG2D ligands (H60, filled gray; Rae1, dashes), as described in Figure 6. As controls, cells stimulated only with anti-CD3 (thin gray line) or left unstimulated (dotted line) are shown. (Right) Murine splenocytes were used as responder cells under the same experimental settings.* ***(B)*** *(Upper panel) Splenocytes from wild-type mice were analyzed after short-term in vitro stimulation with anti-CD3. Dot plots of live lymphocytes are shown, with staining for CD8 (x axis) and NKG2D ligand/SA-APC multimers (y axis). As a control, cells were stained with SA-APC and CD8. (Lower panel) Under the same setting as in A, splenocytes were labeled with CFSE to monitor their proliferation profile in combination with staining for MICA multimers, H60 or SA-APC as a control.* ***(C)*** *Murine splenocytes as described in A were depleted daily of H60/MICA-8 binding cells by using H60/MICA-8 coated beads. H60/MICA-8 depleted cultures in the presence (long dashes) or absence of H60 (gray line) are shown together with cultures stimulated in the presence of H60 (filled gray), Rae1 (black line) or unstimulated cells (dashed gray).* ***(D)*** *Splenocytes derived from IL10$^{-/-}$ mice were treated as described under B, stainings for CD8 vs. MICA-8 or SA-APC control are shown.*

3.3 Generation of a cDNA library to identify the H60/MICA-8 binding receptor

As our data strongly indicated that MICA-8 and H60 can bind also to a receptor different from NKG2D and mediate via this receptor inhibitory signals, several approaches to identify the unknown receptor were anticipated.

3.3.1 Floating Phoenix cells bind specifically H60- and MICA-8-tetramers

During screening of several cell lines with H60 and MICA-8 multimers, we identified a HEK293 derivate, Phoenix cells, which can be selectively stained with H60 and MICA-8 multimers (Figure 10A left), but not with NKG2D mAb or MULT1 and Rae1 multimers. Interestingly, this staining pattern was not observed on normal adherently growing cells (Figure 10A right), but only when using “stressed” cells, which had been cultured for three to four days in petri dishes that prevent a sticking to the surface, in this way generating “floating” cells. Phoenix cells (or φ-Nx Helper-free Retrovirus Producer lines) are based on the 293T cell line (Kinsella and Nolan, 1996); they are a human embryonic kidney cell line transformed with adenovirus E1a and carry a temperature sensitive T antigen co-selected with

neomycin. Their unique characteristic is that they are highly transfectable with several transfection protocols; therefore, they are commonly used to generate libraries for retroviral gene transfer experiments.

HEK293 cells also seem to upregulate like the Phoenix cells the H60/MICA-8-binding receptor when grown in petri dishes (data not shown), but H60/MICA-8-staining intensity was highest with floating Phoenix cells.

3.3.2 Phoenix cells contain mRNA for DAP10 and DAP12 but not for NKG2D

To further confirm that H60/MICA-8-multimer staining does not correlate with NKG2D expression on these cells, we performed RT-PCR analysis on extracted RNA from Phoenix and HEK293 cells for human NKG2D. As Figure 10B clearly shows, no NKG2D product for Phoenix or HEK293 cells was generated, as a control the human NK cell line NKL was used. Furthermore, we measured mRNA levels of the NKG2D adaptor molecules DAP10 and DAP12 by RT-PCR to get more information on possible adaptor molecule dependency of the unknown receptor (Figure 10C). As all tested cell lines revealed products for DAP10 and DAP12 at various amounts, a possible association of DAP10/DAP12 with the unknown receptor could not be excluded. However, experiments using single DAP10-deficient (Figure 8A) and DAP12-deficient (Figure 10D) mice suggest a DAP10/DAP12-independent expression and functionality of the unknown receptor. To definitely rule out conceivable DAP10/DAP12 complementary effects, the usage of DAP10/DAP12 double-knock-out mice would be necessary; unfortunately, the T cell proliferation experiments with these mice failed, and we have at the moment no further access to these mice to ultimately answer this question.

In summary, $NKG2D^-$ Phoenix cells show a staining pattern specific for a H60/MICA-8-binding receptor, although we never observed a functional correlation like growth inhibition of Phoenix cells in the presence of H60 or MICA-8.

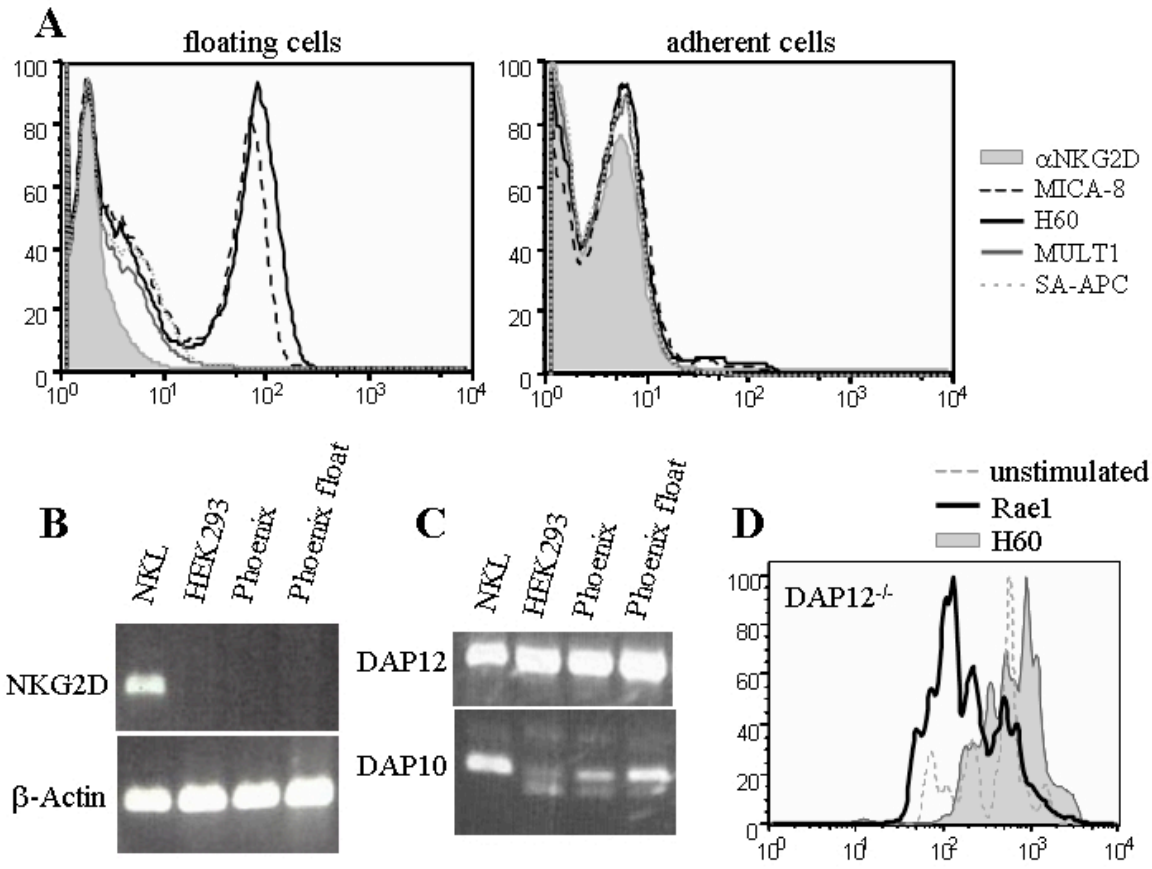

Figure 10: H60- and MICA-8 multimers are specifically bound by floating Phoenix cells

(A) *Floating Phoenix (4 days, left) and adherent Phoenix (right) cells were stained with multimers of NKG2D ligands or NKG2D mAb, as indicated in the legends. Dotted gray lines show background control staining using SA-APC.* ***(B and C)*** *Expression of NKG2D (417bp), DAP10 (306bp) and DAP12 (650bp) was examined in NKL, HEK293, Phoenix and floating Phoenix cells by RT-PCR. Loading controls were measured by β-actin (208bp) RT-PCR.* ***(D)*** *Splenocytes of DAP12$^{-/-}$ mice were short-term anti-CD3 stimulated in the presence of Rae1 or H60 or left unstimulated; CFSE profiles of CD8^{+} T cells are shown as described for Figure 8 (same symbols were used).*

3.3.3 Phoenix mRNA-isolation and synthesis of cDNA

As floating Phoenix cells apparently express the H60/MICA-8 receptor, we generated a cDNA expression library with the help of a commercially available kit from these cells. Large amounts of RNA were extracted from H60/MICA-8 multimer positive cells and mRNA was purified to yield optimal synthesis results. Figure 11A shows extracted RNA rich of ribosomal RNA and purified mRNA with little ribosomal RNA contamination. This mRNA was

subjected to first and second strand cDNA synthesis, and subsequently quality controlled by incorporation of radioactive [α-^{32}P]dATP, as depicted in Figure 11B. First and second strand synthesis samples without any secondary structure, corresponding to the entire size distribution of mRNA, incorporated the radioactive nucleotide, whereas radioactivity of 2nd strand synthesis is only 1/10 of 1st strand synthesis. After completion of unidirectional cloning of yielded cDNA fragments (*Eco*RI and *Xho*I digestion sites at 5' and 3' end, respectively, Figure 2), the cDNA was size fractionated to get rid of small fragments, encoding no genes and unincorporated radioactive nucleotides, as shown in Figure 11C. The amount of the remaining large cDNA products was quantified (~250ng, Figure 11D) and ligated into the Lambda ZAP-CMV XR vector.

3.3.4 Packaging, amplification and excision of the cDNA-library

Thereafter, the ligated cDNA fragments were packaged to lambda phages, the number of primary clones determined (2x10^6 pfu/ml), and amplified to about 1x10^{10} pfu/ml (Figure 11E). In order to allow screening of the library in eukaryotic cells, the library was mass excised, and plasmid DNA from the pCMV-Script® EX Vectors (Figure 3) containing the cDNA inserts was prepared from 600 cDNA pools, each consisting of 200-500 single clones. The representation of the library was controlled by digesting DNA of 18 single colonies with *Eco*RI/*Xho*I (Figure 11F), which revealed a good representation, as cDNA inserts of various sizes were excised, reaching from ~750-3000bp.

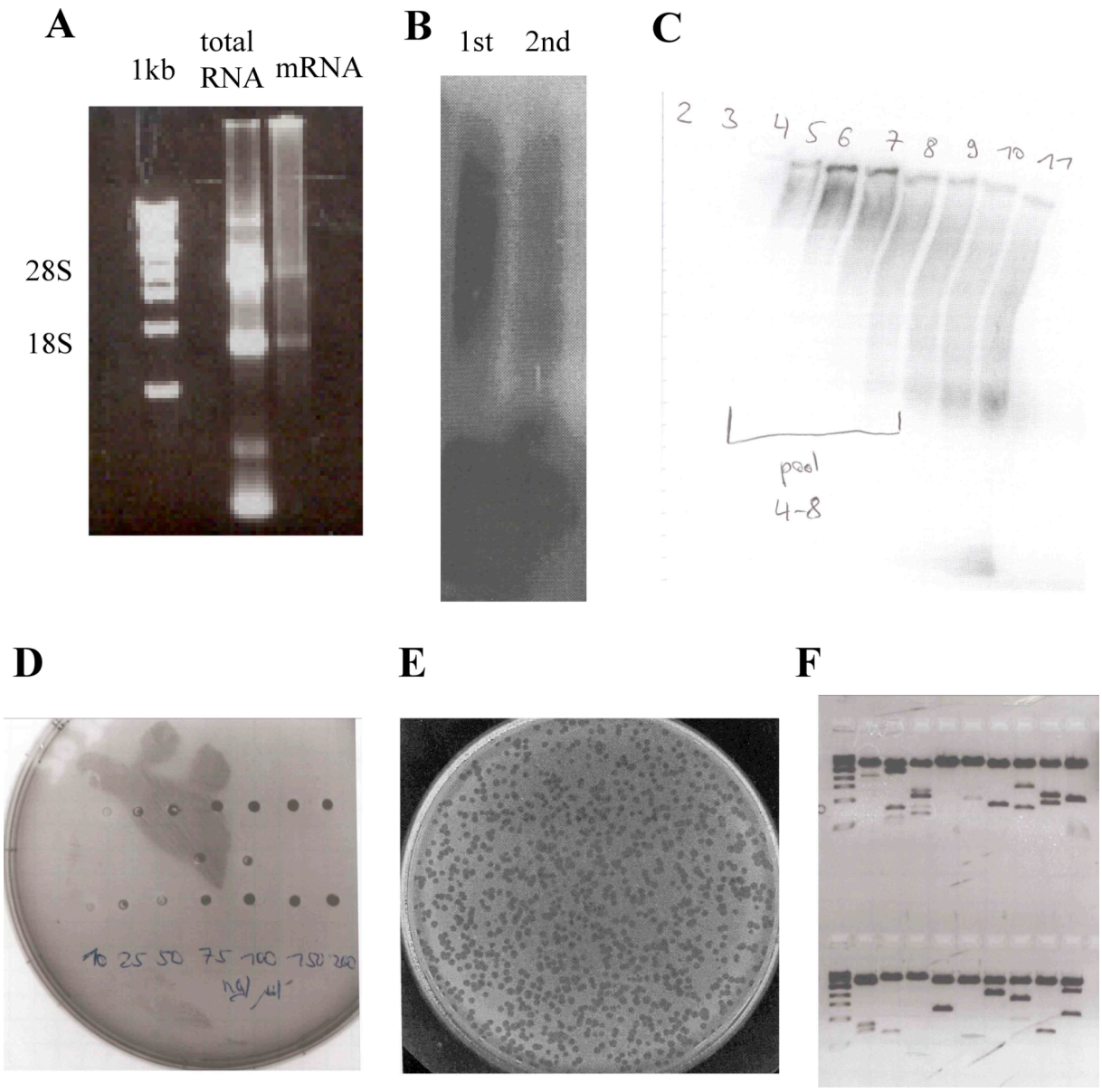

Figure 11: Generation of a cDNA library from floating Phoenix cells

(A) *Analysis of extracted total RNA and purified mRNA of floating Phoenix cells on an agarose gel. Size was controlled by 1kb ladder; ribosomal RNA of 18S and 28S as indicated.* ***(B)*** *Alkaline agarose gel of control of first and second strand synthesis reaction developed by a phospho-imager.* ***(C)*** *Phospho-imager analysis of a 5% nondenaturing acrylamide gel with fractions 2-11 from the size fractionation. Fractions 4-8 were pooled for further cloning.* ***(D)*** *Ethidium bromide assay to quantitate cDNA samples. Several standard concentrations were spotted (10-200ng/µl), so that the DNA amount of the unknown sample could be estimated (~50ng/µl).* ***(E)*** *Example of lambda phage plaques.* ***(F)*** *EcoRI/XhoI digestion of 18 single colonies analyzed on an agarose gel. Inserts of 750-3000bp were excised as depicted by the 1kb ladder.*

3.3.5 Screening of the cDNA library

Two different cell lines, CHO and HEK293, were transfected with the cDNA plasmid pools in order to identify the gene of interest. CHO cells were used because of high transfection efficiencies and minimal background staining due to their hamster origin. HEK293 cells, on the other hand, were used because of their close relationship to Phoenix cells and therefore the presence of potentially required adaptor molecules. Transfection efficiencies usually yielded 70-95% with both cell types (Figure 12A) as observed by transfecting with control plasmids encoding for human CD4 or Histidin. FACS analyses of transfected cells two days after transfections or after culture for three weeks in selective medium (G418) were performed with either using single cDNA pools in 96 well plates or using all 600 cDNA pools at once in 5cm culture plates. Figure 12B shows representative multimer (H60 or MICA-8) staining results on HEK293 cells transfected with single cDNA pools. Nearly all transfected cells show certain multimer binding with some reaching higher positive frequencies, which were never reproducible in further experiments. Transfection of CHO cells produced especially with MICA-8 multimer unexpected high background stainings, and also when mass transfections were repeatedly sorted, no stable positive signal was detected, sometimes even the negative controls exceeded potentially “positive” frequencies (Figure 12C). The once measured 3.5% MICA-8/H60 positive cells (Figure 12C) were probably caused by an artifact, as repetitive stainings never confirmed again these results. In summary, although performing extensive screening of the cDNA library in two different cell systems with both analyzing either transient or stable transfections, no positive plasmid pool could be identified for further subcloning of the wanted H60/MICA-8-binding receptor.

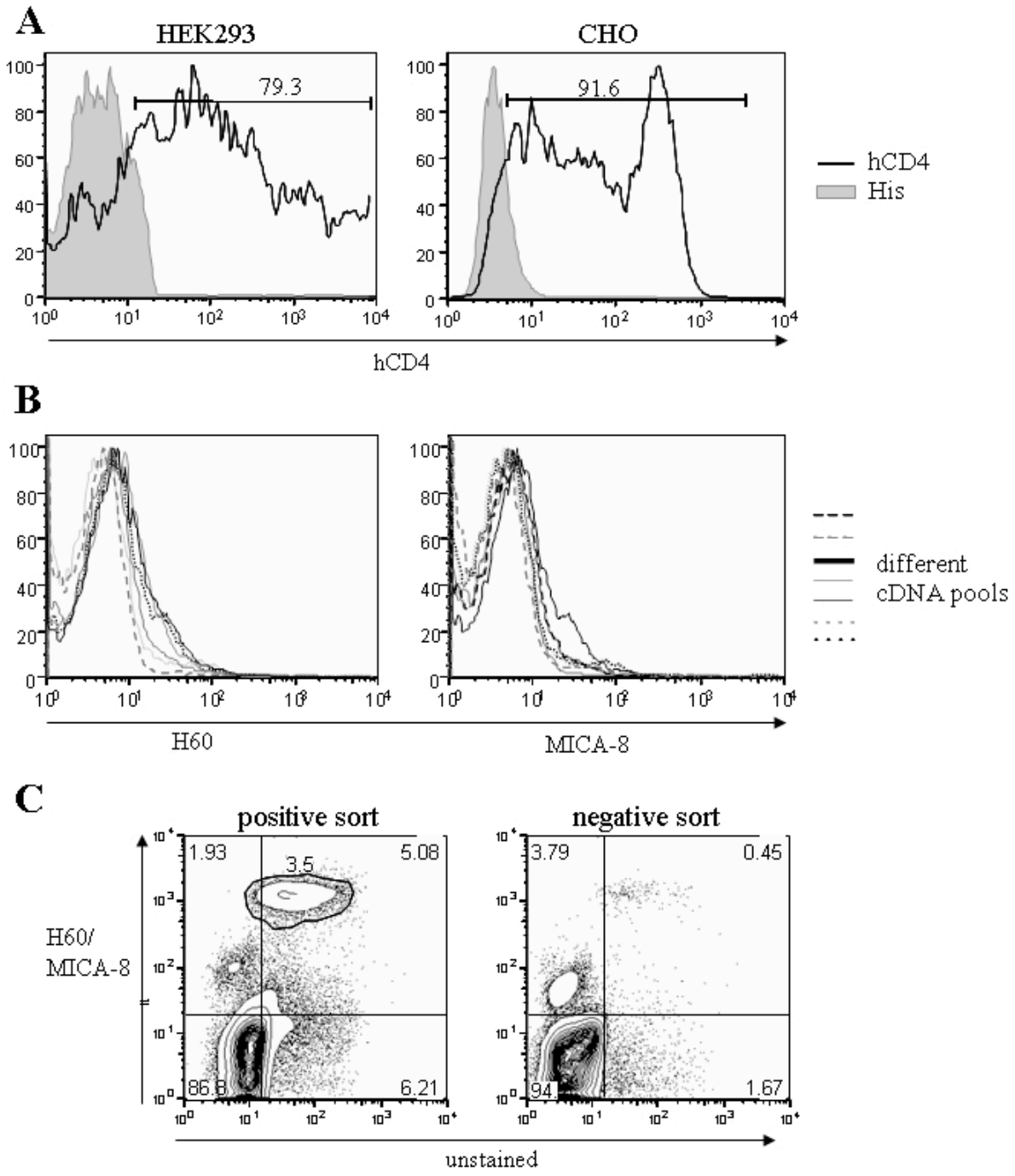

Figure 12: Screening of the cDNA library identified no positive clone

Representative FACS analyses of transfections with cDNA plasmid pools of HEK293 ***(A left and B)*** *or CHO* ***(A right and C)*** *cells are shown.* ***(A)*** *Transfection efficiency was measured by staining transfections with control plasmids hCD4 or Histidin with anti-CD4 mAb; efficiencies of hCD4 positive cells as indicated.* ***(B)*** *HEK293 cells were transfected with various single cDNA pools and stained after two days or after three weeks in G418-selective medium with H60 (left) or MICA-8 (right) multimers.* ***(C)*** *CHO cells were mass tranfected*

with all 600 cDNA pools; H60 or MICA-8 positive cells and negative control cells were repeatedly sorted, cultured in G418-medium and analyzed with H60/MICA-8 multimers.

3.4 Other approaches to identify the inhibitory receptor

As the cDNA expression library screen failed to find the inhibitory receptor, additional techniques were approached.

3.4.1 Affymetrix analysis of different growth forms of Phoenix cells

As floating Phoenix cells have upregulated the putative H60/MICA-8 receptor, whereas adherently growing Phoenix cells have not, we extracted RNA of MICA-8^{+}-sorted floating Phoenix cells and MICA-8^{-}- sorted adherent Phoenix cells. This RNA was used for Affymetrix microarray analyses using two different gene chips, HG U133 A 2.0 with more than 20.000 probe sets and HG U133 Plus 2.0 with more than 50.000 probe sets; the array was performed in collaboration with the Affymetrix Core Facility of Dr. Roland Lang at our institute. Both analyses detected about 22.000 differentially regulated hits (not all different genes, because of several probe sets for each gene). Quality controls by setting the fold change between floating Phoenix and adherent Phoenix to 1.5, as well as defining a maximum minus minimum value of at least 20, restricted the significantly differentially regulated genes to about 300. Table 2 shows combined the upregulated genes on both gene chips together with their individual fold change (FC).

Gene Title	FC	Gene Title	FC
1-acylglycerol-3-phosphate O-acyltransferase 7	1,737	influenza virus NS1A binding protein	2,182
3-hydroxy-3-methylglutaryl-Coenzyme A reductase	1,961	inhibitor of DNA bind. 2, dom. neg. helix-loop-helix prot.	2,143
3-hydroxy-3-methylglutaryl-Coenzyme A synthase 1	4,106	insulin induced gene 1	3,469
6-pyruvoyltetrahydropterin synthase	1,628	interleukin enhancer binding factor 3, 90kDa	1,575
7-dehydrocholesterol reductase	1,729	isopentenyl-diphosphate delta isomerase 1	2,195
A kinase (PRKA) anchor protein 8-like	2,024	Josephin domain containing 3	2,485
abl interactor 2	1,675	jumonji domain containing 1A	1,996
activating transcription factor 3	2,711	jun D proto-oncogene	1,955
acyl-Coenzyme A binding domain containing 3	3,117	karyopherin alpha 2 (RAG cohort 1, importin alpha 1)	1,767
acyl-Coenzyme A dehydrogenase, very long chain	1,760	karyopherin alpha 2 (RAG cohort 1, importin alpha 1)	1,635
acylphosphatase 1, erythrocyte (common) type	2,030	KDEL (Lys-Asp-Glu-Leu) ER protein retention rec. 2	1,604
ADAM metallopept. with thrombospondin type 1 m.	1,614	kelch-like 24 (Drosophila)	2,355
adiponectin receptor 1 /// adiponectin receptor 1	1,578	KIAA0174	1,550
ADP-ribosylation factor 1	1,769	KIAA0251 protein	1,837
ADP-ribosylation factor 4	1,543	KIAA0907	1,609

ADP-ribosylation factor GTPase activating protein 3	1,536	kinesin family member 20A	1,735
ADP-ribosylation factor-like 1	1,594	kinesin family member 22	1,524
adrenomedullin	1,559	kinesin family member 2C	1,728
annexin A2	1,872	Kruppel-like factor 6	1,782
antigen identified by monoclonal antibody Ki-67	2,611	La ribonucleoprotein domain family, member 6	1,844
ARP1 actin-related prot. 1 homolog A, centractin alpha	1,555	lectin, galactoside-binding, soluble, 3 (galectin 3)	1,537
ARS2 protein	1,624	LETM1 domain containing 1	1,582
aryl hydrocarbon receptor interacting protein	1,564	leucine rich repeat containing 59	1,603
ATPase, H+ transporting, lysosomal 34kDa, V1 sub. D	1,821	LUC7-like (S. cerevisiae)	1,666
ATPase, H+ transporting, lysosomal 9kDa, V0 subunit e	1,587	Lymphocyte-specific protein 1	1,594
ATP-binding cassette, sub-family B, member 7	1,654	makorin, ring finger protein, 1	3,071
ATP-binding cassette, sub-family F (GCN20), member 1	1,777	makorin, ring finger protein, 1	1,687
aurora kinase A	2,170	mannosyl-glycoprot. b-1,4-N-acetylglucosaminyltransfer.	1,543
basic helix-loop-helix domain containing, class B, 2	2,104	MAP/microtubule affinity-regulating kinase 4	1,697
B-cell translocation gene 1, anti-proliferative	1,727	membrane-associated ring finger (C3HC4) 5	1,732
bicaudal D homolog 2 (Drosophila)	1,759	membrane-associated ring finger (C3HC4) 6	1,712
bromodomain containing 2	1,807	metal response element binding transcription factor 2	1,617
BTAF1 RNA polymerase II, B-TFIID transcr. factor-ass.	1,682	metallothionein 1X	1,530
BTB (POZ) domain containing 3	1,560	metallothionein 2A	1,815
BTG family, member 3	2,198	microtubule-associated protein 1 light chain 3 beta	1,527
BUB1 budding uninhibited by benzimidazoles 1 hom.	1,973	mitochondrial ribosomal protein S30	1,823
C1q domain containing 1	1,830	M-phase phosphoprotein 9	1,565
CAAX box 1	1,635	myeloid cell leukemia sequence 1 (BCL2-related)	1,540
calcium modulating ligand	1,806	myeloid leukemia factor 1	1,613
calmodulin-like 4	1,797	myeloid leukemia factor 2	1,567
calumenin	1,883	myeloid/lymphoid or mixed-lineage leukemia	1,771
casein kinase 2, alpha 1 polypeptide	1,843	NADH dehydrogenase 1 beta subcomplex, 8, 19kDa	1,736
CD46 molecule, complement regulatory protein	1,685	nascent-polypeptide-associated complex alpha polypept.	7,727
CD59 molecule, complement regulatory protein	1,527	neutral sphingomyelinase 3 /// FLJ41352 protein	1,650
CDC23 (cell division cycle 23, yeast, homolog)	1,510	N-myc downstream regulated gene 1	1,964
CDC28 protein kinase regulatory subunit 1B	1,592	N-myristoyltransferase 1	2,101
CDC28 protein kinase regulatory subunit 2	2,895	nuclear factor, interleukin 3 regulated	1,865
CDC5 cell division cycle 5-like (S. pombe)	1,659	nuclear receptor subfamily 2, group C, member 1	1,650
CDC-like kinase 3	1,936	nucleolar and spindle associated protein 1	1,821
CDNA FLJ11904 fis, clone HEMBB1000048	1,587	nucleoside phosphorylase	1,940
centrosomal protein 57kDa	1,530	nudE nuclear distribution gene E homolog like 1	1,525
chemokine-like factor	1,586	nudix (nucleoside diphos. linked moiety X)-type motif 21	1,956
CHK1 checkpoint homolog (S. pombe)	1,537	oxysterol binding protein-like 2	1,714
choline kinase beta /// carnitine palmitoyltransferase 1B	1,599	peptidylprolyl isomerase G (cyclophilin G)	1,639
chromatin licensing and DNA replication factor 1	1,822	phosphatase and tensin homolog	3,845
chromosome 1 open reading frame 63	1,952	phosphatidylinositol glycan, class L	2,549
chromosome 16 open reading frame 61	1,866	phosphatidylserine receptor	2,266
Chromosome 19 open reading frame 42	1,537	phosphofructokinase, platelet	1,573
chromosome 20 open reading frame 111	1,604	pleckstrin homology domain contain., family A member 1	1,633
chromosome 20 open reading frame 44	1,528	poly (ADP-ribose) polymerase family, member 2	1,902
Chromosome 21 open reading frame 66	1,738	poly(A) polymerase alpha	1,786
chromosome 6 open reading frame 111	2,441	polycomb group ring finger 1	1,949
chromosome 6 open reading frame 75	1,691	potassium channel modulatory factor 1	2,048
chromosome 9 open reading frame 16	1,692	prefoldin subunit 5	1,805

chromosome X open reading frame 40A	1,790	proline rich 14	1,657
chromosome X open reading frame 40B	1,819	proline/serine-rich coiled-coil 2	1,604
cisplatin resistance-associated overexpressed protein	1,843	proteasome (prosome, macropain) subunit, alpha type, 1	1,526
coatomer protein complex, subunit beta	1,839	protein kinase, IFN-inducible ds RNA dep. activator	1,934
coatomer protein complex, subunit beta 2 (beta prime)	1,595	protein phosphatase 1, regulatory (inhibitor) subunit 15A	2,124
collagen, type IV, alpha 2	1,722	protein regulator of cytokinesis 1	1,595
COP9 constitutive photomorphogenic homolog sub.2	1,630	PRP3 pre-mRNA processing factor 3 homolog	1,643
cortactin	1,710	PRP4 pre-mRNA processing factor 4 homolog B (yeast)	2,434
craniofacial development protein 1	1,598	PRP4 pre-mRNA processing factor 4 homolog B (yeast)	1,812
CSAG family, member 2	1,526	PTK2 protein tyrosine kinase 2	1,687
CTTNBP2 N-terminal like	1,740	PTK9 protein tyrosine kinase 9	1,569
C-type lectin domain family 11, member A	1,847	putative nucleic acid binding protein RY-1	1,609
cyclic AMP phosphoprotein, 19 kD	3,022	Rab geranylgeranyltransferase, beta subunit	1,807
cyclin B1	1,724	RAB GTPase activating protein 1	1,566
Cyclin I	1,688	RAB11A, member RAS oncogene family	1,677
cyclin L1	2,152	RANBP2-like and GRIP domain containing 5	1,550
cyclin-dependent kinase inhibitor 2C (p18, inhib.CDK4)	1,580	ras homolog gene family, member B	2,545
cysteine and glycine-rich protein 2	1,580	receptor associated protein 80	1,868
cysteine conjugate-beta lyase; cytoplasmic	1,517	regulator of G-protein signalling 10	1,689
cysteine-rich, angiogenic inducer, 61	1,572	Rho GTPase activating protein 19	1,827
cytidylate kinase	1,567	ribosomal protein L10 /// similar to ribosomal prot. L10	1,647
cytoplasmic FMR1 interacting protein 1	1,553	ribosomal protein L13 /// similar to ribosomal prot. L13	1,740
DAZ associated protein 2	1,592	ribosomal protein L15 /// similar to rs protein L15	1,630
DDHD domain containing 2	1,566	ribosomal protein L17 /// similar to 60S rs protein L17	6,360
DEAD (Asp-Glu-Ala-Asp) box polypeptide 41	1,541	ribosomal protein L18	1,698
DEAD/H (Asp-Glu-Ala-Asp/His) box polypeptide 11	1,551	ribosomal protein L28	2,019
discs, large homolog 7 (Drosophila)	1,655	ribosomal protein L31	3,095
DNA segment on chromosome X and Y 155 expr. sequ.	2,231	ribosomal protein L36a-like	1,956
DnaJ (Hsp40) homolog, subfamily A, member 1	1,525	ribosomal protein L37a	2,000
DnaJ (Hsp40) homolog, subfamily B, member 1	3,940	ribosomal protein L5 /// similar to ribosomal protein L5	1,511
DnaJ (Hsp40) homolog, subfamily B, member 6	1,668	ring finger protein 4	1,541
DnaJ (Hsp40) homolog, subfamily B, member 9	1,589	ring finger protein 5	1,730
downstream neighbor of SON	1,527	RNA binding motif protein 15	2,755
dual specificity phosphatase 1	3,307	RNA binding motif protein 25	1,656
dynamin 1	1,779	S100 calcium binding protein A10	1,810
embryonic ectoderm development	1,766	Sec23 homolog A (S. cerevisiae)	1,589
enhancer of zeste homolog 1 (Drosophila)	1,543	SEC24 related gene family, member B (S. cerevisiae)	1,884
epithelial membrane protein 3	2,863	SEC31-like 1 (S. cerevisiae)	1,624
eukaryotic translation initiation factor 2-alpha kinase 1	1,521	serine/arginine repetitive matrix 1	2,271
eukaryotic translation init. factor 3, subunit 10 theta	1,620	SERTA domain containing 2	1,501
eukaryotic translation initiation factor 4A, isoform 2	1,580	SH3-domain GRB2-like endophilin B1	1,685
eukaryotic translation initiation factor 4E member 2	1,871	similar to splicing factor, arginine/serine-rich 4	2,256
far upstream element (FUSE) binding protein 1	1,706	similar to TFIIH basal transcript. factor compl. p44 sub.	1,981
farnesyl-diphosphate farnesyltransferase 1	2,198	Sin3A-associated protein, 30kDa	1,795
ferritin, heavy polypeptide 1	1,519	single-stranded DNA binding protein 1	2,809
ferritin, light polypeptide	1,794	SNW domain containing 1	1,605
fibronectin 1	1,575	solute carrier family 5 (inositol transporters), member 3	1,815
filamin A, alpha (actin binding protein 280)	1,593	sorting nexin 6	1,521
formin binding protein 4	1,541	sperm associated antigen 7 /// sperm associated antigen 7	1,532

fragile X mental retardation, autosomal homolog 1	1,889	spermidine/spermine N1-acetyltransferase	9,709
fragile X mental retardation, autosomal homolog 2	1,631	splicing factor proline/glutamine-rich	1,578
Full-length cDNA clone CS0DH006YD11 of T cells	1,849	splicing factor, arginine/serine-rich 14	2,118
GABA(A) receptor-associated protein like 1	2,295	splicing factor, arginine/serine-rich 4	1,751
GDP dissociation inhibitor 1	1,542	squalene epoxidase	2,695
general transcr. factor IIE, polypeptide 2, beta 34kDa	1,657	sterol-C4-methyl oxidase-like	3,891
general transcription factor IIH, polypeptide 5	1,541	stress 70 protein chaperone, microsome-associated, 60kDa	1,675
general transcript. factor IIIC, polypeptide 3, 102kDa	1,544	survival motor neuron domain containing 1	1,635
glutamate-ammonia ligase (glutamine synthetase)	2,081	SYF2 homolog, RNA splicing factor (S. cerevisiae)	2,257
golgi autoantigen, golgin subfamily a, 2	1,780	syndecan 2	1,612
golgi autoantigen, golgin subfamily a, 3	1,594	syntaxin 3	1,612
golgi autoantigen, golgin subfamily a, 4	1,826	TBP-like 1	1,614
golgi transport 1 homolog B (S. cerevisiae)	1,644	tetratricopeptide repeat domain 3	1,599
growth arrest and DNA-damage-inducible, alpha	1,797	TIA1 cytotoxic granule-associated RNA bind. prot.-like 1	1,760
growth arrest and DNA-damage-inducible, beta	1,867	TIMP metallopeptidase inhibitor 1	2,316
GTP cyclohydrolase 1 (dopa-responsive dystonia)	1,567	topoisomerase (DNA) II alpha 170kDa	1,867
Guanine nucleotide bind. prot., beta polypept. 2-like 1	3,546	TPX2, microtubule-associated, homolog (Xenopus laevis)	1,733
H2B histone family, member S	1,500	transcription elongation regulator 1	1,515
hairy and enhancer of split 1, (Drosophila)	2,064	transcription factor Dp-2 (E2F dimerization partner 2)	1,629
HCF-binding transcription factor Zhangfei	2,001	translocase of outer mitochondrial membrane 20 homolog	1,708
headcase homolog (Drosophila)	2,417	transmembrane protein 41B	1,600
heat shock 27kDa protein 1	1,648	tribbles homolog 1 (Drosophila)	1,708
heat shock 70kDa protein 1A	3,734	TTK protein kinase	2,668
heat shock 70kDa protein 1B	3,590	TNF receptor superfamily, member 12A	1,652
heat shock 70kDa protein 5	1,688	TNF superfamily, member 5-induced protein 1	1,576
heat shock 70kDa protein 8	1,822	ubiquitin-conjugating enzyme E2C	1,604
hepatitis B virus x interacting protein	1,601	ubiquitin-conjugating enzyme E2G 1 (UBC7 homolog)	1,555
heterogeneous nuclear ribonucleoprotein A1	6,817	unknown protein LOC51035	1,616
Heterogeneous nuclear ribonucleoprotein D	3,649	v-akt murine thymoma viral oncogene homolog 3	1,573
Heterogeneous nuclear ribonucleoprotein D-like	1,666	vesicle amine transport protein 1 homolog (T californica)	1,530
hexokinase 1	1,531	v-maf musculoaponeurotic fibrosarcoma oncogene hom. F	1,767
histidyl-tRNA synthetase-like	1,500	WAS protein family, member 3	1,589
histone 1, H2bk	1,743	Wolf-Hirschhorn syndrome candidate 1	1,598
histone 2, H2aa	1,973	YY1 associated protein 1	1,798
HLA-B associated transcript 1	1,547	zinc finger and BTB domain containing 43	1,684
hypothetical protein LOC92482	1,556	zinc finger and BTB domain containing 5	2,727
immediate early response 2	1,580	zinc finger protein 36, C3H type-like 1	1,666
immunoglobulin (CD79A) binding protein 1	2,023	zinc finger protein 451	1,822
importin 7	1,594	zinc finger, A20 domain containing 2	2,229

Table 2: Results of the microarray analysis of floating Phoenix vs. adherent Phoenix cells

Most of the upregulated genes are transcription factors or seem to be only expressed in the nucleus or intracellularly. Unfortunately, we couldn't filter the data for the presence of a transmembrane domain; this would have been a useful tool in finding a molecule, which is expressed on the surface. As no prominent gene with regulatory function was detected, we

selected three promising candidate genes for first experiments, CD79a, epithelial membrane protein 3 (EMP-3), and 70-kDa heat-shock protein (HSP70). CD79a, also known as Igα, is part of the B cell receptor and is required for surface expression and signal transduction of the BCR. EMP3 is described to be involved in cell proliferation, cell to cell interactions, and suggested to be a tumor suppressor gene in neuroblastoma and glioma (Alaminos et al., 2005). The third candidate, HSP70, belongs to the group of chaperones, which are expressed at high levels of cell stress, e.g. heat shock; it is involved in protein folding and unfolding, and has also been examined to play a role as mitogen for B and T cells (Aosai et al., 2002; Haug et al., 2005). We examined a potential influence on the staining intensity of MICA-8- and H60-multimers on floating Phoenix in the presence of commercially available antibodies against these three candidate proteins (Figure 13A-D), but we detected no significant decrease or increase in staining intensities, which could have pointed to an interference with the same receptor. Surface staining of CD79a, EMP3 and HSP70 revealed a different pattern (Figure 13E). While no specific staining could be yielded with the CD79a and EMP3 antibodies, HSP70 stained brightly on floating Phoenix cells, whereas on adherent Phoenix cells no specific staining at all could be measured (Figure 13F). A double staining with the NKG2D ligand tetramers showed that exactly the same population within the floating Phoenix cells (about 50%) expresses HSP70 and the H60/MICA-8-binding receptor (Figure 13G), suggesting that HSP70 could be the H60/MICA-8 receptor.

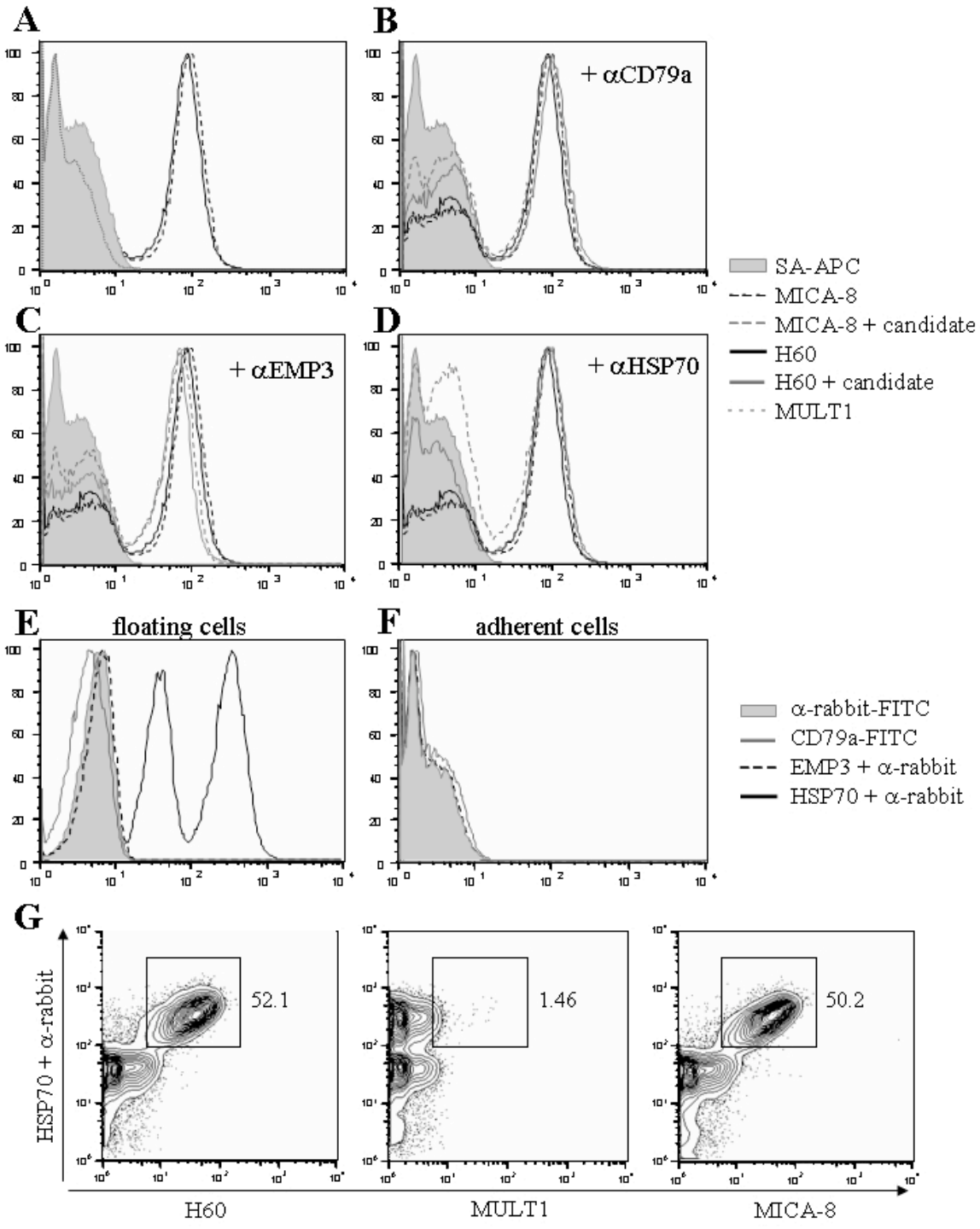

Figure 13: HSP70-antibody binds to the same population as H60 and MICA-8

(A-D) *Floating Phoenix cells were stained with MICA-8 (dashed black), H60 (black line) or MULT1 (dotted gray) multimers; the filled gray histogram shows background control staining using SA-APC.* ***(B-D)*** *In addition to A, MICA-8 (dashed gray) and H60 (gray line) multimer stainings are shown in the presence of antibodies against CD79a* ***(B)****, EMP3* ***(C)*** *and HSP70* ***(D)****.* ***(E)*** *Floating Phoenix cells were stained with anti-CD79a-FITC (gray line), anit-EMP3 plus anti-rabbit-FITC (dashed black) or anti-HSP70 plus anti-rabbit-FITC (black line); the*

filled gray histogram shows background control staining using secondary antibody anti-rabbit-FITC alone. ***(F)*** *Same staining as in E but performed on adherent Phoenix cells.* ***(G)*** *Double staining of anti-HSP70 plus anti-rabbit-FITC and NKG2D ligand multimers H60, MULT1 and MICA-8 as indicated on floating Phoenix cells.*

Further analyses have to be approached to confirm or reject the finding, e.g. by cloning the gene for HSP70 and testing it in transfection experiments for multimer-binding, by using blocking reagents against HSP70, or by small interfering RNA (siRNA) approaches. If HSP70 proves not to be the wanted H60/MICA-8 receptor, the other candidates will have to be systematically tested in the same way.
In summary, the microarray data detected several differentially upregulated genes in floating Phoenix cells in comparison to adherent Phoenix cells; we have identified several candidate genes with HSP70 being the most promising one for the H60/MICA-8 receptor.

3.4.2 Generation of monoclonal antibodies against Phoenix cells

By generating monoclonal antibodies specific for the H60/MICA-8 receptor, we expect to receive a potent reagent for subsequent precipitation approaches of receptor-antibody complexes, which could lead to the identification of the unknown receptor. In addition, blocking antibodies against the receptor could be used to study the inhibitory mechanism on the molecular level. Most importantly, they could provide us with an essential tool to be able to therapeutically intervene inhibitory mechanisms of NKG2D ligands in tumor settings. Therefore, we started a collaboration with Stipan Jonjic in Rijeka, Croatia. His group immunized mice three times with floating Phoenix cells together with CFA as adjuvant and fused then efficiently spleen cells with myeloma cells. They received about 2000 hybridomas, whose supernatants we are currently testing for their specific binding on the floating Phoenix cells together with potential blocking capacities of the H60/MICA-8 binding on the floating Phoenix cells.

3.4.3 Mass spectrometric analysis of membrane protein complexes

The observation, that not only multimeric H60 and MICA-8 can bind specifically to floating Phoenix cells, but that the receptor/ligand binding affinity is also with their monomeric forms high enough to result in a stable staining (Figure 14), offered us the possibility to try to pull-down the receptor with soluble MICA-8 or H60.

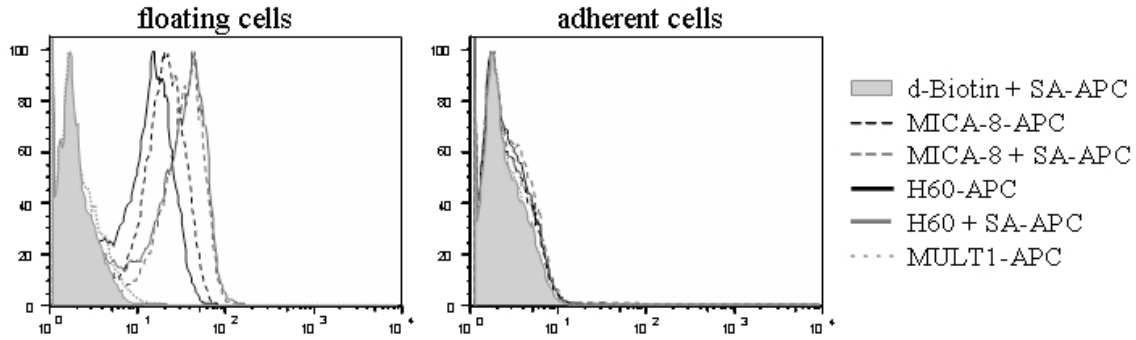

Figure 14: Monomeric H60 and MICA-8 bind stably to floating Phoenix cells

Floating Phoenix cells (left) or adherent Phoenix cells (right) were stained directly with multimeric NKG2D ligands MICA-8 (dashed black), H60 (black line) or MULT1 (dotted gray), or in two steps with first monomeric NKG2D ligands MICA-8 (dashed gray) or H60 (gray line), followed by a secondary staining with SA-APC; the filled gray histogram shows background control staining using d-Biotin and SA-APC.

In collaboration with Marius Üffing, GSF Neuherberg, we try to separate the membrane-integrated protein complex of the unknown receptor with the soluble ligand, whose composition can be determined by mass spectrometric analyses afterwards. By this approach we could not only identify the H60/MICA-8 receptor, but also detect possible receptor-associated adaptor molecules, which could be of unutterable value for the cDNA transfection experiments. First receptor/ligand precipitations are currently under investigation.

3.5 Characterization of the H60-induced cell cycle arrest

We further analyzed the nature of the H60- (and MICA-8-) induced growth inhibition, since this might give us additional insights into the underlying signaling pathway(s).

3.5.1 H60-mediated inhibition is reversible and independent of Fas

A key question was, if H60-mediated inhibition triggered cell death or rather growth arrest. A recent publication has observed an NKG2D ligand-dependent depletion of T cells caused by Fas/Fas-L interaction with $NKG2D^{+}CD4^{+}$ T cells (Groh et al., 2006). In contrast to their observations, we measured no increase in apoptotic cells (Annexin-V single positive) in the presence of H60 or MICA-8 in comparison to the presence of MULT1 or SA-control (Figure

15A), and only slightly higher frequencies of dead cells (Annexin-V/7-AAD positive), probably due to lower cell numbers in H60-treated cultures. By culturing CFSE-labeled splenocytes for three days together with NKG2D ligands, followed by vigorous washing and continued culture for another three days without any further addition of NKG2D ligands (Figure 15B), we confirmed that H60-inhibited T cells don't die, but subsequently proliferate as vigorously as control cells, when the negative signal by H60 multimers is removed. To exclude Fas/Fas-L interaction in our system, we stimulated splenocytes of MRL/lpr mice, which carry a dysfunctional Fas gene, under addition of NKG2D ligands. The lpr mutation in these mice causes a defect in Fas, which leads to a spontaneous autoimmune disease at about the age of 12 weeks similar to lupus erythematosus. We tested several MRL/lpr mice at different age, and observed at least in young animals (up to 6 weeks) a strong H60-mediated suppression as in BALB/c mice (Figure 15C), indicating a Fas independent mechanism.

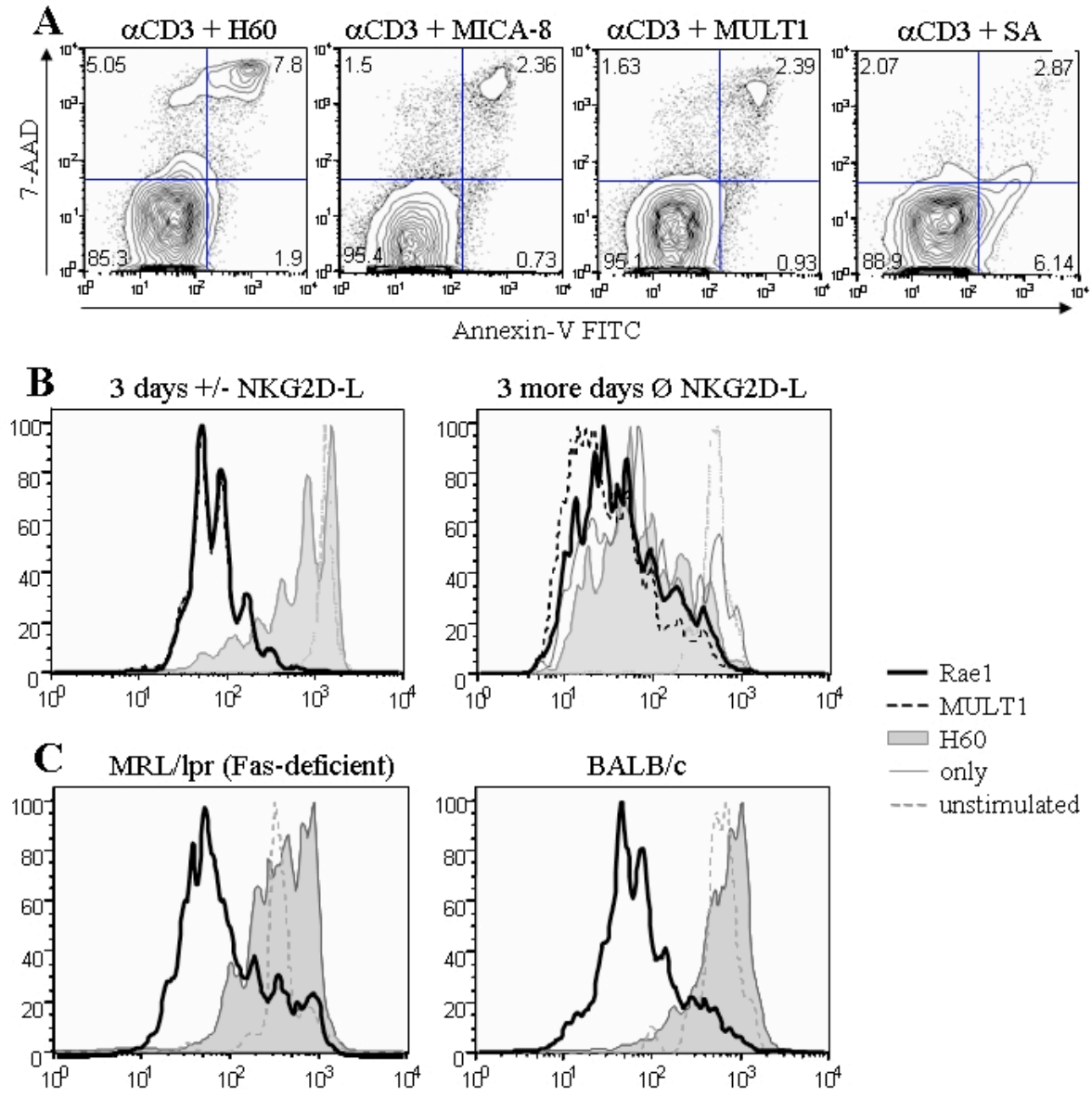

Figure 15: H60-triggered suppression is reversible and not mediated by Fas

Splenocyte cultures show measurements gated on CD8$^+$ T cells, similar results were obtained, when measuring CD4$^+$ T cells. ***(A)*** *Splenocytes of BALB/c mice were analyzed after short-term in vitro stimulation with anti-CD3 in the presence or absence of NKG2D ligands as labeled. Cells were stained with Annexin-V and the vital dye 7-amino-actinomycin-D (7-AAD) to determine apoptotic, necrotic and dead cells.* ***(B)*** *(Left) CFSE proliferation profile of CD8$^+$ T cells upon anti-CD3 stimulation in the presence or absence of NKG2D ligands as described for Figure 6 (same symbols used for ligands and controls). (Right) CFSE proliferation profile of splenocytes from the left histogram, which were washed and cultured for additional 3 days upon anti-CD3 stimulation but no additional NKG2D ligands.* ***(C)*** *(Left) CFSE proliferation*

profile of splenocytes derived from 6-week-old MRL/lpr mice or BALB/c mice (right) was determined as above.

3.5.2 H60-addition leads to cell cycle arrest

As H60-inhibition seems to be reversible, we analyzed splenocytes cultured under addition of NKG2D ligands for their cell cycle status. Propidum iodide (PI) intercalates into DNA and one can determine dependent on the amount of bound PI (which correlates with the DNA content) the cell cycle status of a cell. Staining with PI (Figure 16A) followed by curve fitting by the Dean-Jett-Fox algorithm (Figure 16B) revealed increased S and G2/M phase frequencies (up to 20% more) for T cells cultured in the presence of H60 or MICA-8. This specific cell cycle arrest was further confirmed by cell cycle progression analyses with BrdU incorporation, which can be detected by anti-BrdU Ab (Figure 16C). Control cultures were treated with cyclosporine, rapamycin or nocodazole, which cause G1, S or G2 phase arrest, respectively, to define gate settings. H60 and MICA-8-inhibited cultures showed also with the BrdU technique accumulation especially at late S and G2/M phases (up to 18% more).

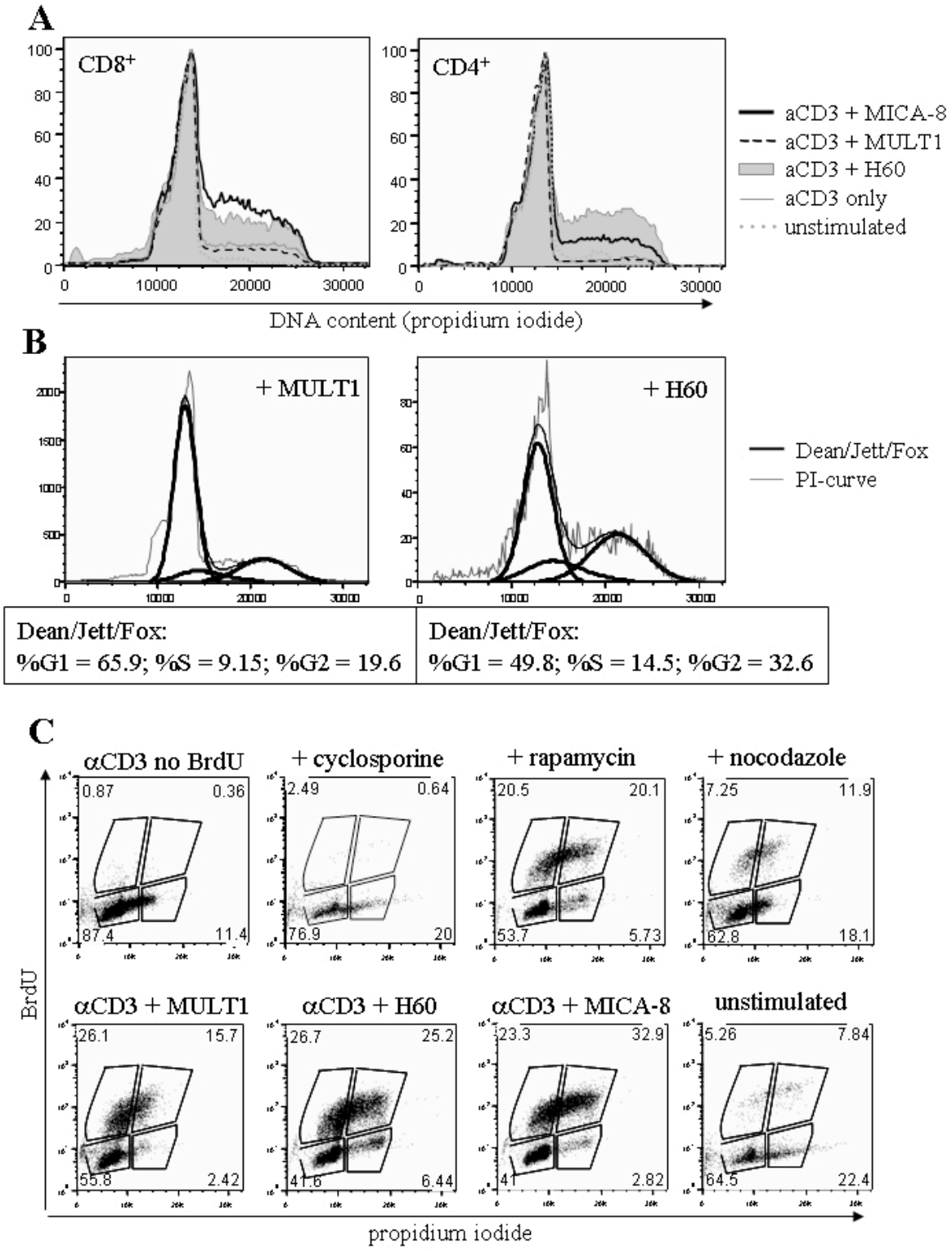

Figure 16: H60-addition causes a cell cycle arrest at S and G2/M phase

(A) *Splenocytes of BALB/c mice were stained for CD8 and CD4, subsequently fixed with ethanol, and stained with propidum iodide after short term in vitro culture upon anti-CD3 stimulation in the presence or absence of NKG2D ligands (same symbols as in Figure 6 used for ligands and controls).* ***(B)*** *Cells as in A. Cell cycle status were calculated by*

Dean/Jett/Fox curve fitting algorithm for splenocytes cultured in the presence of MULT1 or H60, as indicated. ***(C)*** *Splenocytes of BALB/c mice were pulsed with 10µM BrdU for 45' after short term in vitro culture upon anti-CD3 stimulation in the presence or absence of NKG2D ligands and then stained with anti-BrdU Ab and PI. To define gate settings for the different cell cycle phases, splenocytes were cultured in the presence of cyclosporine, rapamycin or nocodazole or left unpulsed, as indicated at the top of each dot plot.*

These data strongly suggest that H60 mediates a reversible cell cycle arrest during and after DNA synthesis phase, which can be also observed by the lymphoblastic state of H60-treated cells (Figure 17A). Furthermore, proliferation experiments, where H60 was added later to the bulk cultures than at the beginning of the stimulation (after one or two days), showed reduced T cell suppression (Figure 17B), indicating that the inhibitory effect of H60 is most effective early after T cell activation.

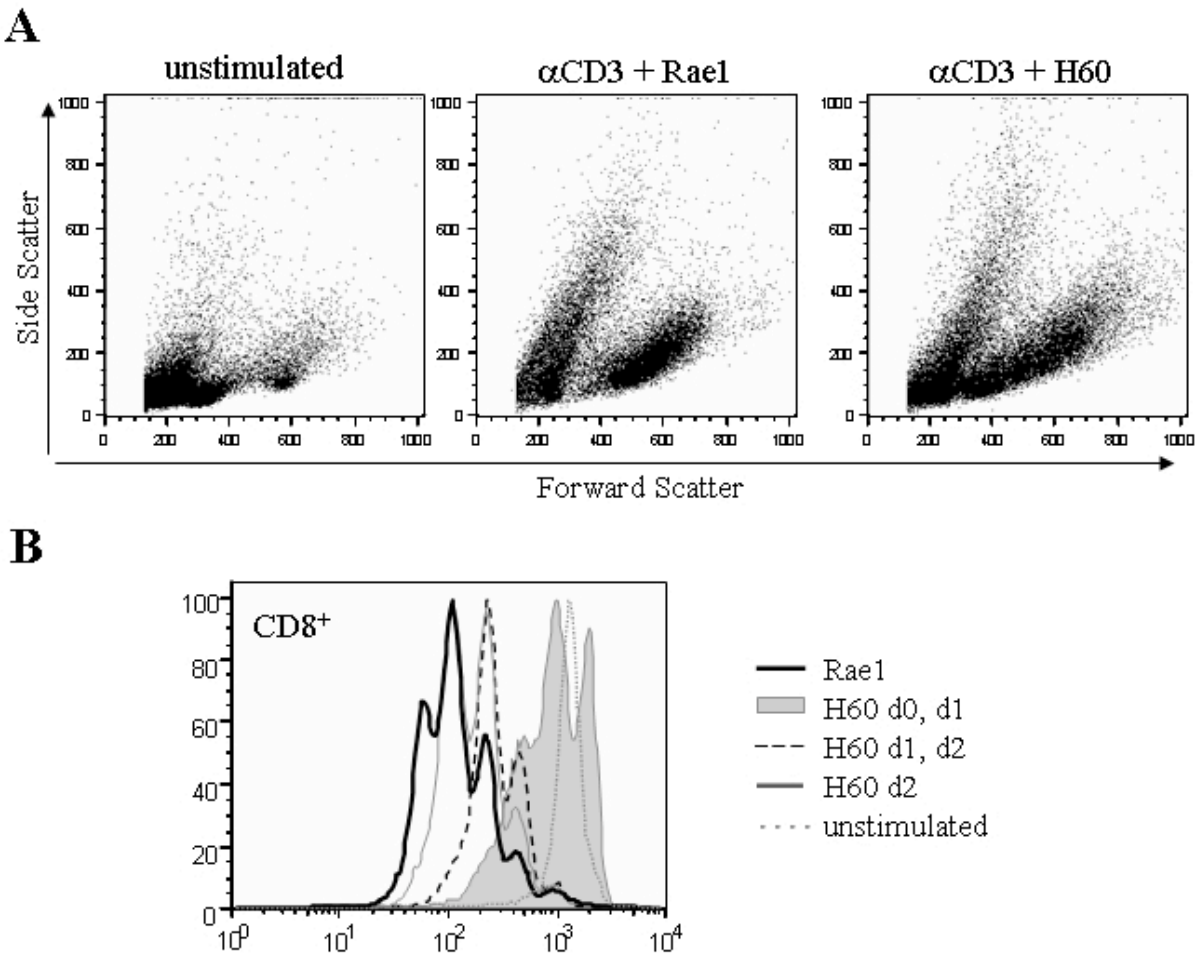

Figure 17: H60-treated cells are lymphoblastic

(A) *Splenocytes of BALB/c mice were anti-CD3 stimulated in the presence of Rae1 or H60, or left unstimulated as a control. After 65h culture cells were analyzed for their size and granularity as defined by forward and side scatter plots.* ***(B)*** *Splenocytes of BALB/c mice were anti-CD3 stimulated in the presence of Rae1 (bold line) or H60 (filled gray) or left unstimulated (dotted gray), and CFSE profiles of $CD8^+$ T cells were analyzed after 67h. H60 was added at the beginning of the culture (filled gray), one day after the beginning (dashed line), or two days after the beginning (gray line).*

3.5.3 Analysis of checkpoint regulators involved in cell cycle arrest

Progression of the cell cycle is tightly controlled by the limited presence of regulatory cyclins and checkpoint regulatory proteins. Synthesis of cyclin A is needed for S phase transition, whereas cyclin B allows cells to pass the G2/M phase checkpoint. We, therefore, analyzed on the protein level the amounts of cyclin A and cyclin B in H60-inhibited cells versus non-inhibited cells. As shown in Figure 18A, we detected no dramatic differences concerning protein levels of the two cyclins. Further analysis of checkpoint regulators controlling the S phase or the G2/M phase transition, namely p21, p27 and p53 (Figure 18A and B), indicated no influence on the observed cell cycle arrest. As control for the cell cycle status, S phase and G2/M phase arrested or unsynchronized 3T3 cells were blotted (Figure 18A), which revealed again S phase and G2/M phase characteristics for H60-suppressed T cells. To determine if prominent signal transduction pathways were altered in lymphocytes cultured in the presence of H60, we compared protein amounts of signaling subunits and kinases as p85α-phosphatidylinositol-3-kinase (PI3K), ζ-associated protein of 70kDa (ZAP-70), phospholipase C-γ1 (PLC-γ1), c-Jun N-terminal kinase (JNK1) and phosphorylation of Akt and mitogen-activated protein kinase p44/p42 (MAPK or Erk1/2). Surprisingly, none of these signaling molecules was significantly altered when analyzing H60- versus MULT1-treated T cells (Figure 18B). Thus, the mainly affected signal transduction molecules and regulators involved in the observed cell cycle arrest remain to be identified.

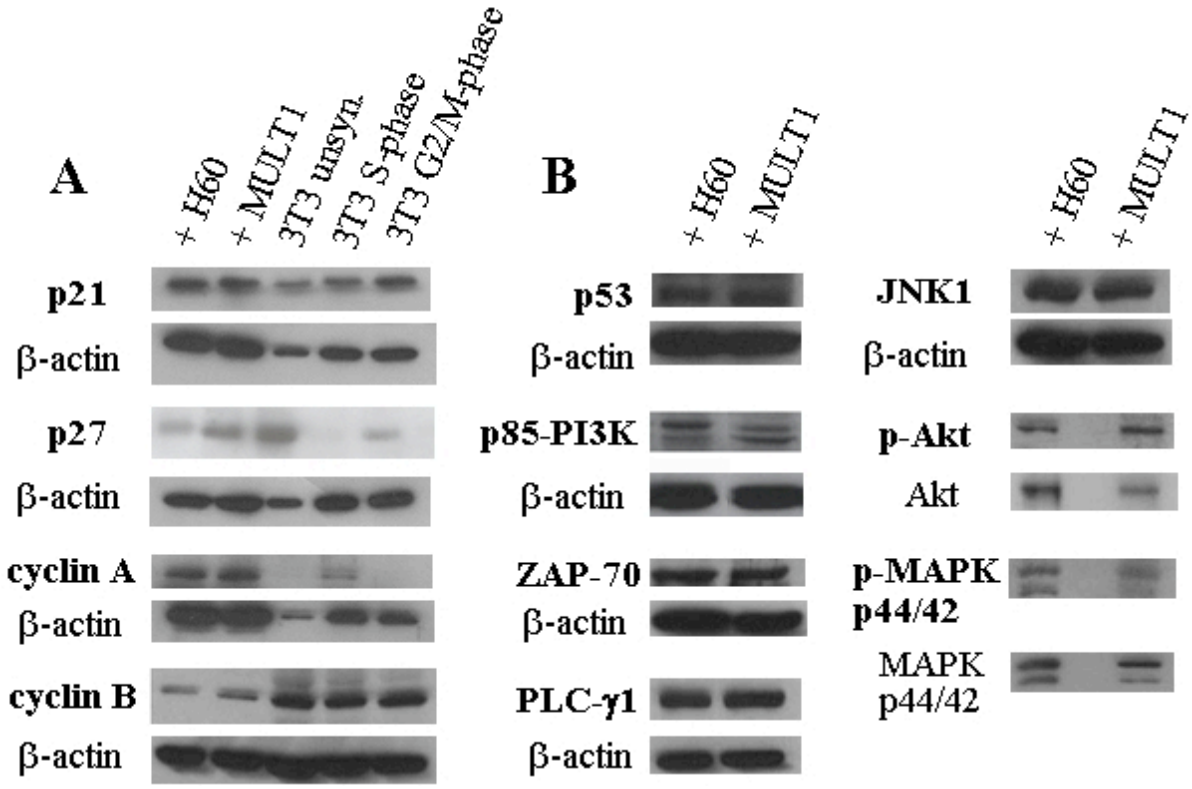

Figure 18: Analysis of cell cycle regulators and signaling molecules

(A and B) *Splenocytes of BALB/c mice were short term in vitro stimulated by anti-CD3 in the presence of H60 or MULT1. Subsequently, $CD8^+$ and $CD4^+$ T cells were sorted; their lysates were blotted and analyzed using the indicated Abs. As loading controls blots were stripped and reprobed with β-Actin or non-phospho Ab.* ***(A)*** *Controls for specific cell cycle phase proteins were measured by blotting unsynchronized, S phase or G2/M phase arrested 3T3 cells.*

4 DISCUSSION

With this work we could demonstrate that distinct NKG2D ligands can in addition to their immune-stimulatory capacities also mediate strong suppressive effects as inhibition of T cell proliferation. We identified so far murine H60 and human MICA-8 as NKG2D ligands able to cause this inhibitory mechanism, but other NKG2D ligands may as well share the same characteristics of this new group of "bifunctional" molecules. The observed suppression of T cell proliferation was independent of NKG2D and its adaptor molecules and applied to murine and human T cells. We discovered that the inhibition of T cells by H60 and MICA-8 leads to a reversible cell cycle arrest mediated by a regulatory lymphocyte subset, suggesting a new mechanism to transiently negatively regulate T cells *in vivo*. Expression cloning analyses to find the H60/MICA-8-binding receptor revealed up to now no positive clone, but further promising strategies to identify the receptor are anticipated, like differential RNA expression analysis by microarray technology, the production of monoclonal antibodies against H60/MICA-8-receptor expressing Phoenix cells, and mass spectrometric analysis of NKG2D ligand-associated membrane protein complexes.

4.1 NKG2D ligands as costimulators of T cells

NKG2D is known as a potent costimulatory receptor for $CD8^+$ T cells in combination with the signal 1 via the T cell receptor (Gilfillan et al., 2002; Groh et al., 2001; Maasho et al., 2005; Roberts et al., 2001). Our group has also measured a slight costimulatory influence of NKG2D ligands, as NKG2D ligand application increased the sensitivity of target cell lysis by cytotoxic T cell lines, and furthermore, higher proliferation rates were measured in thymidine assays upon Rae1 administration (experiments performed by F. Gebhardt). Indeed, *in vivo* immunization with NGK2D ligand-overexpressing tumor cell lines induces effective tumor-specific immunity (Cerwenka et al., 2001; Diefenbach et al., 2003; Diefenbach et al., 2000; Diefenbach et al., 2001), and controversially, in human patients high levels of MICA are correlated with a good prognosis in colorectal cancer (Watson et al., 2006). Expression of different types of NKG2D ligands could serve as a strategy to prevent tumor escape, similar like it has been described for MCMV infection (Krmpotic et al., 2002; Krmpotic et al., 2005; Lodoen et al., 2004). The observation that $CD8^+$ effector memory T cells express high levels of NKG2D (Jamieson et al., 2002), suggests a possible role of NKG2D ligand expressing mucosa tissue in mediating necessary survival signals to the memory T cells. Basic to this speculation is the finding that $CD4^+$ effector memory T cells, which are negative for NKG2D,

poorly survive in non-lymphoid organs like mucosa-associated tissue, while $NKG2D^+CD8^+$ T_{EM} are long-living in these tissues. For further studies concerning $CD8^+$ T cell memory development NKG2D-deficient mice could be useful tools.

4.2 NKG2D ligands as suppressors of T cells

The high expression of NKG2D ligands on tumor cells remains poorly understood, as NK and $CD8^+$ T cells can potently reject NKG2D ligand expressing targets cells. In this context, the active shedding of MICA/B from the tumor cell surface (Groh et al., 2002; Salih et al., 2002), together with NKG2D internalization and degradation by binding of soluble MIC proteins to surface NKG2D (Jinushi et al., 2005; Tieng et al., 2002; Wu et al., 2004) has been discussed as one possibility to explain this discrepancy. Actually, chronic stimulation of NKG2D with soluble NKG2D ligands, as seen in some cancer patients, leads to loss of NKG2D surface expression and therefore an impairment of lymphocyte responses. A recent report has even stated that in late-stage tumor patients $CD8^+$ T cells, which have downregulated NKG2D, are suppressed in their proliferation and killed via a Fas/Fas-L-dependent mechanism by a unique $NKG2D^+CD4^+$ T cell population (Groh et al., 2006).

Our data demonstrate another mechanism, by which T cells can be inhibited in an NKG2D-independent way. Application of H60 or MICA-8 to primary T cell cultures results in a strong and reversible suppression on the proliferation of $CD8^+$ and $CD4^+$ T cells. Our collaborator Antonio Siccardi has established an experimental system, where NKG2D ligands can be directly associated to the surface of transplanted tumor cells. When mice were treated with H60- or Rae1-coated tumor cells, totally opposing effects were obtained; Rae1 on the surface reduced tumor growth in comparison with the control group, whereas H60-targeted tumors grew significantly faster than the control group (Kriegeskorte et al., 2005), impressively confirming our *in vitro* data in an *in vivo* model. These findings allow new interesting speculations of the consequences of NKG2D ligand expression or shedding of soluble molecules from the tumor surface, because the expression of NKG2D ligands with inhibitory functions would certainly be a selective advantage and potent immune evasion mechanism for tumor cells *in vivo*. A better understanding of the participating molecules might provide insights into possible therapeutic interventions. Apart from tumor cells, such a mechanism, which induces a regulatory lymphocyte subset, could represent a more general role in the immune system in preventing excessive, possibly dangerous immune reactions against antigens presented in the periphery. The induced regulatory T cells could stop effector and

memory T cells from too easily re-expanding by selectively suppressing their proliferation without destroying their effector functions. Moreover, autoreactive T cells could be maintained in an antigen-specific tolerogenic state. NKG2D ligand expression has been described for bone marrow stem cells (Ogasawara et al., 2005; Poggi et al., 2005) and thymocytes (Diefenbach et al., 2000; Li et al., 2005), but a direct correlation to its importance has not been found up to now. Here, expression of suppressive ligands together with the H60/MICA-8 receptor could help to trigger necessary growth arrests until further developmental signals are delivered.

4.3 The effects of H60-inhibition

We could show with the help of cell cycle analyses and Annexin-V measurements that the inhibitory effect delivered by H60 and MICA-8 does not lead to apoptosis of the T cells but to a reversible growth arrest at the S and G2/M phase transition points. Further experiments with Fas-deficient MRL/lpr mice could clearly distinguish our NKG2D ligand-dependent effects from the findings of the group of Thomas Spies (Groh et al., 2006). Proliferation assays with CFSE and thymidine incorporation upon human PBMCs in the presence of antagonist anti-Fas mAb are under current investigation, but we are quite confident that these experiments will present also for human cells a Fas/Fas-L independent mechanism of H60-suppression. The analysis of checkpoint regulators and cyclins involved in S and G2/M phase transition has not yet revealed a clearer understanding of the regulatory molecules contributing to the observed cell cycle arrest. Indeed, the transition of S to G2/M phase has up to now not been found to be tightly regulated, as known checkpoint molecules control mostly cells before DNA synthesis or before mitosis. Therefore, the here-described arrest could result more of a delayed cell cycle progression rather than a regulated arrest. The mechanism is clearly distinct from other coinhibitory signal transduction pathways (e.g. CTLA-4) that interfere mostly early at the cell cycle by preventing p21 or p27 degradation or cyclin synthesis. Also intensive comparisons on protein level of prominent signaling adaptor molecules and kinases have not been successful to reveal the signaling pathways altered in H60-treated cells. Analyses of further molecules and of cells at an earlier stage of stimulation, as H60 seems to act at least in the first 24h on the T cells, might detect eventually the signal molecules participating in the induced growth arrest or slowed down cell cycle. Knowledge about these molecules might allow targeted intervention at the signal cascades for therapeutic treatments.

Studies with several knockout mice depicted that the only known population associated with regulatory functions possibly involved in our modulatory system are antigen-induced T regulatory cells (Tr1). Supporting this assumption, IL-10 was found to be essential for the mediation of the inhibited T cell proliferation by H60, thereby presenting IL-10 as a major cytokine driving the generation and/or expansion of H60-responsive Tr1 cells that can suppress T cells mainly via cell contact-dependent mechanisms. Figure 19 shows a model, how regulatory T cells could function in the described system. A similar mode of operation could be thinkable for tumor cells expressing or shedding NKG2D ligands with suppressive functions, thereby impairing host tumor immunosurveillance.

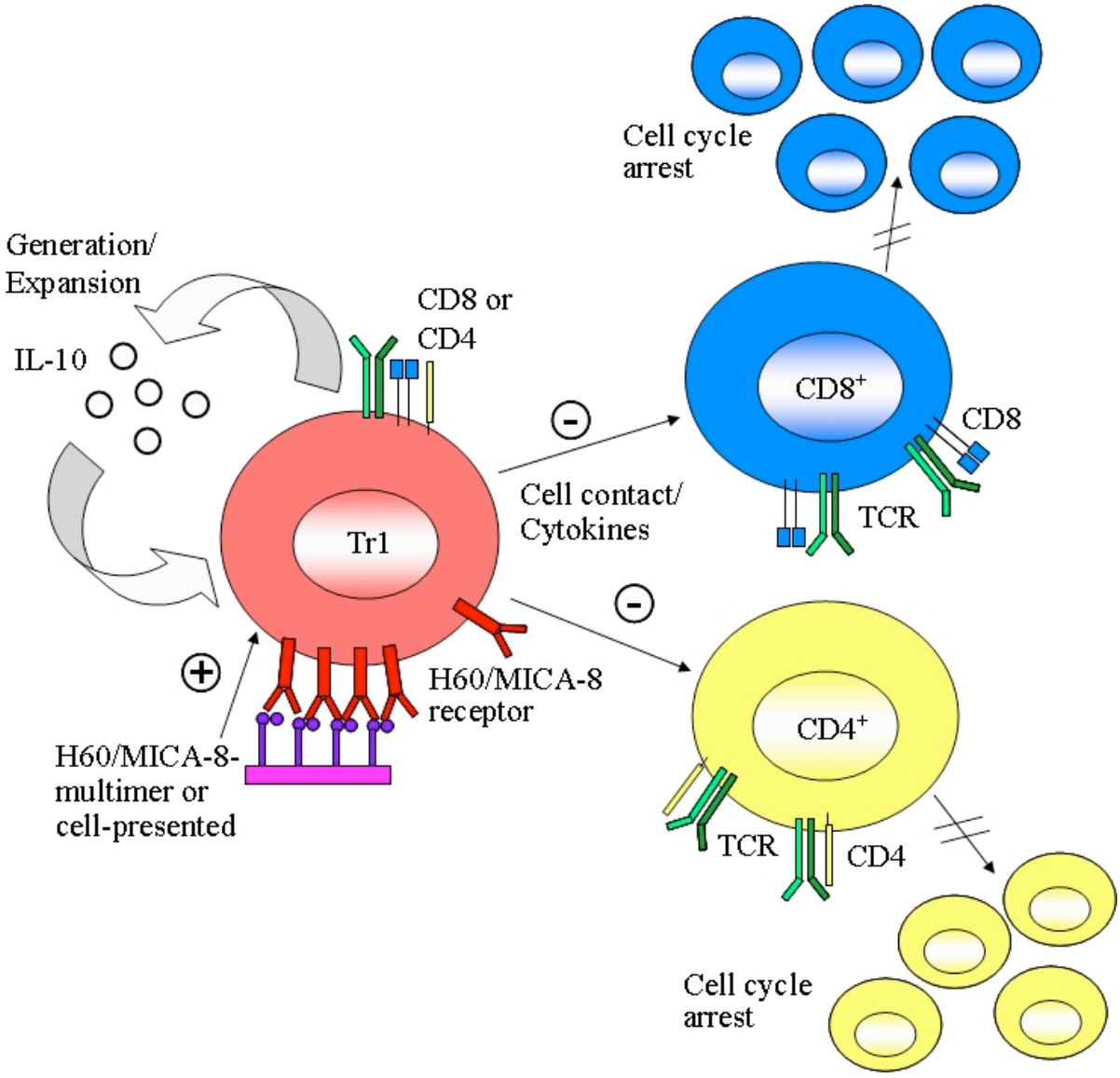

Figure 19: Model of T cell suppression via H60 bound by regulatory T cells

4.4 The H60/MICA-8 receptor

A main project of this thesis work was dedicated to the identification of the molecule that mediates the suppressive effects of H60 and MICA-8 on T cell proliferation. We provided multiple lines of evidence that this receptor is different from NKG2D. $CD4^+$ T cells, which are negative for surface expression and mRNA transcripts of NKG2D, are even in purified cultures strongly and selectively inhibited by H60. Neither blocking antibodies for NKG2D diminished the suppressive effects of H60, nor the absence of the NKG2D adaptor molecule DAP10 influenced the block in proliferation. Furthermore, human MICA-8, which does not stably bind to murine NKG2D, inhibits the proliferation of murine T cells in a similar manner as H60. Finally, experiments with $NKG2D^{-/-}$ mice confirmed the completely NKG2D-independent mechanism.

4.4.1 Reasons for failure to identify the unknown receptor by expression cloning

In order to identify the H60/MICA-8 binding receptor, we generated a cDNA library of floating Phoenix cells, which show exactly the staining pattern expected for cells expressing the unknown receptor. Despite of extensive screenings of two different cell lines, which were both transiently and stably transfected, we couldn't isolate a single cDNA clone for further subcloning. There are several reasons imaginable, why we weren't successful. Of course, the simplest explanation could be that the cDNA library does not contain enough copies of the corresponding mRNA due to low RNA-transcription of the molecule, which would then lead to transfection efficiencies below the detection limit. Also the necessary usage of the H60/MICA-8 tetramers for the read-out could have impeded the recognition of a low expressed protein, as we always had to deal with certain amounts of background staining. In addition, we have no knowledge about a possible adaptor molecule dependency of the receptor. We could exclude a necessary association with DAP10 and DAP12, which are essential for NKG2D surface expression and signaling, by using DAP10 and DAP12 knock-out mice, but presence of other adaptors, which are lacking in the transfected cell lines, could be required for correct surface expression of the H60/MICA-8 receptor. There might be a high probability that the unknown receptor somehow resembles NKG2D, as the receptor binds at least two NKG2D ligands; NKG2D itself builds a homodimer. If the H60/MICA-8 receptor is also formed of two independent subunits, the simultaneous transfection with two monomers, which have to form then a homodimer or even a heterodimer, would impair the chances of

success with the cDNA library approach. Another possibility, which we cannot definitely exclude and which would affect the whole project of the search for the receptor, is that the molecule expressed by floating Phoenix cells is different from the receptor participating in the suppression of T cell proliferation. Therefore, in parallel to the experiments on Phoenix cells, we will as well focus on murine splenocytes to find the unknown receptor, e.g. with microarray analyses of stimulated splenocytes of NKG2D$^{-/-}$ versus wildtype mice, where disturbing NKG2D-effects could be subtracted.

4.4.2 The nature of the H60/MICA-8 receptor

Until now we don't know much about the nature of the H60/MICA-8 receptor. Upon staining of stimulated splenocytes, we detected surface expression of the receptor together with CD8 or CD4, implicating an expression on (a subset of) T cells. Somehow the presence of IL-10 seems to be required for the mediation of the inhibitory effect by providing an essential stimulus for the expression of the receptor or the generation and/or expansion of the regulatory subpopulation that executes the suppressive mechanism. Additional to the model presented in Figure 19, an alternative conceivable mode of action concerning the inhibitory effect of H60 is demonstrated in Figure 20, suggesting a direct interaction of H60/MICA-8 molecules with the in that way subsequently inhibited CD8^{+} and CD4^{+} T cells, which express the inhibitory receptor themselves.

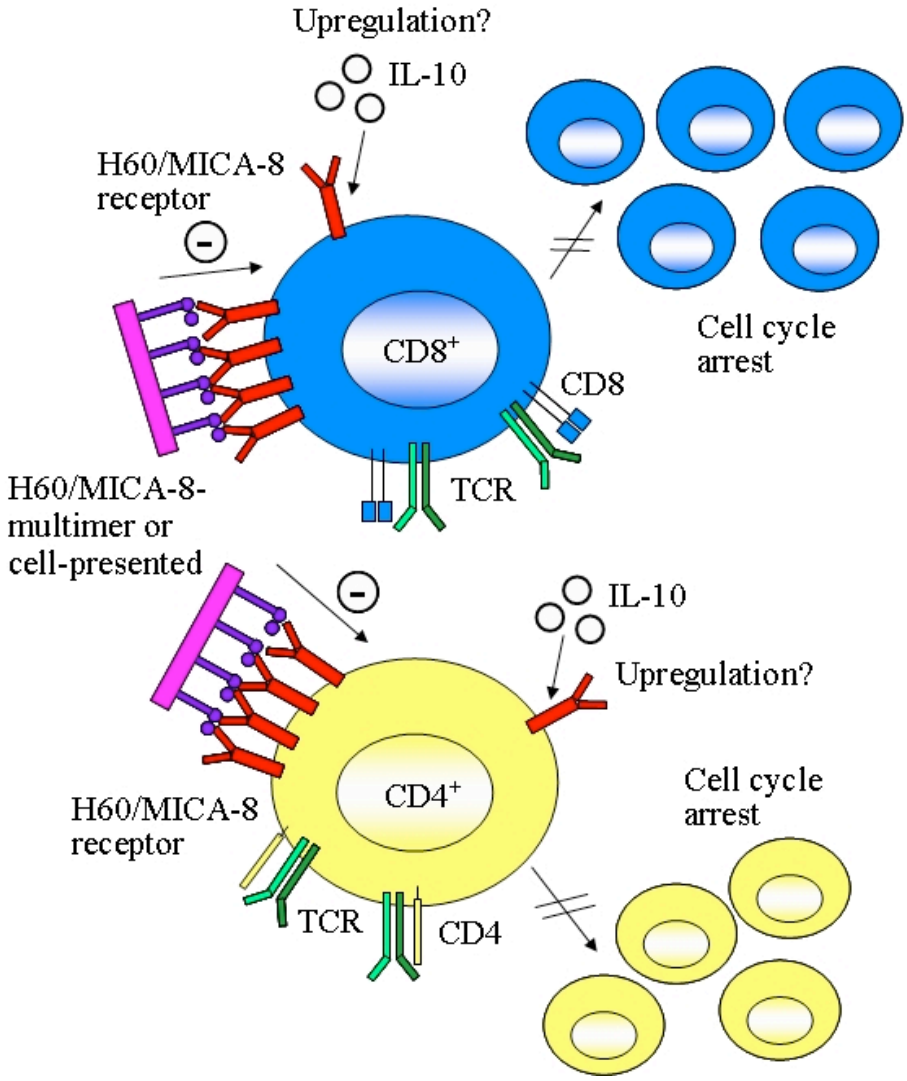

Figure 20: Model of direct interaction of H60/MICA-8 with the regulated T cells

In favor of this model, the finding of the microarray analyses would stand that HSP70 could be the wanted H60/MICA-8 receptor, and also our staining data identified HSP70 mAb- and H60/MICA-8 tetramer-binding on the same cells. The molecular chaperone HSP70 is highly conserved between species, and its primary function is to bind to nascent polypeptides or aberrantly folded proteins to prevent their aggregation. In our context, partially misfolded H60 or MICA-8 molecules could induce and bind to HSP70 on T cells. This could subsequently lead to a distinct cell cycle stopping or delaying signal, until the proteins are correctly folded. On the other hand, binding of H60/MICA-8 to HSP70 could disturb the activity of HSP70, which is known to be important for cellular growth and survival (Kwak et al., 1998; Rohde et al., 2005), thereby preventing cell cycle progression. Another interesting capacity of HSP70, studied in patients with autoimmune diseases as e.g. rheumatoid arthritis, constitutes the role of an “autoantigen”. Application of HSP70 induced HSP-reactive T cells

with a regulatory phenotype (van Eden et al., 2005) and led to downregulation of inflammation. In our cell cultures, the presence of potentially misfolded H60/MICA-8 could promote HSP70 expression; HSP70 in complex with H60/MICA-8 could be recognized by cross-reactive T cells and could turn these to regulatory cells that can negatively influence the other T cells. In contrast to this immune-regulatory effect of HSP70, HSP70/peptide complexes have been found to stimulate peptide-specific T cell responses like proliferation by probably improving the peptide uptake and presentation of APCs (Haug et al., 2005). Concerning this issue, it would be conceivable that H60/MICA-8 could block or impede an activatory adaptor or signal like HSP70 so that the stimulatory effect could not take place and that the responding T cells would lack signals to divide.

Besides HSP70, we could also imagine an integrin-like molecule to bind to H60 and MICA-8, as this could explain the deficiency in proliferation as a result of disturbed cell to cell crosstalk, further providing evidence for the latter model, in which H60/MICA-8 inhibit by blocking a stimulatory event or by directly mediating an inhibitory signal, similar as e.g. CTLA-4 or BTLA. The question, which of the models is more correct, or if maybe the real conditions are a mixture of both models, can only be answered when we get to know more about the affected signaling pathways and the characteristics of the function and the nature of the still unidentified H60/MICA-8 receptor.

4.5 Outlook and future perspectives

For the future work on this project the final identification of the H60/MICA-8 binding receptor has the highest priority. We are confident in succeeding, as we can fall back to many different approaches grateful to various flourishing collaborations. The microarray comparison of floating Phoenix and adherent Phoenix cells yielded several promising candidates for the unknown receptor, especially HSP70, which will be subsequently cloned and tested in transfection experiments for multimer binding. With the generation of monoclonal antibodies against the unknown receptor, we expect to get a powerful reagent for precipitation experiments of receptor-antibody complexes. Furthermore, blocking antibodies against the receptor could be used to study the inhibitory mechanism and could provide an important tool for future therapeutic intervention strategies, especially in the tumor model. The pull-down of membrane-integrated protein complexes with soluble ligands could not only lead to a mass spectrometric-based characterization of the receptor, but in addition we could fish essential receptor-associated adaptor molecules, which would be of great value for the

transfection experiments with the cDNA library. Further insights into the participating signal cascades by western blot analyses could identify possible targets for intervening with the suppression of T cells, and measurements of remaining effector functions of inhibited versus uninhibited T cells could help to reveal the possible *in vivo* relevance of the system.

To study the complex involvement of the H60/MICA-8 receptor in tumor settings, we are establishing an *in vivo* tumor model, in which the expression of NKG2D ligands is inducible by tetracycline. This model could help to answer the open question, to which extent the type, amount, and time point of NKG2D ligand expression influences tumor progression. The access to $NKG2D^{-/-}$ mice generated in collaboration with Bojan Polic in Rijeka, Croatia, will also allow the examination of NKG2D ligand mediated-effects in the absence of NKG2D, e.g. by using the inducible adoptive tumor model. Complementary to the for this work utilized MICA-8 molecule, we plan to clone and refold further MICA alleles and other human NKG2D ligands as MICB and ULBPs, in order to define, if additional NKG2D ligands share these potent inhibitory capacities. By knowing more about the functions of human NKG2D ligands, we will analyze in collaboration with Birgit Luber/ Heinz Höfler, TU München, expression patterns of NKG2D ligands in primary tumor tissue with the target to be able to make prognostic statements on individual NKG2D ligand expression levels.

5 SUMMARY

NKG2D is believed to be an important activating immunoreceptor and is expressed on NK cells, $CD8^+$ T cells and γδ T cells in mice and humans. NKG2D binds to a large variety of structurally diverse ligands, which are found to be only poorly expressed on "normal" resting tissue, but can become upregulated on tumors and otherwise stressed or infected cells. Although the ligands for NKG2D seem to be differentially expressed, only similar redundant stimulatory effects have been described so far for all of them, and the system has been therefore interpreted as a sensor system for the recognition of stressed or transformed cells, crucially involved in tumor immune surveillance and triggering of immune responses of NK and $CD8^+$ T cells. However, especially the high expression of NKG2D-ligands on progressively growing tumor cells remained puzzling.

With this thesis work possible non-redundant functions of NKG2D ligands should be investigated and further analyzed. In order to achieve this, soluble recombinant ligands for murine and human NKG2D were generated. Their specific staining capacities to NKG2D expressing cell populations were monitored, and different relative binding affinities were measured, whereby H60 and MULT1 showed a much greater binding strength than Rae1 for NKG2D. When we compared the effect of NKG2D ligand multimer addition to murine splenocyte cultures, we were surprised to find a strong inhibitory effect on the proliferation of $CD8^+$ and $CD4^+$ T cells by H60, but not by any other murine NKG2D ligand. By testing several gene-deficient or transgenic mouse strains, we could show, that neither CD1d-restricted NKT cells, nor γδ-T cells, nor naturally occurring regulatory cells, but rather a mechanism similar to antigen-induced regulatory cells seems to be crucially involved in the inhibition of T cell proliferation via H60. The immune-regulatory cytokine IL-10 is involved in the suppression of T cells, since the inhibition of T cell proliferation was found to be reduced in IL-10-deficient mice. Most surprisingly by using DAP10- and NKG2D-deficient mice as well as NKG2D blocking antibodies, the involvement of the NKG2D receptor in mediating the inhibitory effects could be excluded. As the murine and human NKG2D/ligand systems show high homology, we investigated, if similar inhibitory effects of NKG2D ligands on human cells could also be found for human cells. Indeed, we identified a cross reactivity between man and mouse, as only the murine ligand H60 was capable of suppressing the proliferation of hPBMCs; vice versa, the human MICA-8 allele could not only inhibit human PBMCs but also murine splenocytes.

In order to identify the unknown receptor binding to H60/MICA-8, we anticipated several approaches. By screening different cell lines, we found that Phoenix cells, a derivate of HEK293 cells, highly express the unknown receptor under growth conditions, in which the normally adherent cells can not attach to the culture plate surface. Again, since Phoenix cells are negative for NKG2D mRNA or protein expression, an involvement of NKG2D in the binding to H60/MICA-8 could be excluded. We isolated mRNA of receptor-expressing Phoenix cells and used it to generate a cDNA library. This cDNA library, containing 600 plasmid pools, was extensively screened by transfecting H60/MICA-8 receptor negative cell lines. Unfortunately, no promising cDNA plasmid pool could be identified for further subcloning. Another approach to find the inhibitory receptor was made by comparing mRNA expression patterns of Phoenix receptor positive and negative cells in an Affymetrix analysis. We identified several candidate genes, which are upregulated during the receptor positive growth stage. Three most promising candidate genes were selected (EMP3, HSP70 and CD79a), and their potential involvement as H60/MICA-8-receptor was studied with presenting HSP70 as a molecule expressed on the very same cells as the wanted receptor.

Additionally to these analyses, we characterized the nature of H60-induced growth inhibition in more detail. We observed, that H60-inhibited T cells don't die; they are reversibly arrested during cell cycle progression. Furthermore, the inhibition appears to be mostly independent of Fas/FasL interactions for murine and human cells, which distinguishes the phenomenon from a recently reported observation of NKG2D ligand-mediated depletion of antigen-specific T cells. The H60-induced T cell suppression was fully reversible and led to a cell cycle arrest in the S and G2/M phase. Analysis of checkpoint regulators as p21, p27, p53 and distinct cyclins demonstrated no upregulation in the observed cell cycle arrest, so that the mainly affected signaling molecules still remain to be identified.

In conclusion, we showed for the first time that distinct NKG2D ligands can also mediate strong suppressive effects, which are independent of the NKG2D receptor itself. The inhibition leads to a completely reversible cell cycle arrest, suggesting a physiologically relevant regulatory function. Furthermore, our novel findings provide new explanations how the expression of distinct NKG2D ligands could become a selective advantage for tumor cells.

6 REFERENCES

Abbas, A., and Lichtman, A. (2003). Cellular and Molecular Immunology, Fifth edn, Elsevier Science).

Alaminos, M., Davalos, V., Ropero, S., Setien, F., Paz, M. F., Herranz, M., Fraga, M. F., Mora, J., Cheung, N. K., Gerald, W. L., and Esteller, M. (2005). EMP3, a myelin-related gene located in the critical 19q13.3 region, is epigenetically silenced and exhibits features of a candidate tumor suppressor in glioma and neuroblastoma. Cancer Res *65*, 2565-2571.

Alberts, B., Johnson, A., Lewis, J., Raff, M., Roberts, K., and Walter, P. (2002). Molecular Biology of THE CELL, Fourth edn, Garland Science).

Andre, P., Castriconi, R., Espeli, M., Anfossi, N., Juarez, T., Hue, S., Conway, H., Romagne, F., Dondero, A., Nanni, M.*, et al.* (2004). Comparative analysis of human NK cell activation induced by NKG2D and natural cytotoxicity receptors. Eur J Immunol *34*, 961-971.

Aosai, F., Chen, M., Kang, H. K., Mun, H. S., Norose, K., Piao, L. X., Kobayashi, M., Takeuchi, O., Akira, S., and Yano, A. (2002). Toxoplasma gondii-derived heat shock protein HSP70 functions as a B cell mitogen. Cell Stress Chaperones *7*, 357-364.

Apostolou, I., Sarukhan, A., Klein, L., and von Boehmer, H. (2002). Origin of regulatory T cells with known specificity for antigen. Nat Immunol *3*, 756-763.

Bacon, L., Eagle, R. A., Meyer, M., Easom, N., Young, N. T., and Trowsdale, J. (2004). Two human ULBP/RAET1 molecules with transmembrane regions are ligands for NKG2D. J Immunol *173*, 1078-1084.

Bahram, S., Bresnahan, M., Geraghty, D. E., and Spies, T. (1994). A second lineage of mammalian major histocompatibility complex class I genes. Proc Natl Acad Sci U S A *91*, 6259-6263.

Bahram, S., Inoko, H., Shiina, T., and Radosavljevic, M. (2005). MIC and other NKG2D ligands: from none to too many. Curr Opin Immunol *17*, 505-509.

Bauer, S., Groh, V., Wu, J., Steinle, A., Phillips, J. H., Lanier, L. L., and Spies, T. (1999). Activation of NK cells and T cells by NKG2D, a receptor for stress-inducible MICA. Science *285*, 727-729.

Bendelac, A., Rivera, M. N., Park, S. H., and Roark, J. H. (1997). Mouse CD1-specific NK1 T cells: development, specificity, and function. Annu Rev Immunol *15*, 535-562.

Billadeau, D. D., Upshaw, J. L., Schoon, R. A., Dick, C. J., and Leibson, P. J. (2003). NKG2D-DAP10 triggers human NK cell-mediated killing via a Syk-independent regulatory pathway. Nat Immunol *4*, 557-564.

Boissel, N., Rea, D., Tieng, V., Dulphy, N., Brun, M., Cayuela, J. M., Rousselot, P., Tamouza, R., Le Bouteiller, P., Mahon, F. X.*, et al.* (2006). BCR/ABL oncogene directly controls MHC class I chain-related molecule A expression in chronic myelogenous leukemia. J Immunol *176*, 5108-5116.

Brandes, M., Willimann, K., and Moser, B. (2005). Professional antigen-presentation function by human gammadelta T Cells. Science *309*, 264-268.

Busch, D. H., and Pamer, E. G. (1998). MHC class I/peptide stability: implications for immunodominance, in vitro proliferation and diversity of responding CTL. J Immunol *160*, 4441-4448.

Busch, D. H., Pilip, I. M., Vijh, S., and Pamer, E. G. (1998). Coordinate regulation of complex T cell populations responding to bacterial infection. Immunity *8*, 353-362.

Busche, A., Goldmann, T., Naumann, U., Steinle, A., and Brandau, S. (2006). Natural killer cell-mediated rejection of experimental human lung cancer by genetic overexpression of major histocompatibility complex class I chain-related gene A. Hum Gene Ther *17*, 135-146.

Cantor, H. (2004). Reviving suppression? Nat Immunol *5*, 347-349.

Carayannopoulos, L. N., Naidenko, O. V., Fremont, D. H., and Yokoyama, W. M. (2002a). Cutting edge: murine UL16-binding protein-like transcript 1: a newly described transcript encoding a high-affinity ligand for murine NKG2D. J Immunol *169*, 4079-4083.

Carayannopoulos, L. N., Naidenko, O. V., Kinder, J., Ho, E. L., Fremont, D. H., and Yokoyama, W. M. (2002b). Ligands for murine NKG2D display heterogeneous binding behavior. Eur J Immunol *32*, 597-605.

Carbone, E., Neri, P., Mesuraca, M., Fulciniti, M. T., Otsuki, T., Pende, D., Groh, V., Spies, T., Pollio, G., Cosman, D.*, et al.* (2005). HLA class I, NKG2D, and natural cytotoxicity receptors regulate multiple myeloma cell recognition by natural killer cells. Blood *105*, 251-258.

Castriconi, R., Cantoni, C., Della Chiesa, M., Vitale, M., Marcenaro, E., Conte, R., Biassoni, R., Bottino, C., Moretta, L., and Moretta, A. (2003). Transforming growth factor beta 1 inhibits expression of NKp30 and NKG2D receptors: consequences for the NK-mediated killing of dendritic cells. Proc Natl Acad Sci U S A *100*, 4120-4125.

Cerwenka, A., Bakker, A. B., McClanahan, T., Wagner, J., Wu, J., Phillips, J. H., and Lanier, L. L. (2000). Retinoic acid early inducible genes define a ligand family for the activating NKG2D receptor in mice. Immunity *12*, 721-727.

Cerwenka, A., Baron, J. L., and Lanier, L. L. (2001). Ectopic expression of retinoic acid early inducible-1 gene (RAE-1) permits natural killer cell-mediated rejection of a MHC class I-bearing tumor in vivo. Proc Natl Acad Sci U S A *98*, 11521-11526.

Chalupny, N. J., Sutherland, C. L., Lawrence, W. A., Rein-Weston, A., and Cosman, D. (2003). ULBP4 is a novel ligand for human NKG2D. Biochem Biophys Res Commun *305*, 129-135.

Chan, C. W., Crafton, E., Fan, H. N., Flook, J., Yoshimura, K., Skarica, M., Brockstedt, D., Dubensky, T. W., Stins, M. F., Lanier, L. L.*, et al.* (2006). Interferon-producing killer dendritic cells provide a link between innate and adaptive immunity. Nat Med *12*, 207-213.

Chen, L. (2004). Co-inhibitory molecules of the B7-CD28 family in the control of T-cell immunity. Nat Rev Immunol *4*, 336-347.

Conejo-Garcia, J. R., Benencia, F., Courreges, M. C., Khang, E., Zhang, L., Mohamed-Hadley, A., Vinocur, J. M., Buckanovich, R. J., Thompson, C. B., Levine, B., and Coukos, G. (2003). Letal, A tumor-associated NKG2D immunoreceptor ligand, induces activation and expansion of effector immune cells. Cancer Biol Ther *2*, 446-451.

Cosman, D., Mullberg, J., Sutherland, C. L., Chin, W., Armitage, R., Fanslow, W., Kubin, M., and Chalupny, N. J. (2001). ULBPs, novel MHC class I-related molecules, bind to CMV glycoprotein UL16 and stimulate NK cytotoxicity through the NKG2D receptor. Immunity *14*, 123-133.

Coudert, J. D., Zimmer, J., Tomasello, E., Cebecauer, M., Colonna, M., Vivier, E., and Held, W. (2005). Altered NKG2D function in NK cells induced by chronic exposure to NKG2D ligand-expressing tumor cells. Blood *106*, 1711-1717.

Croft, M. (2003). Co-stimulatory members of the TNFR family: keys to effective T-cell immunity? Nat Rev Immunol *3*, 609-620.

Diefenbach, A., Hsia, J. K., Hsiung, M. Y., and Raulet, D. H. (2003). A novel ligand for the NKG2D receptor activates NK cells and macrophages and induces tumor immunity. Eur J Immunol *33*, 381-391.

Diefenbach, A., Jamieson, A. M., Liu, S. D., Shastri, N., and Raulet, D. H. (2000). Ligands for the murine NKG2D receptor: expression by tumor cells and activation of NK cells and macrophages. Nat Immunol *1*, 119-126.

Diefenbach, A., Jensen, E. R., Jamieson, A. M., and Raulet, D. H. (2001). Rae1 and H60 ligands of the NKG2D receptor stimulate tumour immunity. Nature *413*, 165-171.

Diefenbach, A., and Raulet, D. H. (1999). Natural killer cells: stress out, turn on, tune in. Curr Biol *9*, R851-853.

Diefenbach, A., and Raulet, D. H. (2003). Innate immune recognition by stimulatory immunoreceptors. Curr Opin Immunol *15*, 37-44.

Diefenbach, A., Tomasello, E., Lucas, M., Jamieson, A. M., Hsia, J. K., Vivier, E., and Raulet, D. H. (2002). Selective associations with signaling proteins determine stimulatory versus costimulatory activity of NKG2D. Nat Immunol *3*, 1142-1149.

Ehrlich, L. I., Ogasawara, K., Hamerman, J. A., Takaki, R., Zingoni, A., Allison, J. P., and Lanier, L. L. (2005). Engagement of NKG2D by cognate ligand or antibody alone is insufficient to mediate costimulation of human and mouse CD8+ T cells. J Immunol *174*, 1922-1931.

Fehervari, Z., and Sakaguchi, S. (2004). Development and function of CD25+CD4+ regulatory T cells. Curr Opin Immunol *16*, 203-208.

Fontenot, J. D., Gavin, M. A., and Rudensky, A. Y. (2003). Foxp3 programs the development and function of CD4+CD25+ regulatory T cells. Nat Immunol *4*, 330-336.

Garrity, D., Call, M. E., Feng, J., and Wucherpfennig, K. W. (2005). The activating NKG2D receptor assembles in the membrane with two signaling dimers into a hexameric structure. Proc Natl Acad Sci U S A *102*, 7641-7646.

Gasser, S., Orsulic, S., Brown, E. J., and Raulet, D. H. (2005). The DNA damage pathway regulates innate immune system ligands of the NKG2D receptor. Nature *436*, 1186-1190.

Gilfillan, S., Ho, E. L., Cella, M., Yokoyama, W. M., and Colonna, M. (2002). NKG2D recruits two distinct adapters to trigger NK cell activation and costimulation. Nat Immunol *3*, 1150-1155.

Girardi, M. (2006). Immunosurveillance and immunoregulation by gammadelta T cells. J Invest Dermatol *126*, 25-31.

Girardi, M., Oppenheim, D. E., Steele, C. R., Lewis, J. M., Glusac, E., Filler, R., Hobby, P., Sutton, B., Tigelaar, R. E., and Hayday, A. C. (2001). Regulation of cutaneous malignancy by gammadelta T cells. Science *294*, 605-609.

Greenwald, R. J., Freeman, G. J., and Sharpe, A. H. (2005). The B7 family revisited. Annu Rev Immunol *23*, 515-548.

Greenwald, R. J., Latchman, Y. E., and Sharpe, A. H. (2002). Negative co-receptors on lymphocytes. Curr Opin Immunol *14*, 391-396.

Groh, V., Bahram, S., Bauer, S., Herman, A., Beauchamp, M., and Spies, T. (1996). Cell stress-regulated human major histocompatibility complex class I gene expressed in gastrointestinal epithelium. Proc Natl Acad Sci U S A *93*, 12445-12450.

Groh, V., Bruhl, A., El-Gabalawy, H., Nelson, J. L., and Spies, T. (2003). Stimulation of T cell autoreactivity by anomalous expression of NKG2D and its MIC ligands in rheumatoid arthritis. Proc Natl Acad Sci U S A *100*, 9452-9457.

Groh, V., Rhinehart, R., Randolph-Habecker, J., Topp, M. S., Riddell, S. R., and Spies, T. (2001). Costimulation of CD8alphabeta T cells by NKG2D via engagement by MIC induced on virus-infected cells. Nat Immunol *2*, 255-260.

Groh, V., Rhinehart, R., Secrist, H., Bauer, S., Grabstein, K. H., and Spies, T. (1999). Broad tumor-associated expression and recognition by tumor-derived gamma delta T cells of MICA and MICB. Proc Natl Acad Sci U S A *96*, 6879-6884.

Groh, V., Smythe, K., Dai, Z., and Spies, T. (2006). Fas-ligand-mediated paracrine T cell regulation by the receptor NKG2D in tumor immunity. Nat Immunol *7*, 755-762.

Groh, V., Wu, J., Yee, C., and Spies, T. (2002). Tumour-derived soluble MIC ligands impair expression of NKG2D and T-cell activation. Nature *419*, 734-738.

Groux, H., O'Garra, A., Bigler, M., Rouleau, M., Antonenko, S., de Vries, J. E., and Roncarolo, M. G. (1997). A CD4+ T-cell subset inhibits antigen-specific T-cell responses and prevents colitis. Nature *389*, 737-742.

Gumperz, J. E., Miyake, S., Yamamura, T., and Brenner, M. B. (2002). Functionally distinct subsets of CD1d-restricted natural killer T cells revealed by CD1d tetramer staining. J Exp Med *195*, 625-636.

Hamerman, J. A., Ogasawara, K., and Lanier, L. L. (2004). Cutting edge: Toll-like receptor signaling in macrophages induces ligands for the NKG2D receptor. J Immunol *172*, 2001-2005.

Harding, F. A., McArthur, J. G., Gross, J. A., Raulet, D. H., and Allison, J. P. (1992). CD28-mediated signalling co-stimulates murine T cells and prevents induction of anergy in T-cell clones. Nature *356*, 607-609.

Hasan, M., Krmpotic, A., Ruzsics, Z., Bubic, I., Lenac, T., Halenius, A., Loewendorf, A., Messerle, M., Hengel, H., Jonjic, S., and Koszinowski, U. H. (2005). Selective down-regulation of the NKG2D ligand H60 by mouse cytomegalovirus m155 glycoprotein. J Virol *79*, 2920-2930.

Haug, M., Dannecker, L., Schepp, C. P., Kwok, W. W., Wernet, D., Buckner, J. H., Kalbacher, H., Dannecker, G. E., and Holzer, U. (2005). The heat shock protein Hsp70 enhances antigen-specific proliferation of human CD4+ memory T cells. Eur J Immunol *35*, 3163-3172.

Hayday, A., and Tigelaar, R. (2003). Immunoregulation in the tissues by gammadelta T cells. Nat Rev Immunol *3*, 233-242.

Hsieh, C. S., Liang, Y., Tyznik, A. J., Self, S. G., Liggitt, D., and Rudensky, A. Y. (2004). Recognition of the peripheral self by naturally arising CD25+ CD4+ T cell receptors. Immunity *21*, 267-277.

Hsieh, C. S., Macatonia, S. E., Tripp, C. S., Wolf, S. F., O'Garra, A., and Murphy, K. M. (1993). Development of TH1 CD4+ T cells through IL-12 produced by Listeria-induced macrophages. Science *260*, 547-549.

Huster, K. M., Busch, V., Schiemann, M., Linkemann, K., Kerksiek, K. M., Wagner, H., and Busch, D. H. (2004). Selective expression of IL-7 receptor on memory T cells identifies early CD40L-dependent generation of distinct CD8+ memory T cell subsets. Proc Natl Acad Sci U S A *101*, 5610-5615.

Irizarry, R. A., Bolstad, B. M., Collin, F., Cope, L. M., Hobbs, B., and Speed, T. P. (2003). Summaries of Affymetrix GeneChip probe level data. Nucleic Acids Res *31*, e15.

Jamieson, A. M., Diefenbach, A., McMahon, C. W., Xiong, N., Carlyle, J. R., and Raulet, D. H. (2002). The role of the NKG2D immunoreceptor in immune cell activation and natural killing. Immunity *17*, 19-29.

Janeway, C., and Travers, P. (2001). Immunobiology, The Immune System in Health and Disease, Third edn, Spektrum Akademischer Verlag GmbH).

Jinushi, M., Takehara, T., Tatsumi, T., Hiramatsu, N., Sakamori, R., Yamaguchi, S., and Hayashi, N. (2005). Impairment of natural killer cell and dendritic cell functions by the soluble form of MHC class I-related chain A in advanced human hepatocellular carcinomas. J Hepatol *43*, 1013-1020.

Jinushi, M., Takehara, T., Tatsumi, T., Kanto, T., Groh, V., Spies, T., Kimura, R., Miyagi, T., Mochizuki, K., Sasaki, Y., and Hayashi, N. (2003). Expression and role of MICA and MICB in human hepatocellular carcinomas and their regulation by retinoic acid. Int J Cancer *104*, 354-361.

Karimi, M., Cao, T. M., Baker, J. A., Verneris, M. R., Soares, L., and Negrin, R. S. (2005). Silencing human NKG2D, DAP10, and DAP12 reduces cytotoxicity of activated CD8+ T cells and NK cells. J Immunol *175*, 7819-7828.

Khattri, R., Cox, T., Yasayko, S. A., and Ramsdell, F. (2003). An essential role for Scurfin in CD4+CD25+ T regulatory cells. Nat Immunol *4*, 337-342.

Kinsella, T. M., and Nolan, G. P. (1996). Episomal vectors rapidly and stably produce high-titer recombinant retrovirus. Hum Gene Ther *7*, 1405-1413.

Krieg, C., Boyman, O., Fu, Y. X., and Kaye, J. (2007). B and T lymphocyte attenuator regulates CD8(+) T cell-intrinsic homeostasis and memory cell generation. Nat Immunol.

Kriegeskorte, A. (2003) Einfluss von NKG2D-Liganden auf CD4+ T-Helferzellen, Diploma thesis, Technical University Munich, Munich.

Kriegeskorte, A. K., Gebhardt, F. E., Porcellini, S., Schiemann, M., Stemberger, C., Franz, T. J., Huster, K. M., Carayannopoulos, L. N., Yokoyama, W. M., Colonna, M.*, et al.* (2005). NKG2D-independent suppression of T cell proliferation by H60 and MICA. Proc Natl Acad Sci U S A *102*, 11805-11810.

Krmpotic, A., Busch, D. H., Bubic, I., Gebhardt, F., Hengel, H., Hasan, M., Scalzo, A. A., Koszinowski, U. H., and Jonjic, S. (2002). MCMV glycoprotein gp40 confers virus resistance to CD8+ T cells and NK cells in vivo. Nat Immunol *3*, 529-535.

Krmpotic, A., Hasan, M., Loewendorf, A., Saulig, T., Halenius, A., Lenac, T., Polic, B., Bubic, I., Kriegeskorte, A., Pernjak-Pugel, E.*, et al.* (2005). NK cell activation through the NKG2D ligand MULT-1 is selectively prevented by the glycoprotein encoded by mouse cytomegalovirus gene m145. J Exp Med *201*, 211-220.

Kronenberg, M. (2005). Toward an understanding of NKT cell biology: progress and paradoxes. Annu Rev Immunol *23*, 877-900.

Kronenberg, M., and Gapin, L. (2002). The unconventional lifestyle of NKT cells. Nat Rev Immunol *2*, 557-568.

Krug, A., French, A. R., Barchet, W., Fischer, J. A., Dzionek, A., Pingel, J. T., Orihuela, M. M., Akira, S., Yokoyama, W. M., and Colonna, M. (2004). TLR9-dependent recognition of MCMV by IPC and DC generates coordinated cytokine responses that activate antiviral NK cell function. Immunity *21*, 107-119.

Kwak, H. J., Jun, C. D., Pae, H. O., Yoo, J. C., Park, Y. C., Choi, B. M., Na, Y. G., Park, R. K., Chung, H. T., Chung, H. Y.*, et al.* (1998). The role of inducible 70-kDa heat shock protein in cell cycle control, differentiation, and apoptotic cell death of the human myeloid leukemic HL-60 cells. Cell Immunol *187*, 1-12.

Lang, R., Patel, D., Morris, J. J., Rutschman, R. L., and Murray, P. J. (2002). Shaping gene expression in activated and resting primary macrophages by IL-10. J Immunol *169*, 2253-2263.

Lanier, L. L., Corliss, B. C., Wu, J., Leong, C., and Phillips, J. H. (1998). Immunoreceptor DAP12 bearing a tyrosine-based activation motif is involved in activating NK cells. Nature *391*, 703-707.

Lee, J. C., Lee, K. M., Kim, D. W., and Heo, D. S. (2004). Elevated TGF-beta1 secretion and down-modulation of NKG2D underlies impaired NK cytotoxicity in cancer patients. J Immunol *172*, 7335-7340.

Li, C., and Wong, W. H. (2001). Model-based analysis of oligonucleotide arrays: expression index computation and outlier detection. Proc Natl Acad Sci U S A *98*, 31-36.

Li, J., Rabinovich, B. A., Hurren, R., Cosman, D., and Miller, R. G. (2005). Survival versus neglect: redefining thymocyte subsets based on expression of NKG2D ligand(s) and MHC class I. Eur J Immunol *35*, 439-448.

Lipscomb, M. F., and Masten, B. J. (2002). Dendritic cells: immune regulators in health and disease. Physiol Rev *82*, 97-130.

Liu, Z., Tugulea, S., Cortesini, R., Lederman, S., and Suciu-Foca, N. (1999). Inhibition of CD40 signaling pathway in antigen presenting cells by T suppressor cells. Hum Immunol *60*, 568-574.

Lodoen, M., Ogasawara, K., Hamerman, J. A., Arase, H., Houchins, J. P., Mocarski, E. S., and Lanier, L. L. (2003). NKG2D-mediated natural killer cell protection against cytomegalovirus is impaired by viral gp40 modulation of retinoic acid early inducible 1 gene molecules. J Exp Med *197*, 1245-1253.

Lodoen, M. B., Abenes, G., Umamoto, S., Houchins, J. P., Liu, F., and Lanier, L. L. (2004). The cytomegalovirus m155 gene product subverts natural killer cell antiviral protection by disruption of H60-NKG2D interactions. J Exp Med *200*, 1075-1081.

Long, E. O. (1999). Regulation of immune responses through inhibitory receptors. Annu Rev Immunol *17*, 875-904.

Maasho, K., Opoku-Anane, J., Marusina, A. I., Coligan, J. E., and Borrego, F. (2005). NKG2D is a costimulatory receptor for human naive CD8+ T cells. J Immunol *174*, 4480-4484.

Malarkannan, S., Shih, P. P., Eden, P. A., Horng, T., Zuberi, A. R., Christianson, G., Roopenian, D., and Shastri, N. (1998). The molecular and functional characterization of a dominant minor H antigen, H60. J Immunol *161*, 3501-3509.

Medzhitov, R., and Janeway, C. A., Jr. (1998). Innate immune recognition and control of adaptive immune responses. Semin Immunol *10*, 351-353.

Meresse, B., Chen, Z., Ciszewski, C., Tretiakova, M., Bhagat, G., Krausz, T. N., Raulet, D. H., Lanier, L. L., Groh, V., Spies, T*., et al.* (2004). Coordinated induction by IL15 of a TCR-independent NKG2D signaling pathway converts CTL into lymphokine-activated killer cells in celiac disease. Immunity *21*, 357-366.

Nomura, M., Zou, Z., Joh, T., Takihara, Y., Matsuda, Y., and Shimada, K. (1996). Genomic structures and characterization of Rae1 family members encoding GPI-anchored cell surface proteins and expressed predominantly in embryonic mouse brain. J Biochem (Tokyo) *120*, 987-995.

O'Callaghan, C. A., Cerwenka, A., Willcox, B. E., Lanier, L. L., and Bjorkman, P. J. (2001). Molecular competition for NKG2D: H60 and RAE1 compete unequally for NKG2D with dominance of H60. Immunity *15*, 201-211.

Ogasawara, K., Benjamin, J., Takaki, R., Phillips, J. H., and Lanier, L. L. (2005). Function of NKG2D in natural killer cell-mediated rejection of mouse bone marrow grafts. Nat Immunol *6*, 938-945.

Oldenhove, G., de Heusch, M., Urbain-Vansanten, G., Urbain, J., Maliszewski, C., Leo, O., and Moser, M. (2003). CD4+ CD25+ regulatory T cells control T helper cell type 1 responses to foreign antigens induced by mature dendritic cells in vivo. J Exp Med *198*, 259-266.

Pende, D., Rivera, P., Marcenaro, S., Chang, C. C., Biassoni, R., Conte, R., Kubin, M., Cosman, D., Ferrone, S., Moretta, L., and Moretta, A. (2002). Major histocompatibility complex class I-related chain A and UL16-binding protein expression on tumor cell lines of different histotypes: analysis of tumor susceptibility to NKG2D-dependent natural killer cell cytotoxicity. Cancer Res *62*, 6178-6186.

Poggi, A., Prevosto, C., Massaro, A. M., Negrini, S., Urbani, S., Pierri, I., Saccardi, R., Gobbi, M., and Zocchi, M. R. (2005). Interaction between human NK cells and bone marrow stromal cells induces NK cell triggering: role of NKp30 and NKG2D receptors. J Immunol *175*, 6352-6360.

Powell, J. D., Lerner, C. G., and Schwartz, R. H. (1999). Inhibition of cell cycle progression by rapamycin induces T cell clonal anergy even in the presence of costimulation. J Immunol *162*, 2775-2784.

Rabinovich, B., Li, J., Wolfson, M., Lawrence, W., Beers, C., Chalupny, J., Hurren, R., Greenfield, B., Miller, R., and Cosman, D. (2006). NKG2D splice variants: a reexamination of adaptor molecule associations. Immunogenetics *58*, 81-88.

Rabinovich, B. A., Li, J., Shannon, J., Hurren, R., Chalupny, J., Cosman, D., and Miller, R. G. (2003). Activated, but not resting, T cells can be recognized and killed by syngeneic NK cells. J Immunol *170*, 3572-3576.

Ravetch, J. V., and Lanier, L. L. (2000). Immune inhibitory receptors. Science *290*, 84-89.

Rieder, C. L., and Cole, R. (2000). Microtubule disassembly delays the G2-M transition in vertebrates. Curr Biol *10*, 1067-1070.

Roberts, A. I., Lee, L., Schwarz, E., Groh, V., Spies, T., Ebert, E. C., and Jabri, B. (2001). NKG2D receptors induced by IL-15 costimulate CD28-negative effector CTL in the tissue microenvironment. J Immunol *167*, 5527-5530.

Rohde, M., Daugaard, M., Jensen, M. H., Helin, K., Nylandsted, J., and Jaattela, M. (2005). Members of the heat-shock protein 70 family promote cancer cell growth by distinct mechanisms. Genes Dev *19*, 570-582.

Romanski, A., Bug, G., Becker, S., Kampfmann, M., Seifried, E., Hoelzer, D., Ottmann, O. G., and Tonn, T. (2005). Mechanisms of resistance to natural killer cell-mediated cytotoxicity in acute lymphoblastic leukemia. Exp Hematol *33*, 344-352.

Rosen, D. B., Araki, M., Hamerman, J. A., Chen, T., Yamamura, T., and Lanier, L. L. (2004). A Structural basis for the association of DAP12 with mouse, but not human, NKG2D. J Immunol *173*, 2470-2478.

Routes, J. M., Ryan, S., Morris, K., Takaki, R., Cerwenka, A., and Lanier, L. L. (2005). Adenovirus serotype 5 E1A sensitizes tumor cells to NKG2D-dependent NK cell lysis and tumor rejection. J Exp Med *202*, 1477-1482.

Saez-Borderias, A., Guma, M., Angulo, A., Bellosillo, B., Pende, D., and Lopez-Botet, M. (2006). Expression and function of NKG2D in CD4(+) T cells specific for human cytomegalovirus. Eur J Immunol *36*, 3198-3206.

Sakaguchi, S., Fukuma, K., Kuribayashi, K., and Masuda, T. (1985). Organ-specific autoimmune diseases induced in mice by elimination of T cell subset. I. Evidence for the active participation of T cells in natural self-tolerance; deficit of a T cell subset as a possible cause of autoimmune disease. J Exp Med *161*, 72-87.

Salih, H. R., Antropius, H., Gieseke, F., Lutz, S. Z., Kanz, L., Rammensee, H. G., and Steinle, A. (2003). Functional expression and release of ligands for the activating immunoreceptor NKG2D in leukemia. Blood *102*, 1389-1396.

Salih, H. R., Rammensee, H. G., and Steinle, A. (2002). Cutting edge: down-regulation of MICA on human tumors by proteolytic shedding. J Immunol *169*, 4098-4102.

Salomon, B., Lenschow, D. J., Rhee, L., Ashourian, N., Singh, B., Sharpe, A., and Bluestone, J. A. (2000). B7/CD28 costimulation is essential for the homeostasis of the CD4+CD25+ immunoregulatory T cells that control autoimmune diabetes. Immunity *12*, 431-440.

Schmitz, F., Mages, J., Heit, A., Lang, R., and Wagner, H. (2004). Transcriptional activation induced in macrophages by Toll-like receptor (TLR) ligands: from expression profiling to a model of TLR signaling. Eur J Immunol *34*, 2863-2873.

Siren, J., Sareneva, T., Pirhonen, J., Strengell, M., Veckman, V., Julkunen, I., and Matikainen, S. (2004). Cytokine and contact-dependent activation of natural killer cells by influenza A or Sendai virus-infected macrophages. J Gen Virol *85*, 2357-2364.

Smyth, M. J., Swann, J., Kelly, J. M., Cretney, E., Yokoyama, W. M., Diefenbach, A., Sayers, T. J., and Hayakawa, Y. (2004). NKG2D recognition and perforin effector function mediate effective cytokine immunotherapy of cancer. J Exp Med *200*, 1325-1335.

Steinle, A., Li, P., Morris, D. L., Groh, V., Lanier, L. L., Strong, R. K., and Spies, T. (2001). Interactions of human NKG2D with its ligands MICA, MICB, and homologs of the mouse RAE-1 protein family. Immunogenetics *53*, 279-287.

Stephens, H. A. (2001). MICA and MICB genes: can the enigma of their polymorphism be resolved? Trends Immunol *22*, 378-385.

Steuerwald, N., Cohen, J., Herrera, R. J., and Brenner, C. A. (1999). Analysis of gene expression in single oocytes and embryos by real-time rapid cycle fluorescence monitored RT-PCR. Mol Hum Reprod *5*, 1034-1039.

Taieb, J., Chaput, N., Menard, C., Apetoh, L., Ullrich, E., Bonmort, M., Pequignot, M., Casares, N., Terme, M., Flament, C.*, et al.* (2006). A novel dendritic cell subset involved in tumor immunosurveillance. Nat Med *12*, 214-219.

Takahashi, T., Kuniyasu, Y., Toda, M., Sakaguchi, N., Itoh, M., Iwata, M., Shimizu, J., and Sakaguchi, S. (1998). Immunologic self-tolerance maintained by CD25+CD4+ naturally anergic and suppressive T cells: induction of autoimmune disease by breaking their anergic/suppressive state. Int Immunol *10*, 1969-1980.

Thornton, A. M., and Shevach, E. M. (1998). CD4+CD25+ immunoregulatory T cells suppress polyclonal T cell activation in vitro by inhibiting interleukin 2 production. J Exp Med *188*, 287-296.

Tieng, V., Le Bouguenec, C., du Merle, L., Bertheau, P., Desreumaux, P., Janin, A., Charron, D., and Toubert, A. (2002). Binding of Escherichia coli adhesin AfaE to CD55 triggers cell-surface expression of the MHC class I-related molecule MICA. Proc Natl Acad Sci U S A *99*, 2977-2982.

Upshaw, J. L., Arneson, L. N., Schoon, R. A., Dick, C. J., Billadeau, D. D., and Leibson, P. J. (2006). NKG2D-mediated signaling requires a DAP10-bound Grb2-Vav1 intermediate and phosphatidylinositol-3-kinase in human natural killer cells. Nat Immunol *7*, 524-532.

van Eden, W., van der Zee, R., and Prakken, B. (2005). Heat-shock proteins induce T-cell regulation of chronic inflammation. Nat Rev Immunol *5*, 318-330.

Verneris, M. R., Karami, M., Baker, J., Jayaswal, A., and Negrin, R. S. (2004). Role of NKG2D signaling in the cytotoxicity of activated and expanded CD8+ T cells. Blood *103*, 3065-3072.

Vieira, P. L., Christensen, J. R., Minaee, S., O'Neill, E. J., Barrat, F. J., Boonstra, A., Barthlott, T., Stockinger, B., Wraith, D. C., and O'Garra, A. (2004). IL-10-secreting regulatory T cells do not express Foxp3 but have comparable regulatory function to naturally occurring CD4+CD25+ regulatory T cells. J Immunol *172*, 5986-5993.

Watson, N. F., Spendlove, I., Madjd, Z., McGilvray, R., Green, A. R., Ellis, I. O., Scholefield, J. H., and Durrant, L. G. (2006). Expression of the stress-related MHC class I chain-related protein MICA is an indicator of good prognosis in colorectal cancer patients. Int J Cancer *118*, 1445-1452.

Wolan, D. W., Teyton, L., Rudolph, M. G., Villmow, B., Bauer, S., Busch, D. H., and Wilson, I. A. (2001). Crystal structure of the murine NK cell-activating receptor NKG2D at 1.95 A. Nat Immunol *2*, 248-254.

Wu, J., Song, Y., Bakker, A. B., Bauer, S., Spies, T., Lanier, L. L., and Phillips, J. H. (1999). An activating immunoreceptor complex formed by NKG2D and DAP10. Science *285*, 730-732.

Wu, J. D., Higgins, L. M., Steinle, A., Cosman, D., Haugk, K., and Plymate, S. R. (2004). Prevalent expression of the immunostimulatory MHC class I chain-related molecule is counteracted by shedding in prostate cancer. J Clin Invest *114*, 560-568.

Zhang, Z. X., Yang, L., Young, K. J., DuTemple, B., and Zhang, L. (2000). Identification of a previously unknown antigen-specific regulatory T cell and its mechanism of suppression. Nat Med *6*, 782-789.

Zompi, S., Hamerman, J. A., Ogasawara, K., Schweighoffer, E., Tybulewicz, V. L., Di Santo, J. P., Lanier, L. L., and Colucci, F. (2003). NKG2D triggers cytotoxicity in mouse NK cells lacking DAP12 or Syk family kinases. Nat Immunol *4*, 565-572.

7 ACKNOWLEDGEMENTS

An dieser Stelle möchte ich die Gelegenheit wahrnehmen all den Leuten zu danken, die mich während meiner Doktorarbeit praktisch und geistig unterstützt haben, und ohne die ein Gelingen der Arbeit nicht möglich gewesen wäre.

Zunächst möchte ich das großartige Labor von Prof. Dirk Busch erwähnen. Ich habe es immer sehr genossen dort zu arbeiten. Das freundliche und kommunikative Umfeld war nicht nur bei zähen und schwierigen Versuchen über all die Jahre eine essentielle Quelle, um neue Kraft zu schöpfen und hilfreiche Anregungen zu erhalten. In erster Linie möchte ich die Arbeit von Dr. Friedemann Gebhardt würdigen, der zahlreiche für das Projekt richtungsweisende Ergebnisse beigesteuert hat. Des Weiteren wären ohne die exzellenten Sortfähigkeiten und „Mädchen für alles"-Qualitäten von Dr. Matthias Schiemann und Evelin Ziegler sowie Katleen Götsch viele Experimente nicht durchzuführen gewesen. Für stimulierende Diskussionen möchte ich im Besonderen PD Dr. Katharina Huster und Florian Anderl danken, sowie Martina Koffler und Anna Hochholzer für technische und freundschaftliche Unterstützung.

Großer Dank geht an meinen Arbeitsgruppenleiter Prof. Dirk Busch, der mich stets vorbildlich betreut hat und entscheidend an der Projektgestaltung teilgenommen hat. Auch für die Möglichkeit an diesem renommierten Institut zu forschen und meine Erfolge auf internationalen Kongressen vorzustellen, möchte ich mich bei Prof. Busch und nicht zuletzt bei unserem Institutsleiter Prof. Herman Wagner erkenntlich zeigen.

Darüber hinaus bin ich dankbar für die zahlreichen fruchtbaren Kooperationen außerhalb unseres Instituts. Von der AG Duyster waren mir Christine von Klitzing und Dr. Lena Illert behilflich mit den Zellzyklusanalysen und der Präparation von synchronisierten 3T3-Zellen. Dr. Nadia Guerra aus der Gruppe von Prof. David Raulet führte mit mir die Experimente an den NGK2D knock-out Mäusen durch. Aus der AG Üffing versucht sich Karsten Boldt an der Aufreinigung der Membranproteinkomplexe, und unter der Leitung von Prof. Stipan Jonjic steht das Projekt der Antikörpergenerierung.

Nicht zuletzt möchte ich mich bei meinen privaten „Kooperationspartnern" bedanken. Hier stehen natürlich meine Eltern an vorderster Stelle, auf die ich mich immer verlassen kann, und deren Finanzspritzen mir auch ein angenehmes Leben neben der Doktorarbeit ermöglichten. Neben meinen Freunden, die für die nötige Abwechslung in der Freizeit unersetzlich waren, war besonders mein Partner Gregor Völtz nicht nur in der Endphase der Arbeit von entscheidender Bedeutung bei der Behebung von EDV-Problemen und der Hauptleidtragende, wenn es mal nicht so gut lief. Vielen Dank, dass du mit mir durchgehalten hast!